NTNU – Trondheim
Norwegian University of
Science and Technology

Design of Centrifugal Pump for Produced Water

Sverre Stefanussen Foslie

EPT-M-2013-146

MASTEROPPGAVE

for

Stud.techn Sverre Stefanussen Foslie

Høst 2013

Design of centrifugal pump for produced water
Design av sentrifugalpumpe for produsert vann

Background and objective
In the process of oil production, there will be water extracted from the oil coming up from the well. This water must be cleaned for oil droplets before it is submitted to the ocean. Cyclone separators are used for cleaning the water. However, if the droplets are too small the separation becomes difficult. A company, Typhonix, is developing a multi stage centrifugal pump where the aim to increase the droplet size during pumping. An ongoing PhD project is working with understanding the mechanism of how to collect the oil droplets during pumping.

A three stage pump is designed and produced by Standart Pumps in Istanbul according to requirements defined by Typhonix. The pump will initially be tested at Typonix and will be sent to the Waterpower Laboratory fro further tests.

The candidate will collaborate with PhD student Alessandro Nocente who will especially address the flow through the diffuser.

Objective
Find the velocity distribution at pump outlet, which is the entrance of the diffuser.

The following tasks are to be considered

1. Establish a suitable test stand for the pump in the Waterpower Laboratory

2. Test the characteristics of the pump and compare with simulated characteristics

3. Find the velocity distribution at the outlet of the pump both theoretically and verified by tests.

” - ”

Within 14 days of receiving the written text on the master thesis, the candidate shall submit a research plan for his project to the department.

When the thesis is evaluated, emphasis is put on processing of the results, and that they are presented in tabular and/or graphic form in a clear manner, and that they are analyzed carefully. The thesis should be formulated as a research report with summary both in English and Norwegian, conclusion, literature references, table of contents etc. During the preparation of the text, the candidate should make an effort to produce a well-structured and easily readable report. In order to ease the evaluation of the thesis, it is important that the cross-references are correct. In the making of the report, strong emphasis should be placed on both a thorough discussion of the results and an orderly presentation.

The candidate is requested to initiate and keep close contact with his/her academic supervisor(s) throughout the working period. The candidate must follow the rules and regulations of NTNU as well as passive directions given by the Department of Energy and Process Engineering.
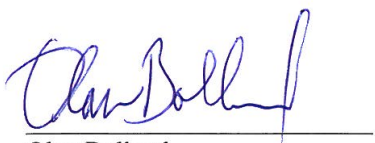
Risk assessment of the candidate's work shall be carried out according to the department's procedures. The risk assessment must be documented and included as part of the final report. Events related to the candidate's work adversely affecting the health, safety or security, must be documented and included as part of the final report.

Pursuant to "Regulations concerning the supplementary provisions to the technology study program/Master of Science" at NTNU §20, the Department reserves the permission to utilize all the results and data for teaching and research purposes as well as in future publications.

The final report is to be submitted digitally in DAIM. An executive summary of the thesis including title, student's name, supervisor's name, year, department name, and NTNU's logo and name, shall be submitted to the department as a separate pdf file. Based on an agreement with the supervisor, the final report and other material and documents may be given to the supervisor in digital format.

☒ Work to be done in lab (Water power lab, Fluids engineering lab, Thermal engineering lab)
☐ Field work

Department of Energy and Process Engineering, 4.August 2013

Olav Bolland
Department Head

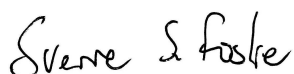Torbjørn K. Nielsen
Academic Supervisor

Preface

This Master's thesis was written at the Waterpower Laboratory, Department of Energy and Process Engineering at the Norwegian University of Science and Technology (NTNU) during the fall of 2013. The aim of the thesis was to verify certain parameters calculated by a pump design program in MATLAB by testing of a multistage centrifugal pump.

In agreement with my supervisor Torbjørn K. Nielsen task number 1 and part of number 2 in the project description has not been performed due to practical limitations. The multistage centrifugal pump was originally planned to be brought to the Waterpower Laboratory, and hopefully this may be done in the near future as it may be valuable to research and to other Master's students.

I would like to thank my supervisor Torbjørn K. Nielsen, who put me in touch with Typhonix and gave me a more hands-on Master's thesis, as was my desire. A special thanks also goes to Typhonix, and above all Trygve Husveg and Olav Austbø. They have provided good answers to all my questions and gave very valuable help during the pump testing in Varhaug. I would also like to thank Alessandro Nocente, PhD-candidate and co-supervisor, for reviewing my thesis, helping me in the lab and answering all my questions.

The employees and PhD-candidates at the Waterpower Laboratory are doing a great job in making a good working environment at the lab, and the final year of my studies have therefore become a highlight. Especially PhD-candidates Bjørn W. Solemslie and Peter Joachim Gogstad should get credit for this. It has been a great motivation socially and professionally, and I hope that the positive environment may be kept intact despite the recent changes at the lab.

Thank you Oddveig for all your patience.

Sverre Stefanussen Foslie
Trondheim, December 18, 2013

Abstract

During the spring of 2008, Jón Bergmann Heimisson developed a pump design program in MATLAB. The program has been further developed during the work with this thesis, as well as in the author's preceding project thesis, giving key information for an existing pump design. The aim of this Master's thesis has been to verify the calculation of pump characteristics and velocity profiles at the impeller outlet through testing.

A detailed description of the relevant theory regarding pump design has been presented, and different calculation models for the pump characteristics have been examined. The analytical approaches for calculating the performance data have been implemented into MATLAB, and a comparison of the different calculation models has been performed.

A multistage centrifugal pump has been used for verifying the velocity profiles, and the pump characteristics have been compared to the different calculation models presented in MATLAB. Measurements of the velocity profiles were carried out in Typhonix' laboratories at Varhaug using a pitot-static probe.

The results achieved from the comparison of the characteristic curves calculated in MATLAB showed that the models provide quite different results. Some of the methods widely used in the literature proved to deviate significantly from the measured results, while other and more advanced methods provided better results.

The results achieved from testing the velocity profiles with the pitot-static probe were not as good as desired. The measured velocities and flow angles did not correlate well with the analytical solutions, and the results are partly unreliable. Some of the trends regarding changes due to increased volume flow or rotational speed were found, but the exact values could not be trusted. The pitot-static probe is an intrusive method, and it probably disturbed the flow in a way making good results difficult to achieve.

Sammendrag

I løpet av våren 2008 utviklet Jón Bergmann Heimisson et program for pumpedesign i MATLAB. I løpet av denne oppgaven og forfatterens foregående prosjektoppgave har programmet blitt utviklet med det mål å gi nøkkelinformasjon ved et eksisterende pumpedesign. Målet med denne masteroppgaven har vært å verifisere beregningen av pumpekarakteristikk og hastighetsprofil ved utløpet av impelleren ved hjelp av testing.

En detaljert beskrivelse av den relevante teorien rundt pumpedesign har blitt presentert, og forskjellige beregningsmodeller for pumpekarakteristikker har blitt undersøkt. De analytiske fremgangsmåtene for å beregne disse nøkkeltallene har blitt implementert i MATLAB, og en sammenligning mellom de ulike beregningsmodellene har blitt gjennomført.

En flertrinns sentrifugalpumpe har blitt brukt til testing av hastighetsprofilene, og pumpens karakteristiske kurver har blitt sammenlignet med de ulike beregningsmodellene i MATLAB. Testing av hastighetsprofilene ble gjort i Typhonix' laboratorier på Varhaug ved hjelp av pitot måleutstyr.

Resultatene som ble funnet fra sammenligningen av de ulike karakteristiske kurvene i MATLAB viste at beregningsmodellene ga ganske forskjellige resultater. Noen av metodene som blir allment brukt i pumpelitteratur hadde store avvik fra de målte resultatene, mens andre og mer avanserte beregningsmodeller ga bedre resultater.

Resultatene som ble funnet fra testing av hastighetsprofilene med pitot var ikke så gode som ønsket. De målte hastighetene og strømningsvinklene korrelerte dårlig med de analytiske løsningene, og resultatene var delvis upålitelige. Noen av trendene når det kommer til endringer ved forskjellig volumstrøm eller rotasjonshastighet ble funnet, men de eksakte verdiene kan ikke regnes som pålitelige. Å bruke pitot til hastighetsmålinger til dette formålet har sannsynligvis forstyrret strømningsbildet så mye at gode resultater ble vanskelig å oppnå.

Contents

List of Figures

List of Tables

Nomenclature

A	area	m^2
a	distance between vanes	m
b	height	m
c	absolute velocity	m/s
C_p	Pfleiderer's correction factor	$-$
d	diameter	m
d_n	hub diameter	m
d_{1i}	inner streamline diameter	m
e	vane thickness	m
g	acceleration due to gravity	m/s^2
H	head	m
h	head loss	m
n	speed of rotation	rpm
n_q	specific speed	$m^{3/4}/\sqrt{s}$
p	pressure	Pa
Q	delivered volume flow	m^3/s
$q*$	flow rate ratio, $q* = Q/Q_{opt}$	$-$
Q_E	flow rate through axial thrust balancing	m^3/s
Q_L	total leakage flow rate	m^3/s
Q_{sp}	leakage flow rate through impeller inlet seal	m^3/s
r	radius	m

u	peripheral velocity	m/s
w	relative velocity	m/s
z	height	m
z	number of blades or vanes	—

Greek letters

α	angle between peripheral and absolute velocity	—
β	angle between relative velocity and peripheral velocity	—
ϵ	absolute roughness	m
η_h	hydraulic efficiency	—
γ	slip factor	—
ν	kinematic viscosity	kg/sm
ρ	density	kg/m^3
τ	blade blockage factor	—
ζ	loss coefficient	—

Sub- and superscripts

$'$	with blockage
1	impeller inlet
2	impeller outlet
3	diffuser inlet
4	diffuser outlet
5	return channel inlet
6	return channel outlet
∞	infinite number of blades
av	average
B	blade or vane angle
f	friction
La	impeller
Le	diffuser
m	geometric average of diameters, e.g. $d_{1m} = \sqrt{0.5(d_1{}^2 + d_{1i}{}^2)}$
m	meridional velocity component

opt	operation at best efficiency point (BEP)
q	throat
ref	reference value
s	shock
sch	blade or vane
th	theoretical flow conditions without losses
u	peripheral velocity component
v	volumetric

Abbreviations

BEP	Best efficiency point
CFD	Computational fluid dynamics
GUI	Graphical user interface
NTNU	Norwegian University of Science and Technology
rpm	rotations per minute

Geometric dimensions
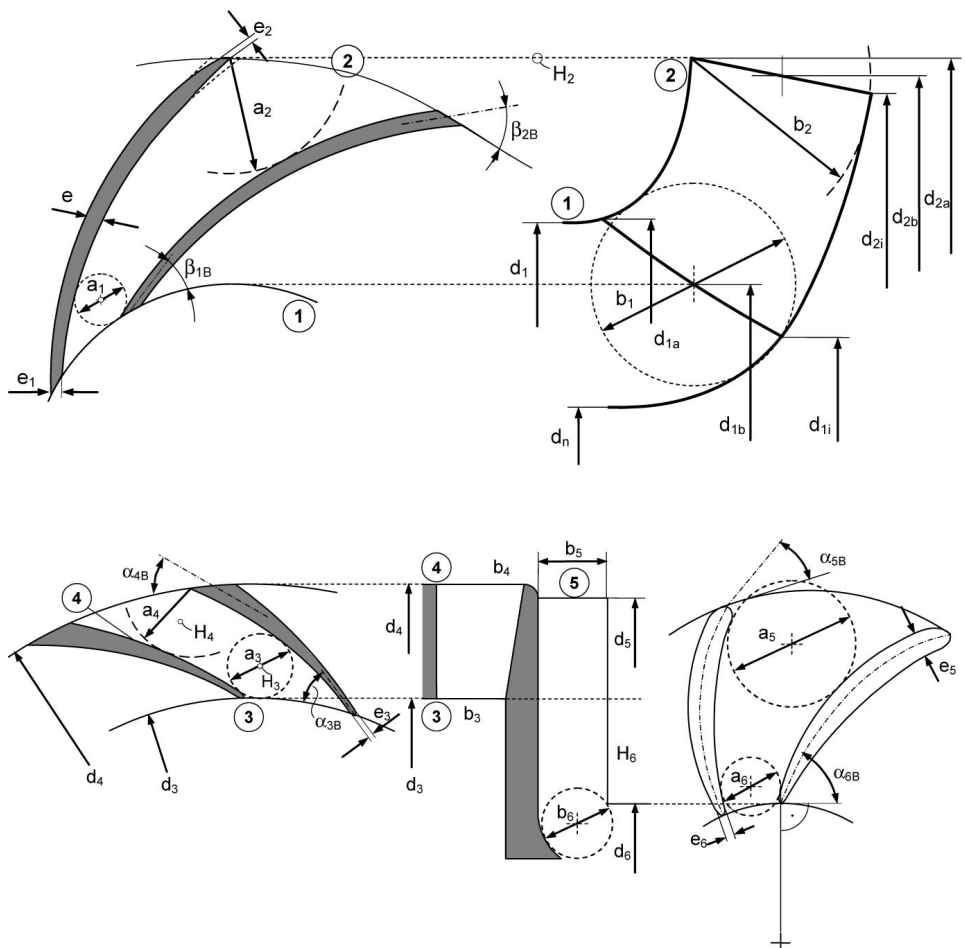
Figure 1: Geometric dimensions as they are denoted in this thesis[12]

Chapter 1

Introduction

The environmental restrictions in the oil and gas industry are constantly developing, requiring new solutions for the processing equipment. One of these restrictions concerns the amount of oil droplets in the leftover water from the process, also known as produced water. The collection of oil droplets from produced water is a difficult operation, and the droplet size is an important parameter in order to collect as much as possible. Produced water pumps available today shatter the oil remains into smaller droplets, causing the requirement of expensive rinsing technology.

Typhonix is a company specialized on handling separation of oil and water in produced water, and they are investigating the possibility of producing a pump for use in these applications. Their research has shown that the oil droplets may be coalesced in the diffuser of the pump, and the development of a suitable pump may give huge advantages in the strive for cleaner production. An ongoing PhD project by Alessandro Nocente is aimed at researching the coalescing of the droplets in the diffuser by performing a CFD analysis of the diffuser section of a multistage pump. To be able to simulate the flow as correctly as possible, accurate inlet conditions to the diffuser is needed.

This Master's thesis is a continuation of a project thesis written the spring of 2013 in which a pump design program in MATLAB was developed to give velocity inlet conditions for the diffuser of a specific pump. The aim of this thesis is to verify the calculations made by the pump design program by testing, and to further develop the program in those areas where it proves to be insufficient.

Testing of the characteristic curves and the outlet velocity profile will be compared to the analytical solutions. This can be used as an indication to whether the analytical solution is accurate and if the pump design program can provide satisfying solutions. If they prove to be accurate, the program may be used to estimate the velocities as a part of the PhD work by Alessandro Nocente and the program may also in the future be used as a pump design tool giving good predictions of the pump behaviour.

Chapter 2

Theory

In this chapter the relevant physics of a pump will be described, and methods to calculate the performance will be given. A brief introduction to methods for measuring the velocity of a fluid will also be given.

2.1 Pump theory

2.1.1 Velocity triangles

In turbo machinery the motion of the fluid needs to be specified according to the rotational motion of the impeller. The absolute velocity c can be regarded as the velocity relative to a stationary part, such as the housing or the diffuser. This can be seen as the sum of two velocities: the peripheral velocity of the impeller u, and the fluid velocity relative to the impellers w [16].

$$c = u + w \tag{2.1}$$

When these velocities are plotted, they form a velocity parallelogram or a velocity triangle. The velocities are normally given subscript 1 or 2, where 1 corresponds to impeller inlet, and 2 to impeller outlet. The subscripts 3 and 4 correspond to the inlet and outlet of the diffuser, while 5 and 6 correspond to the inlet and outlet of the return channels of multistage pumps. The velocity parallelograms can be seen in Figure 2.1. Figure 2.2 shows how these can be rearranged in order to form velocity triangles that show the relation between the relative and absolute velocities.

α and β represent the angles of the absolute and relative velocities at the inlet and outlet of the impeller. When dealing with an axial inlet we usually assume zero swirl, meaning $\alpha_1 = 90°$. In multistage pumps this is difficult to obtain because
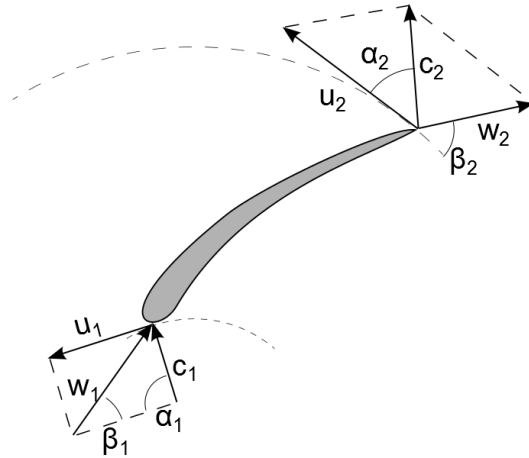
Figure 2.1: Velocity diagram in an impeller stage
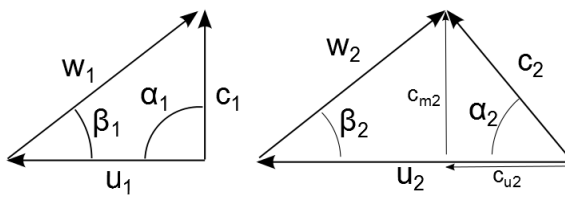
Figure 2.2: Velocity triangles
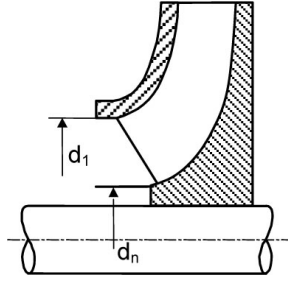
Figure 2.3: Inlet dimensions

of disturbances in the flow caused by the previous stage. According to theory, the angle at the outlet, β_2, aligns with the camber angle of the impeller [12, p. 70]. In reality this angle deviates due to slip and blade blockage, as we shall see later.

The peripheral velocity u may easily be calculated by knowing the rotational speed n of the impeller, by the following relation:

$$u = \pi d \frac{n}{60} \tag{2.2}$$

in which d is the diameter where the velocity is evaluated.

The absolute velocity, c, can be decomposed into meridional and peripheral components with subscripts m and u [20, p. 32]. With zero swirl at the inlet c_{u1} is negligible, and $c_{m1} = c_1$. By taking into account conservation of mass, the relation between c_{m1} and c_{m2} can be found.

$$c_{m2} = \frac{Q_{La}}{A_2} = c_{m1} \frac{A_1}{A_2} \tag{2.3}$$

In Equation (2.3), Q_{La} is the volume flow passed through the impeller, A_1 is the area at the inlet and A_2 is the outlet area of the impeller. The areas are calculated from equations (2.4) and (2.5), where d_n is the hub diameter as seen in Figure 2.3, d_1 is the impeller eye diameter, d_2 is the diameter at the outlet and b_2 is the height of the outlet of the impeller.

$$\text{Inlet area:} \qquad A_1 = \frac{\pi}{4} d_1^2 - d_n^2 \tag{2.4}$$

$$\text{Outlet area:} \qquad A_2 = \pi \, d_2 b_2 \tag{2.5}$$

The calculation of c_{u2} is a bit more difficult due to slip, and will be discussed further in subsection 2.1.4.

This basic knowledge of velocity triangles will be used throughout the following sections, and they are important parameters when designing the diffusing elements.

2.1.2 Specific speed

In order to classify pumps into different categories, the specific speed was first introduced by Camerer in 1914 and further developed by Stepanoff in 1948 [20]:

$$n_q = n \frac{\sqrt{Q_{La,opt}}}{H_{opt}^{0.75}} \tag{2.6}$$

When calculating the specific speed with Equation (2.6) H_{opt} is the head. The subscript *opt* indicates that they are evaluated at the best efficiency point of the pump, also called BEP. By calculating the specific speed it is possible to classify which kind of pump would be suitable for different applications, and it is also possible to compare pumps in different operating conditions. n_q is not dimensionless, but is a number used for classifications in the same way as the Reynolds' number [20].

2.1.3 Euler's equation, theoretical head

By combining Newton's 2.law and the law of momentum, Euler's equation can be obtained in order to calculate the theoretical head of the pump [5, p. 133].

$$H_{th\infty} = \frac{u_2 c_{u2} - u_1 c_{u1}}{g} \tag{2.7}$$

In a pump with an axial inlet c_{u1} is negligible and Euler's equation reduces to:

$$H_{th\infty} = \frac{u_2 c_{u2}}{g} \tag{2.8}$$

To obtain this theoretical head we assume an infinitely amount of infinitely thin blades. Reducing the number of blades reduces the friction area in the pump, but also increases the pressure differences between the suction side and pressure side of the blades. When this difference grows we experience a flow pattern on the trailing edge of the blade called slip. This will be further discussed in the following section.

2.1.4 Slip

To fully understand what happens at the trailing edge of the blades, it is necessary to know a bit about what goes on within the impeller. The impeller is a curved channel in constant movement in which the blades act upon the fluid to create an increased velocity and pressure. This leads to the fact that the pressure will be higher at the pressure side than at the suction side of the blades. Since the pressure distribution correlates with the velocities, there must be a difference in the velocity of the fluid at these two surfaces. The flow is therefore not able to follow the blade

(a) Velocity distribution between two blades

(b) Streamline deviation from blade shape
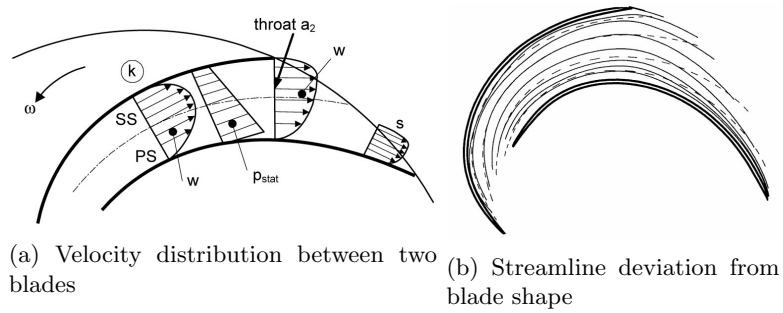
Figure 2.4: Flow between blades [12]
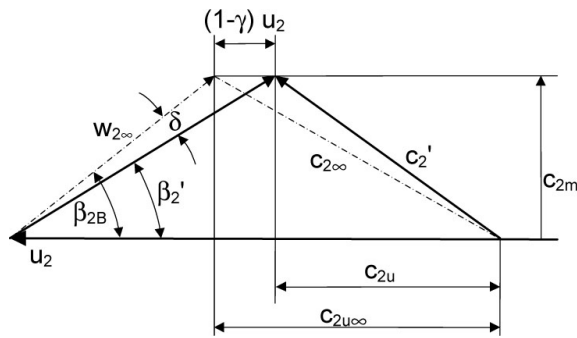
Figure 2.5: Outlet velocities with slip [12]

exactly, and deviates from the shape of the blade [12, p. 75]. This can be seen in Figure 2.4.

When the flow passes the trailing edge, the pressure difference immediately vanishes and the streamlines curve around the trailing edge to satisfy the outlet conditions. This can be seen in Figure 2.4 where most of the deviation from the blade shape happens in the triangular section after the throat a_2 at the impeller outlet [12, p. 76]. In total, this leads to a deviation between the angle of the trailing edge of the blade and the flow, called slip.

Slip is an important design parameter when designing pumps, and it has a significant influence when computing head and flow properties. Although slip is a well known phenomena, exact calculations of the process can only be done by testing [12, p. 77]. In Figure 2.5 the effect of the slip on the outlet angle β_2 can be seen. The Figure uses a slightly different notation, but the difference in outlet angle δ between the flow and the blade angle β_{2B} can clearly be seen, as well as the changed peripheral component of the absolute velocity c_{u2}.

Getting a complete knowledge of the effects of slip is a difficult operation, with several uncertainties. Nevertheless it is important to take the slip into account when designing centrifugal pumps, and the following approaches give us good ap-

proximations in design operations.

Slip calculation

Figure 2.5 introduces the slip coefficient γ. The slip coefficient is defined by Gülich [12] and Tuzson [22] as:

$$c_{u2\infty} - c_{u2} = (1 - \gamma)u_2 \tag{2.9}$$

In Equation (2.9) $c_{u2\infty}$ represents the peripheral component of the absolute velocity with infinite number of blades. c_{u2} is the peripheral component of the real velocity, taking slip into account.

The most accurate values which exist for the slip coefficient were calculated by Busemann in 1928, and later reviewed and adjusted by Wiesner in 1967 [22, p. 66]. Wiesner derived the following expression for calculating the slip coefficient with a standard deviation of about $\pm 4\%$ [12, p. 78]:

$$\gamma = f_1 \left(1 - \frac{\sqrt{\sin \beta_{2B}}}{z_{La}^{0.70}} \right) \tag{2.10}$$

In Equation (2.10) β_{2B} is the blade angle at the outlet and z_{La} is the number of impeller blades. The factor f_1 is for radial impellers set to 0.98. With $\gamma = 1$ there is no slip. This equation is valid for a limited range of mean diameter ratios, given by the following expression[7]:

$$\varepsilon_{\lim} = \exp \left(-\frac{8.16 \sin \beta_{2B}}{z_{La}} \right) \tag{2.11}$$

The limit is defined as $\frac{d_{1m}}{d_{2m}} = \varepsilon_{\lim}$, where the subscript m represents a mean streamline. The mean streamline corresponds to the streamline ending on the geometric mean diameter at the outlet. For values of $\frac{d_{1m}}{d_{2m}} > \varepsilon_{\lim}$, the right side of Equation (2.10) can be multiplied by the factor k_w, calculated by the following equation[12]:

$$k_w = 1 - \left(\frac{\frac{d_{1m}}{d_{2m}} - \varepsilon_{\lim}}{1 - \varepsilon_{\lim}} \right)^3 \tag{2.12}$$

Pfleiderer's correction

Another approach, presented by Stepanoff and by Łazarkiewicz and Troskolański, is to use Pfleiderer's correction factor C_p to calculate the theoretical head with a finite number of blades directly. The relation is given in *Impeller Pumps* as:

$$H_{th} = \frac{1}{1 + C_p} H_{th\infty} \tag{2.13}$$

The correction factor is by Pfleiderer defined by the semi-empirical formula [2, p. 94]

$$C_p = 2 \frac{\psi}{z_{La}} \frac{1}{1 - \left(\frac{r_{1m}}{r_{2m}}\right)^2} \tag{2.14}$$

in which z_{La} is the number of impeller blades, r_{1m} and r_{2m} are the inner and outer mean radius, while ψ can be calculated from the following formula: s, while ψ can be calculated from the following formula:

$$\psi = f(1 + \sin \beta_{2B}) \left(\frac{r_{1m}}{r_{2m}}\right) \tag{2.15}$$

where f is chosen between 1.0 and 1.2. The Pfleiderer correction thus gives a simple way to calculate the reduced head due to slip, but the two methods give slightly different results, as we shall see later.

2.1.5 Impeller outlet velocities

To accurately calculate the outlet velocities from the impeller, it is important to obtain as thorough information about the flow as possible. This includes slip, blade profile, trailing edge profile, and of course the main parameters such as flow, head, rotational speed and so on. To calculate the velocity triangle at the outlet, the preceding knowledge is used combined with geometry. The meridional component of the absolute velocity c_{m2} is calculated with Equation (2.3), while the peripheral component c_{u2} can be found from geometry in Figure 2.5:

$$c_{u2} = \gamma u_2 - \frac{c_{m2}}{\tan \beta_{2B}} \tag{2.16}$$

These values represent the velocities at the mean streamlines. They can also be calculated at the inner and outer streamlines, which is recommended in detailed design.

2.1.6 Diffuser inlet velocities

At the outlet of the impeller, the fluid has an angular momentum of $\rho Q c_{u2} r_2$. Between the impeller and the diffuser the fluid is not affected by any external forces, and following Newton's law of inertia the angular momentum must be conserved.

As both the density and the volume flow is constant, we can tell that the motion of the fluid can be described by the following expression:

$$c_u \times r = c_{u2} \times r_2 = \text{constant} \tag{2.17}$$

In order to calculate the approach angle before the diffuser inlet, Equation (2.17) may be rewritten as:

$$c_{u3} = c_{u2} \frac{d_2}{d_3} \tag{2.18}$$

which together with Equation (2.19)

$$c_{m3} = \frac{Q}{\pi d_3 b_3} \tag{2.19}$$

may be used to calculate the approach angle of the flow:

$$\tan \alpha_3 = \frac{c_{m3}}{c_{u3}} = \frac{Q}{\pi b_3 d_2 c_{u2}} \tag{2.20}$$

From Equation (2.20) it may be seen that the approach angle of the flow at the inlet of the diffuser does not depend on the diameter of the diffuser inlet d_3, but the parameters at the outlet of the impeller have a major impact.

By multiplying c_{m3} with the blade blockage factor τ, the velocity immediately after the diffuser inlet may be calculated, as well as the flow angle [12].

$$c_{m3}{}' = \frac{Q\tau_3}{\pi d_3 b_3} \tag{2.21}$$

$$\tan \alpha_3 = \frac{c_{m3}{}'}{c_{u3}} = \frac{Q\tau_3}{\pi b_3 d_2 c_{u2}} \tag{2.22}$$

The blade blockage factor can be calculated by:

$$\tau_3 = \frac{1}{1 - \frac{z_{Le} e_3}{\pi d_3 \sin \alpha_{3B}}} \tag{2.23}$$

where z_{Le} is the number of diffuser vanes, e_3 is the diffuser inlet vane thickness and α_{3B} is the vane angle at the inlet of the diffuser.

The velocity in the diffuser inlet throat may also easily be calculated for a diffuser with known throat dimensions with the following formula:
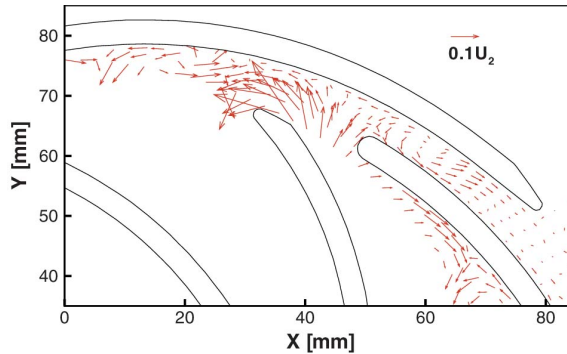
Figure 2.6: Flow variations at impeller trailing edge [8]

$$c_{q3} = \frac{Q}{z_{Le}a_3 b_3} \tag{2.24}$$

where a_3 and b_3 are the throat width and height, respectively.

2.1.7 Impeller-diffuser interaction

In rotating machinery there will always be some interaction between the rotating and the stationary part. In a centrifugal pump the gap between the impeller and the diffuser is usually small due to size limitations, and therefore the interaction between those parts will be significant. Feng, Benra and Domen [8] investigated this phenomena both by CFD simulations and by LDV measurements. They investigated the outer region of the impeller and the diffuser, and discovered that the impeller trailing edge to a large extent affects the flow in the diffuser.

Because of the differential pressure between the pressure and suction side of the impeller blade, the absolute flow angle α varies by more than 35 degrees each time the blade passes, for a pump with a specific speed of $n_q = 22.6$ and with a gap between the impeller and diffuser of 3% of the impeller radius. This creates an unsteadiness in the flow in the diffuser inlet which is significant also after the diffuser inlet throat. The suction side of the diffuser is more exposed to this unsteadiness than the pressure side.

Vector plots from the LDV measurements are also presented, showing the periodic variations of the velocity. They show that the variations are very strong in the triangular area before the diffuser throat, and the flow here is very dependent on the impeller blade position. The flow velocity changes by blade position also after the diffuser inlet throat, but the variations decrease very fast in the rear end of the diffuser. An illustration of this can be seen in Figure 2.6. Note that this is not a plot of the absolute velocities, but only the periodic variations of it.
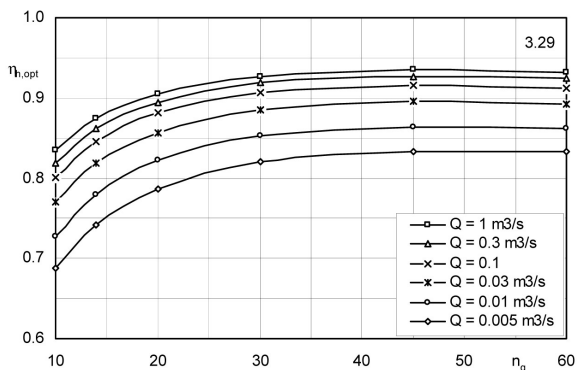
Figure 2.7: Hydraulic efficiency of multistage, single entry, radial pumps [12]

At part load, decreasing the flow rate from Q_{opt} to $0.5Q_{opt}$ increased the unsteadiness significantly before the diffuser inlet throat, while it is actually lower after the diffuser outlet throat.

2.2   Efficiency and losses

Losses will always arise in rotating machinery, causing the useful power to be lower than the power applied to the pump shaft. The theoretical study of efficiency and losses is difficult with uncertainties of $\pm 20 - 30\%$ [12, p. 83].

The losses which affect the delivered head are mainly the hydraulic losses [21, p. 36]. In addition, the volumetric losses indirectly affect the delivered head, by reducing the delivered volume flow. The other losses, such as mechanical, disk friction, axial thrust friction losses and other more or less significant losses do not affect the delivered head. They do, however, affect the power needed to drive the pump, and such the overall efficiency.

2.2.1   Hydraulic losses

The hydraulic efficiency is a result of the hydraulic losses in the casing, impellers and diffuser, and reduces the useful head to $H = \eta_h H_{th}$ [12, p. 107].

The hydraulic losses are generated by skin friction and vortex dissipation in all parts of the pump, but especially where the flow is disturbed by leading edges, curves or other irregularities. The losses are very difficult to calculate analytically, and therefore statistical data have been used to estimate a realistically achievable hydraulic efficiency.

The pump characteristics are of course of great importance, and different relations

exist for different pumps. In multistage pumps there will be additional losses in the return channels between each stage. In Figure 2.7 the measured hydraulic efficiencies of multistage pumps are plotted. These statistical data can be approximated by the following equation [12, p. 142]:

$$\eta_{h,opt} = 1 - 0.065\left(\frac{Q_{ref}}{Q}\right)^m - 0.23\left\{0.3 - \log\frac{n_q}{23}\right\}^2 \left(\frac{Q_{ref}}{Q}\right)^{0.05} \tag{2.25}$$

In this equation the calculated $\eta_{h,opt}$ is the achievable hydraulic efficiency at BEP. The reference volume flow, Q_{ref}, is always set as $Q_{ref} = 1m^3/s$, and the factor m is calculated by Equation (2.26).

$$m = 0.08a\left(\frac{Q_{ref}}{Q}\right)^{0.15}\left(\frac{45}{n_q}\right)^{0.06} \qquad a = \begin{cases} 1 & \text{if } Q \le 1m^3/s \\ 0.5 & \text{if } Q > 1m^3/s \end{cases} \tag{2.26}$$

2.2.2 Volumetric losses

The volumetric losses, or leakage losses, in a pump take place between the stationary and the rotary parts of the pump. They reduce the available capacity at the pump discharge compared to the volume passed through the impeller [21]. The leakage loss is difficult to approximate without having detailed information about the pump, and even then it is difficult to obtain accurate estimates. Across a gap, the leakage loss can be calculated by

$$h_L = f\frac{L}{d}\frac{v^2}{2g} \tag{2.27}$$

where h_L is the pressure difference across the gap, f is a friction coefficient, L is the length of the gap, d is the hydraulic diameter and v is the velocity of the leakage water [21]. This results in the leakage being proportional to $\sqrt{h_L}$, which gives a higher leakage flow for higher heads. This can be seen illustrated in Figure 2.8.

The leakage loss will not reduce the head of the pump itself, but it will drain some of the high-energy flow delivered by the impeller. Indirectly this will cause a reduced head for the delivered flow. The volumetric losses which mainly contribute to the reduced head in a multistage centrifugal pump are the losses through the annular seal at the impeller inlet Q_{sp} and the axial thrust balancing losses Q_E. In total, the hydraulic efficiency can be expressed as [12]:

$$\eta_v = \frac{Q}{Q_{La}} = \frac{Q}{Q + Q_{sp} + Q_E} \tag{2.28}$$

In the above equation Q_{La} is the volume flow which is passed through the impeller, and Q is the flow actually delivered by the pump. Gülich also presents simplified
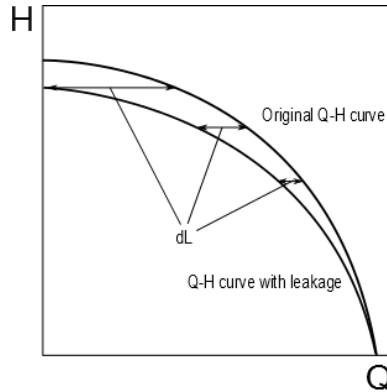
Figure 2.8: The effect of leakage on a head-capacity curve

approximations to the leakage flow, based on pumps designed according to the recommendations by the American Petroleum Institute (API).

$$\frac{Q_{sp}}{Q_{opt}} = \frac{Q_E}{Q_{opt}} = \frac{4.1}{n_q^{1.6}} \tag{2.29}$$

As a consequence of the increased leakage for increased head, as shown in Figure 2.8, it is clear that the volumetric efficiency is not constant for all volume flows. For high heads, most of the volume flow is recirculated through the leakages, while at low heads the leakages may be negligible [18]. Taking this into account, the relation in Equation (2.29) and the common approximation of the leakage losses as being in the order of $1 - 2\%$ of the total flow [1, 14, 22] must be information which is only valid at BEP. For other operational points than BEP, the leakage losses can be calculated by the relation $Q_L \propto \sqrt{H}$. This makes it possible to estimate the volumetric losses by the following relation where the constant K_v is the only unknown:

$$Q_L = K_v \sqrt{H} \tag{2.30}$$

Using BEP as a reference, K_v can be calculated and used to find the leakage Q_L for all operational points of the pump. This gives a total volume flow passed through the impeller as

$$Q_{La} = Q + Q_L \tag{2.31}$$

2.3 Head-capacity curves

The characteristic curves of a pump describe the relation between volume flow and different properties such as efficiency, power consumption and head. The latter is called a head-capacity curve including head H and volume flow Q, taking into account slip, pre-rotation, hydraulic losses and volume flow losses. The shape of the curve is an important parameter for the pump behaviour. For most pump applications, stable operation requires a Q-H curve which is constantly decreasing with increasing volume flow giving maximum head at zero flow. This is called a stable characteristic, in contrast to a curve with sections of increasing head [12]. Examples of stable and unstable characteristics can be seen in Figure 2.9.

(a) Stable characteristics   (b) Unstable characteristics
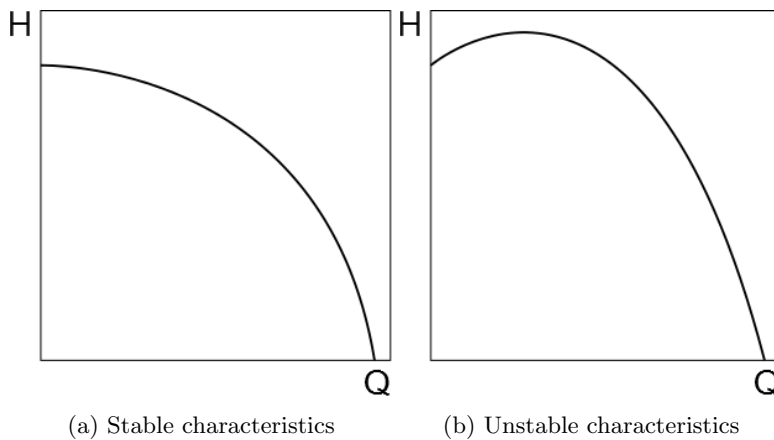
Figure 2.9: Examples of characteristic curves

Creating accurate Q-H curves is difficult, and different approaches exist. The traditional way is described well by Łazarkiewicz and Troskolański in *Impeller Pumps* and gives quite simple relations between head, flow, slip and losses. Gülich, however, uses a somewhat different approach providing more advanced physical relations for calculating the losses, making the creation of the Q-H curves a more complex study. He also presents empirical data which can be used to approximate the Q-H curve for a certain pump. In the following subsection the process of calculating the head-capacity curves will be presented. All three approaches will be presented, and they will later during this work be compared through testing to find which is better.

2.3.1 Creating head-capacity curves

The first step in creating the Q-H curves of a pump is using Euler's equation in its reduced form (2.8). This gives the theoretical head of a pump with infinitely many

blades and no inlet rotation or losses. This can be related to the volume flow in
the following way, using notation for flow with no slip [4]:

$$H_{th\infty} = \frac{u_2 c_{u2\infty}}{g}$$

(2.32)

The term $c_{u2\infty}$ can be rewritten using geometrical relations from figures 2.2 and 2.5:

$$c_{u2\infty} = u_2 - \frac{c_{m2}}{\tan\beta_{2B}}$$

(2.33)

We also know from subsection 2.1.1 that the meridional component of the absolute
velocity c_{m2} is proportional to the volume flow:

$$c_{m2} = \frac{Q_{La}}{A_2} = \frac{Q_{La}}{\pi d_2 b_2}$$

(2.34)

Combining the equations (2.32), (2.33) and (2.34) gives us the following relation
between theoretical head and volume flow with no slip:

$$H_{th\infty} = \frac{u_2}{g}\left(u_2 - \frac{Q_{La}}{\pi d_2 b_2 \tan\beta_{2B}}\right)$$

(2.35)

As all the factors in this relation except the volume flow are constants for a specific
pump, it can be rewritten as $H_{th\infty} = K_1 - K_2 Q_{La}$ in which K_1 and K_2 are positive
constants for $\beta_{2B} < 90°$. As we can see, the theoretical head is linearly dependent
of the volume flow.

The next step is to include slip into the calculations, and here the differences
between the traditional approach and the approach described by Gülich start.

2.3.2   Traditional method

Including slip into these calculations will give a lower head than $H_{th\infty}$. Pfleiderer
introduces a correction factor, described in section 2.1.4, giving a head H_{th} cor-
rected by C_p. Assuming this correction factor as constant and combining it with
Equation (2.35), the theoretical head including slip can be expressed as:

$$H_{th} = \frac{H_{th\infty}}{1 + C_p} = \frac{1}{1 + C_p}\left(\frac{u_2}{g}\left(u_2 - \frac{Q_{La}}{\pi d_2 b_2 \tan\beta_{2B}}\right)\right)$$

(2.36)

For simplicity, this can also be rewritten as $H_{th} = \frac{1}{1+C_p}(K_1 - K_2 Q_{La})$, giving a
head-capacity curve as seen in Figure 2.10.
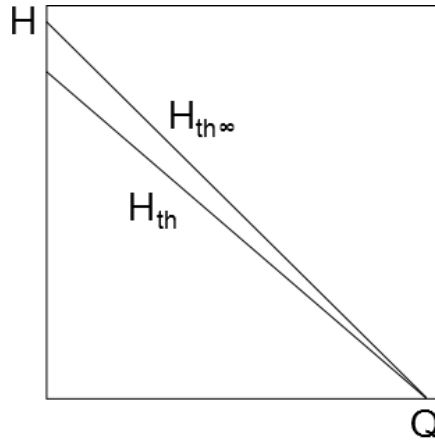
Figure 2.10: Theoretical head with and without slip

After the head curves including slip have been calculated, the losses have to be included. There are two main hydraulic losses, the friction losses and the vortex dissipation (including shock) losses. In addition, the volumetric losses should be included into the calculations, as they will affect the Q-H curves by reducing the delivered volume flow [6].

Stepanoff [21], Brekke [5] and Łazarkiewicz and Troskolański [2] present a calculation of the hydraulic losses where the friction and vortex dissipation losses are calculated separately in the following manner:

$$\text{Friction losses:} \qquad h_f = K_f Q_{La}^2 \qquad (2.37)$$
$$\text{Vortex dissipation losses:} \qquad h_s = K_s(Q_{La} - Q_{La,opt})^2 \qquad (2.38)$$

We now have the following relation:

$$
\begin{aligned}
H &= H_{th} - h_s - h_f \\
&= \frac{1}{1+C_p}\left(\frac{u_2}{g}\left(u_2 - \frac{Q_{La}}{\pi d_2 b_2 \tan\beta_{2B}}\right)\right) - K_s(Q_{La} - Q_{La,opt})^2 - K_f Q_{La}^2
\end{aligned}
$$
$$(2.39)$$

Here K_f and K_s are constants which are different from pump to pump, and they may only be established by solving the actual Q-H curve for a pump [20, p. 176]. There have been several attempts to establish accurate estimates for the hydraulic losses, but none of them are very helpful [2].
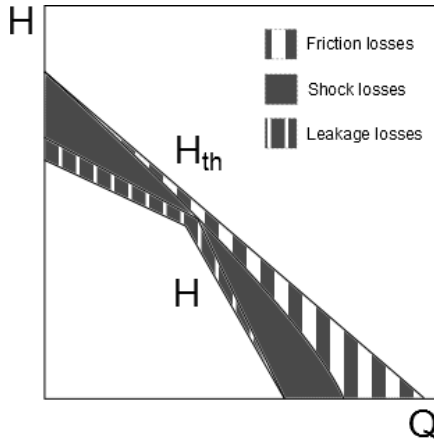
Figure 2.11: Total head including losses

If no established Q-H curve for a specific pump exists, one way to make an approximation of the losses is to assume that all the losses caused by shock at the inlet can be given by [6]:

$$h_s = \left| \frac{u_1 c_{u1}}{g} \right| \tag{2.40}$$

By assuming this, the only unknown will be K_f in Equation (2.37). After doing tests it is possible to analyse the results and calculate a reasonable K_f for the actual pump.

In total this gives the final head of the pump expressed by:

$$
\begin{aligned}
H &= H_{th} - h_s - h_f \\
&= \frac{1}{1 + C_p} \left(\frac{u_2}{g} \left(u_2 - \frac{Q_{La}}{\pi d_2 b_2 \tan \beta_{2B}} \right) \right) - \left| \frac{u_1 c_{u1}}{g} \right| - K_f Q_{La}^2
\end{aligned} \tag{2.41}
$$

in which K_f is the only term which has to be found experimentally. This will typically provide a head-capacity curve as seen in Figure 2.11. In reality, the total head curve will be a parabola, but the simplification of the shock losses h_s gives it a more linear shape.

2.3.3 Loss calculation method

This method is based on calculating the hydraulic losses in the impeller and diffuser, based on relations given by Gülich in *Centrifugal Pumps*. A detailed description
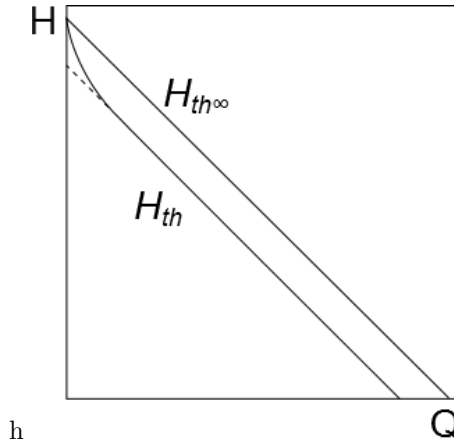
Figure 2.12: Theoretical head with and without slip

of calculation of the volumetric losses will not be covered, as extensive information about the clearances in the pump is needed, and it usually does not exceed $1 - 2\%$ of the total volume flow. Calculation of the leakages will therefore be based on the procedure described in subsection 2.2.2.

By taking slip from Equation (2.16) into account in the relation between theoretical head and volume flow (2.35) the following relation for theoretical head including slip is obtained:

$$H_{th} = \frac{u_2}{g} \left(\gamma u_2 - \frac{Q_{La}}{\pi d_2 b_2 \tan \beta_{2B}} \right) \tag{2.42}$$

Rewriting this equation gives the expression $H_{th} = \gamma K_1 - K_2 Q$ where γ is a factor between 0 and 1. This gives a lower theoretical head for all flows which can be seen in Figure 2.12. Close to Q=0 the slip factor is no longer constant due to recirculation, explaining why the curve is deflecting up towards $H_{th\infty}$ at the left side.

Gülich divides the hydraulic losses into two main parts, the losses in the impeller and the losses in the diffuser. The losses in the impeller are further divided into shock losses at impeller inlet and friction and mixing losses through the impeller. The diffuser losses consist of losses in the vaneless space between impeller and diffuser, losses in the diffuser, and losses in the return channels. The calculation of all these losses is complicated, but they can be found in tables A.1 and A.2 in the appendices.

In total, these calculations will provide head-capacity curves like the ones seen in Figure 2.13.
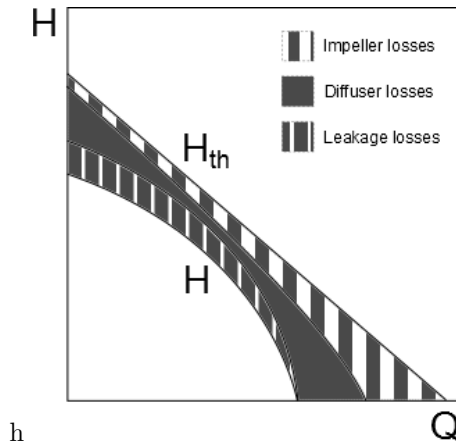
Figure 2.13: Total head including losses

2.3.4   Empirical method

In *Centrifugal Pumps* [12] an empirical method for predicting the characteristics of a pump is also presented. The data is based on several tested pumps, and may give an indication of how a new pump may perform. In order to calculated the predicted characteristic about the pump, the design volume flow Q_{opt}, the design head H_{opt} and the speed of rotation n is needed, as well as the dimensions of the pump. With this information and some statistical data, a prediction of the pump characteristics can be made.

First the achievable hydraulic efficiency $\eta_{h,opt}$ and the slip factor γ_{opt} has to be calculated from the previously described methods. Both the slip factor and the hydraulic efficiency depend on the flow rate, and the relations in figures 2.14 and 2.15 have been established by testing. As the figures show, the uncertainty rises at flow rates much lower and much higher than design flow, so this method should be used carefully at off-design conditions.

By using the flow rate ratio $q^* = Q/Q_{opt}$, the hydraulic efficiency can also be found from the following equation:
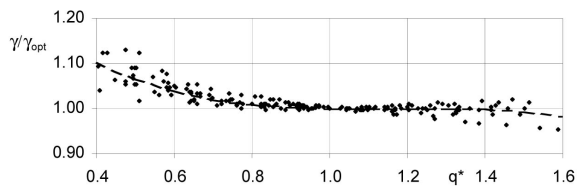
Figure 2.14: Variation of slip factor
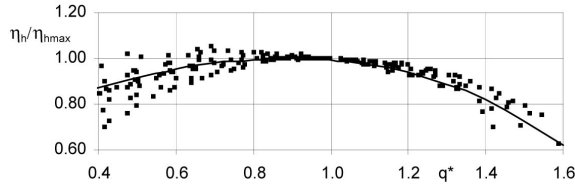
Figure 2.15: Variation of hydraulic efficiency

$$\frac{\eta_h}{\eta_{h,BEP}} = 1 - 0.6(q^* - 0.9)^2 - 0.25(q^* - 0.9)^3 \tag{2.43}$$

This equation will give a maximum efficiency at $q^* = 0.9$. Even though the shock losses may be smallest at Q_{opt}, the sum of the losses is usually smaller at a lower flow rate because of the increasing frictional losses.

By calculating γ and η_h for several flow rates from $Q = 0$ to $Q = Q_{max}$ and using them as input in Equation (2.44), the head may be calculated and plotted in a head-capacity diagram.

$$H = \frac{\eta_h u_2}{g} \left\{ \gamma u_2 - \frac{\tau_2 Q_{La}}{A_2 \tan \beta_{2B}} \right\} \tag{2.44}$$

In Equation (2.44), the volume flow Q_{La} is the total flow passing through the impeller, including the leakages. The inlet is assumed to be without swirl $\alpha_1 = 90°$, and τ_2 is the blade blockage factor which can be calculated from the following equation:

$$\tau_2 = \frac{1}{1 - \frac{z_{La} e_2}{\pi d_2 \sin \beta_{2B}}} \tag{2.45}$$

As described above, this method will only give predictions based on statistical data from other pumps. This means that the more a new pump differs from the ones in the statistics, the more the actual performance will deviate from the predictions.

2.4 Velocity measurements

Several techniques for measuring fluid velocity exist. The methods which have been considered here are mainly Pitot-static probe and Laser Doppler Velocimetry (LDV), and following is a short description of the principles upon which the two methods are based. The following is mainly based on the theory written by Håkon Hjort Francke [11] in his PhD thesis.

2.4.1   Pitot-static probe

The pitot-static probe is a very common device used for measuring the velocity of
a fluid. It uses sidewall holes to measure the static pressure in the flow and a hole
in the front to measure the stagnation pressure [24]. Bernoulli's equation describes
the relation between static pressure and velocity along a frictionless streamline:

$$p + \frac{1}{2}\rho c^2 + \rho g z = \text{constant} \tag{2.46}$$
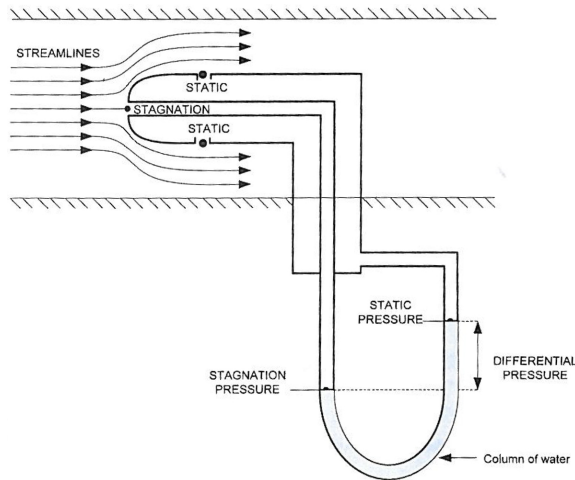
Figure 2.16: Principle of pitot-static probes [11]

The differential pressure between the two measurements can then be used to cal-
culate the absolute velocity c at this point.

$$\Delta p = (p_{stagnation}) - (p_{static}) = (p_{static} + \frac{1}{2}\rho c^2) - (p_{static}) \tag{2.47}$$

Which, when rearranged, gives an expression for the absolute velocity at a point:

$$c = \sqrt{\frac{2\Delta p}{\rho}} \tag{2.48}$$

The relation is valid only when the velocity at the points where the static pres-
sure is measured is orthogonal to the measurements. This introduces the need for
calibration of a knife pitot, as the holes for measuring the static pressure are not
orthogonal to the flow. The knife pitot is commonly used when the angle of the
flow is to be measured, as it is more sensitive to angular variations.
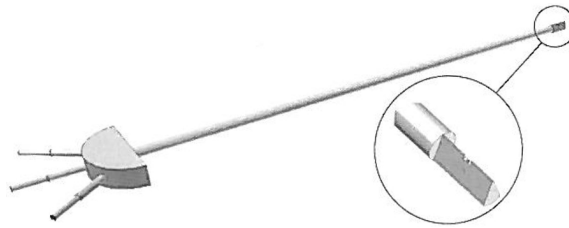
Figure 2.17: Knife pitot tube [11]

The main advantage of the pitot-static probe is the simplicity of the setup, as well as the simplicity of the physics. The disadvantages are that it needs to be aligned with the flow direction, which may be difficult to achieve, and that it is an intrusive method which will disturb the flow [24].

2.4.2 Laser Doppler Velocimetry

LDV is a non-intrusive method to calculate the velocity of particles in a fluid based on laser light. The most used system today is a dual-beam laser where a laser beam is split into two beams, and one of the beams is given a frequency shift [23]. The two beams are focused on the point of interest, and the scattered light at the intersection is registered through the receiving optics into a detector. A signal processor then calculates the velocity of the fluid based on the frequency of the light and the distance of the interference pattern at the intersection.

The main advantages of LDV is that it is very accurate, non intrusive and does not need calibration. Nevertheless it is an expensive and complex set-up which is both less common and more time consuming than the pitot-static probe.
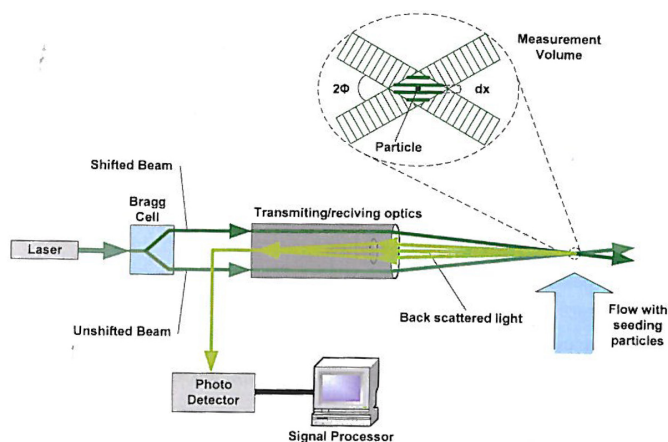
Figure 2.18: Principle of LDV [11]

Chapter 3

Design program in Matlab

This chapter describes the work and calculations performed in Matlab. A pump design program has been modified to give velocity triangles for a specific pump, and several analytic approaches to approximate pump characteristics have been tested.

3.1 Background

The pump design program has its origin from a Master's thesis written in 2007 by Jón Bergmann Heimisson [13] where the program was developed as a tool to help a pump designer to create a basic design of a centrifugal pump. During my project thesis, the program was significantly changed in order to simulate an existing pump geometry and to give necessary information regarding inlet conditions to the diffuser. The calculations of slip and velocity triangles were also changed, basing most of the calculations on the approaches given by Johann Friedrich Gülich [12]. A detailed description of this work can be found in the author's project thesis [10].

The purpose of the work performed in Matlab in this thesis has been to calculate the velocity triangles at the outlet of the impeller and at the inlet of the diffuser, as well as approximating the characteristics of a specific pump based on a known geometry. The velocity profiles will be important input to CFD simulations which are to be performed by PhD candidate Alessandro Nocente, while the pump characteristics can be used to verify the proposed design done in Matlab.

3.2 Introduction

As mentioned in the section above, the Matlab-program was originally made to provide a suggested pump design for a specific application. For this thesis the

program has been changed to be able to take input of the dimensions of a specific pump, rather than the operating conditions. Most of this work was performed in the author's project thesis [10], but further changes have also been made.

The program is written in MATLAB and gives a graphical user interface (GUI) in which the user can handle all the input values. The program is started by running the file *pump.m* in MATLAB which will run the *Main menu* and the *Main dimensions* figures. This is where most of the design parameters for the pump is handled, and a graphical presentation of the impeller, the inlet- and outlet velocities and the pump characteristics is presented, as seen in Figure 3.1.
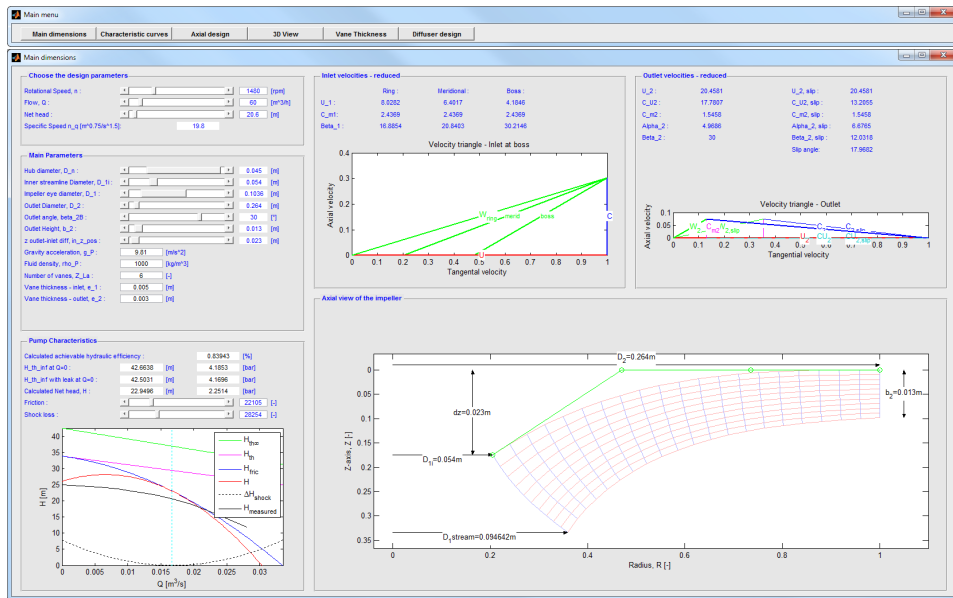
Figure 3.1: The main menu and main dimensions window

After running *Main dimensions*, the next window is the *Characteristic curves* in which the different approaches of calculating the pump characteristics have been tested. Then follows the *Axial design*, *3D View*, *Vane thickness* and finally the *Diffuser design*-window where the inlet velocities to the diffuser are given.

3.3 Velocity triangles

The calculations of the velocity triangles are based on the previously outlined theory where zero rotation at the inlet is assumed and where the slip factor γ is calculated according to section 2.1.

The necessary input parameters are:

- Rotational speed n
- Volume flow Q
- Impeller eye diameter d_1
- Impeller outlet diameter d_2
- Impeller outlet height b_2
- Impeller outlet angle β_{2B}
- Number of impeller blades z_{La}

- Blade thickness at outlet e_2
- Diffuser inlet diameter d_3
- Diffuser inlet height b_3
- Diffuser vane angle at inlet α_{3B}
- Number of diffuser vanes z_{Le}
- Diffuser vane thickness at inlet e_3

In total, these provide the information necessary to calculate the theoretical velocities at the outlet of the impeller and at the inlet of the diffuser. The results are presented both graphically and numerically, as shown in figures 3.2a and 3.2b.
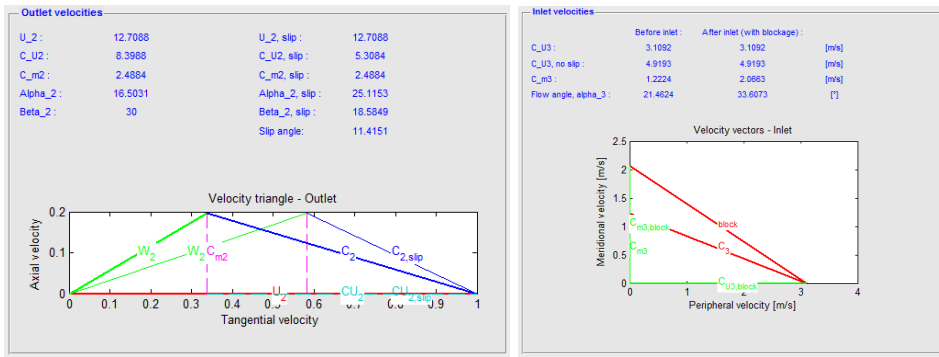
(a) Impeller outlet velocities

(b) Diffuser inlet velocities

Figure 3.2: Presentation of fluid velocities in a pump

Figure 3.2a shows a presentation of the outlet velocities from the impeller both with and without slip. The inlet velocities to the diffuser are presented in Figure 3.2b. These are presented both with and without the slip calculations from the impeller and both before and after the diffuser inlet.

3.4   Pump characteristics

One of the major drawbacks of the pump design program in the earlier version was the calculation of the characteristic curves. The pump characteristics needed a friction factor and a shock factor which had to be found experimentally, taking away the aspect of predicting the characteristic curves of a pump design in advance. This introduced the need for experimentation to find the most suitable calculation procedure for the characteristic curves.

3.4.1 Test setup

In the literature several different methods for estimating the characteristic curves of a pump can be found. A more detailed description of these can be found in section 2.3 about head-capacity curves. Four different methods were chosen to be used for further testing. Two of these are based on the approach described by Stepanoff [21], Brekke [5] and Łazarkiewicz and Troskolański [2], one is based on a more detailed loss calculation described by Gülich [12] requiring a lot more input about the pump dimensions, and one is based on empirical data for similar pumps, also described by Gülich.

In order to find which method is most suitable, the calculations were to be compared with the characteristics of the pump delivered by Standart Pompa to Typhonix for their research regarding produced water treatment. A new window was created in Matlab to be used for testing of different calculations of the characteristic curves. The four different calculation models were placed side by side, and compared to the measured head-capacity curve from Standart. This can be seen in Figure 3.3.
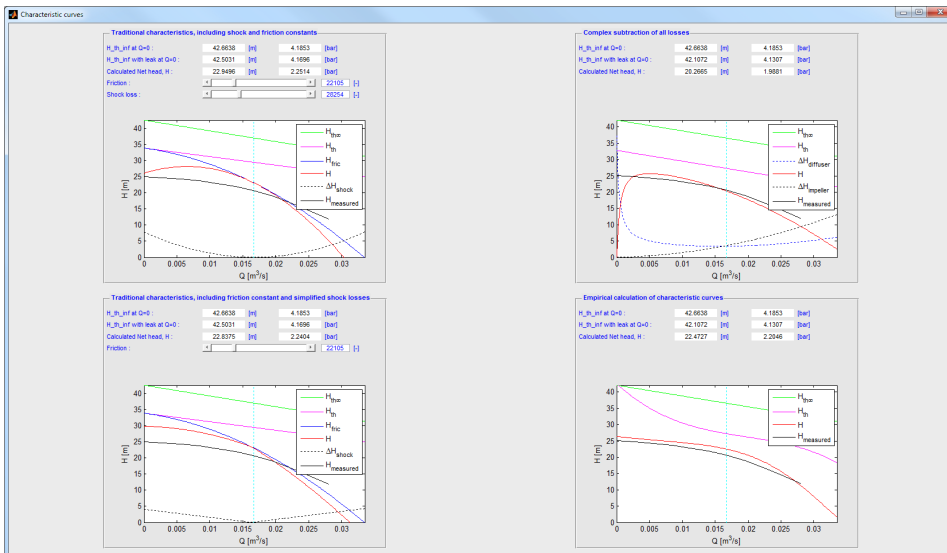
Figure 3.3: Test setup for calculation of characteristics

3.4.2 Input parameters

The four different calculation models require very different input parameters. All of the models need basic information about the impeller regarding rotational speed, volume flow, outlet area, diameters and blade angle. In addition, the most detailed calculations also need input about for example roughness, blade length, viscosity, diffuser dimensions and return channel design. More about the calculations can be

found in section 2.3. Most of the input have been obtained from the lab personnel in Typhonix, some of them from drawings of the pump and the diffuser, and for some of the values it has been necessary to make estimates.

Listed in the table below are all the input parameters which have been used in the calculations. All the information is taken from the pump which has been tested, unless other is noted.

Parameter	Value	Parameter	Value
Rotational speed:	1480 rpm	Volume flow:	60 m^3/h
Net head:	20.6 m	Hub diameter:	0.045 m
Impeller outlet diameter:	0.264 m	Impeller eye diameter:	0.1036 m
Inner streamline diameter:	0.054 m	Impeller outlet blade angle:	30°
Impeller outlet height:	0.013 m	Gravity:	9.81 m/s^2
Distance between blades, inlet:	0.018 m^a	Distance between blades, outlet:	0.04 m^b
Channel height, inlet:	0.0324m	Impeller blade length:	0.14 m^c
Fluid density:	1000 kg/m^3	Impeller blades:	6
Blade thickness, inlet:	0.005 m	Blade thickness, outlet:	0.003 m
Diffuser inlet diameter:	0.270 m	Diffuser inlet height:	0.0155 m
Diffuser outlet diameter:	0.468 m	Diffuser outlet height:	0.0208 m
Diffuser inlet vane angle:	8°	Diffuser vanes:	10
Distance between vanes, inlet:	0.0127 m	Distance between vanes, outlet:	0.0276 m
Vane thickness at inlet:	0.0093 m	Volumetric efficiency:	2%^{d}
Water temperature:	50°C	Absolute roughness:	0.0005 m^e

[a]Estimate based on pictures from Typhonix
[b]Estimate based on pictures from Typhonix
[c]Estimate based on pictures from Typhonix
[d]Estimate based on available literature [1, 14, 22]
[e]Absolute roughness of moderately corroded carbon steel [17]

Table 3.1: Input parameters

Chapter 4

Experimental work

This chapter describes all the experimental work that has been performed through this thesis. Three different rigs have been used for the measurements. Two of these have been used for calibration purposes at the Waterpower Laboratory, while the pump measurements were performed in Typhonix' laboratory in Varhaug. Originally it was planned to do the pump measurements at the Waterpower Laboratory, but due to time limitations and other practicalities the measurements were performed in Varhaug. This resulted in difficulties in measuring the pump characteristics, and the measurements from Standart laboratories in Istanbul were used for this purpose.

The measurement methods which were considered were using a pitot-static probe or LDV measurements. After discussions with prof. James Dawson and PhD Håkon H. Francke, the conclusion was to use a pitot-static probe which Francke used in his PhD thesis [11]. The decision was based on the simplicity of the pitot-static probe and the availability of the equipment, especially as the measurements were to be performed in several locations. The pitot-static probe is an intrusive measurement method, but after discussions with Francke and prof. Torbjørn Nielsen it was considered to be able to provide good results for this application.

4.1 Swirl rigg calibration

As mentioned in section 2.4, the use of a knife pitot introduces the need for calibration. The calibration was performed according to the three-quarters radius method, described in Kjølle [15, p. 63], where a circular pipe with a known volume flow is the necessary rig setup. At the Waterpower Laboratory, a swirl rigg built as a part of the work by Francke [11] for research regarding injection of water in the draft tube of a francis turbine exist, and is suitable for the purpose. The rig has later been used also by Skodje [19].

4.1.1 Rig description

A centrifugal pump delivers water to the rig where it can be distributed into three different pipes. All three pipes have valves and flow meters, but in the calibration of the pitot only the main pipe was used. A schematic of the rig can be seen in Figure 4.1.
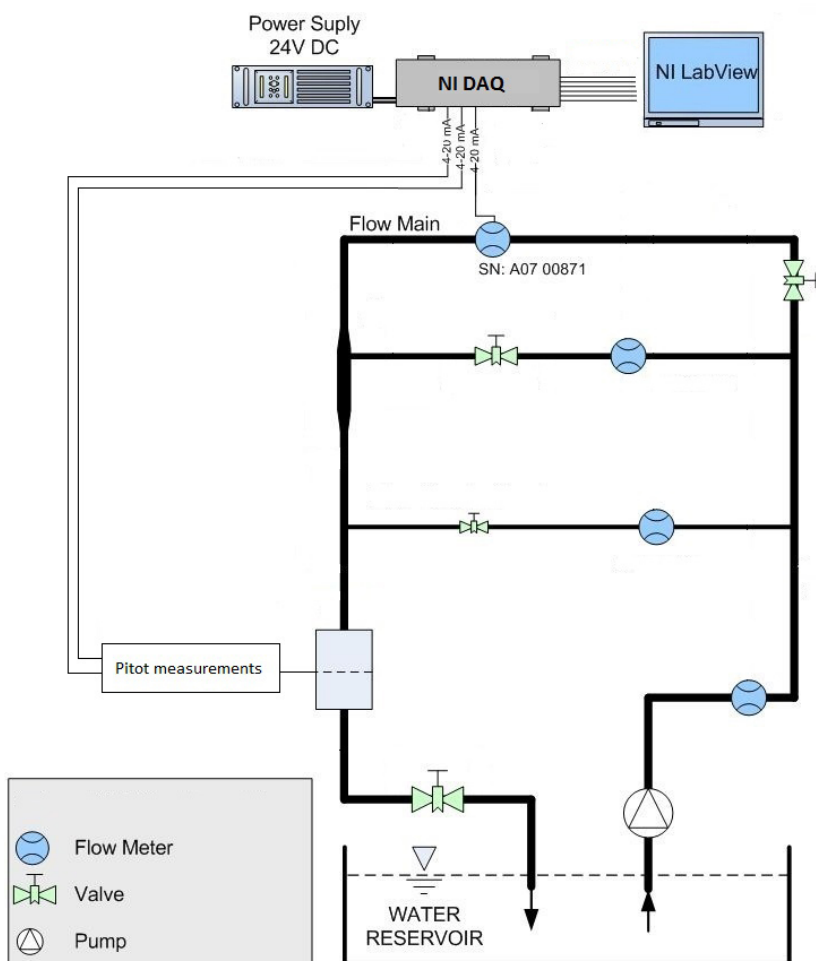
Figure 4.1: Schematic of swirl rig, modified from [19]

4.1.2 Measurement setup

The setup used in the swirl rigg calibration consisted of the flow meter on the main pipe, the knife pitot with two differential pressure transmitters, a DAQ-card for data acquisition and a computer for logging. The centrifugal pump was controlled from the control room, while the valves and the measuring equipment were controlled from the rig.

Data acquisition

For the data acquisition, a DAQ-card from National Instruments was used and registered in LabView on a computer. The DAQ-card uses a 0-10 volt range, and converts the current from the measuring equipment to a voltage through a 500 ohm resistance. The program in LabView registers the voltage, and calculates the desired parameters. The front panel of the calibration program in LabView can be found in Appendix B.1.

Flow measurements

The volume flow was measured using the flow meter on the main pipe on top of the rig. The flow meter was of the type Krohne Optiflux 2300C, using the electromagnetic principle. This was connected to the DAQ and registered in LabView. The calibration of the flow meter was perfomed by Skodje [19]. As the calibrations were done by logging the flow versus a mA signal, the voltage signal from the DAQ had to be converted to a mA signal before calculating the pressure. The calibration gives a calibration formula on the form $dp = aX + b$ where a and be can be found from Table 4.1.

Name	Serial number	a	b	Max error %
Optiflux 2300C	A07 00871	6.187273	-0.025382	0.189443

Table 4.1: Calibration results for flow meter on swirl rig [19]

Pitot measurements

The pitot measurements were performed using a knife pitot from United Sensors. The knife pitot has three holes for pressure measurements, one for stagnation pressure in the front P2, an two on the sides P1 and P3. The technical data for the pitot tube are presented in Appendix C.Two differential pressure transmitters were connected to the pitot to measure the pressure difference between P1-2 and P3-2. The differential pressure transmitters were of the type Fuji FCX, and the calibration of these were performed by Skodje [19].
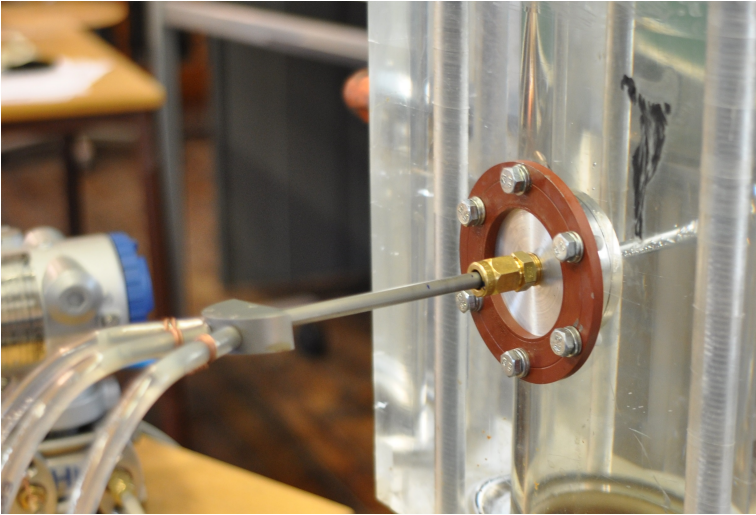
Figure 4.2: Introduction of pitot probe through hull fitting

Name	Serial number	a	b	Max error %
Fuji FCX	9602 N 0004 CK1	157.112975	-0.628592	1.145053
Fuji FCX	A5A5304F	81.391035	-0.319467	0.162098

Table 4.2: Calibration results for differential pressure transmitters [19]

The pitot probe was introduced to the flow through a hull fitting in the measurement section, making it possible to adjust both the angle and the radial position of the pitot. This can be seen in Figure 4.2.

4.1.3 Execution of measurements

The pitot calibration was performed by running the pump at a constant rotational speed, adjusting the volume flow with the back pressure valve. An attempt was made to run the pump at 1300 rpm, but as it gave serious cavitation at full opening of the valve, the maximum rotational speed possible was 1150 rpm. This gave a maximum calibration velocity of approximately 5 m/s, significantly lower than the desired 20 m/s which was assumed to be the maximum velocity in Typhonix' multistage pump .

21 measurements were performed at different velocities, providing a linear relation between the average differential pressures between P1-2 and P3-2. The measurements were performed when the difference between the two differential pressures were at ± 0.005 bar, as this was considered as giving satisfying accuracy.

It was observed that at back pressure valve openings from 65-100%, the volume flow

was nearly constant, giving an overweight of measurements in the upper velocity region. Vibration of the pitot was also observed at the largest flow rates, increasing the uncertainty of the measurements.

The different difficulties experienced during the calibration in the swirl rig made the results uncertain. After discussions with prof. Torbjørn Nielsen and PhD-candidate Bjørn Solemslie, it was decided to do a re-calibration in the pelton rig after the pump measurements had been carried out.

The results from the pitot calibration can be found in Appendix E.

4.2 Pump measurements

After the calibration of the pitot-static probe had been carried out, testing the outlet velocities on Typhonix' multistage pump was to be carried out. The laboratory facilities of Typhonix are located at Varhaug in Rogaland. The measurements that were planned to be carried out were velocity measurements in three positions at the inlet of the diffuser, see Figure 4.3.
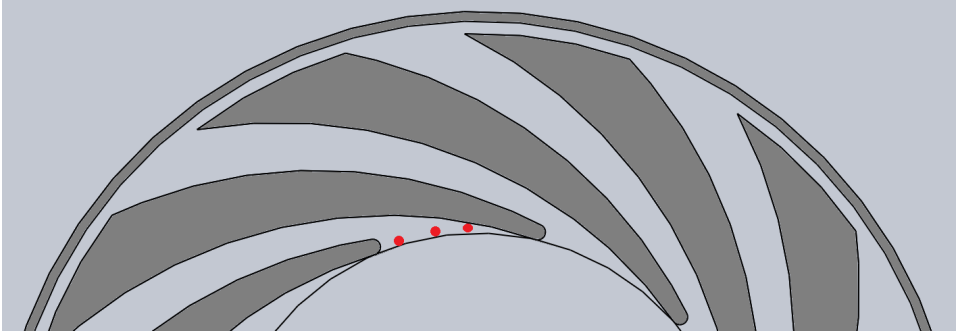
Figure 4.3: The planned measurement points

4.2.1 Rig description

The rig in the laboratory of Typhonix is very complex, as it is equipped to be able to run with different inlet pressures and also with seeding possibilities of oil and minerals. For the measurements in this thesis, the necessary components were only a volume flow meter upstream the pump and a back pressure valve downstream the pump to control the volume flow through the pump. The pump with inlet on the right and outlet on the top can be seen in Figure 4.4.
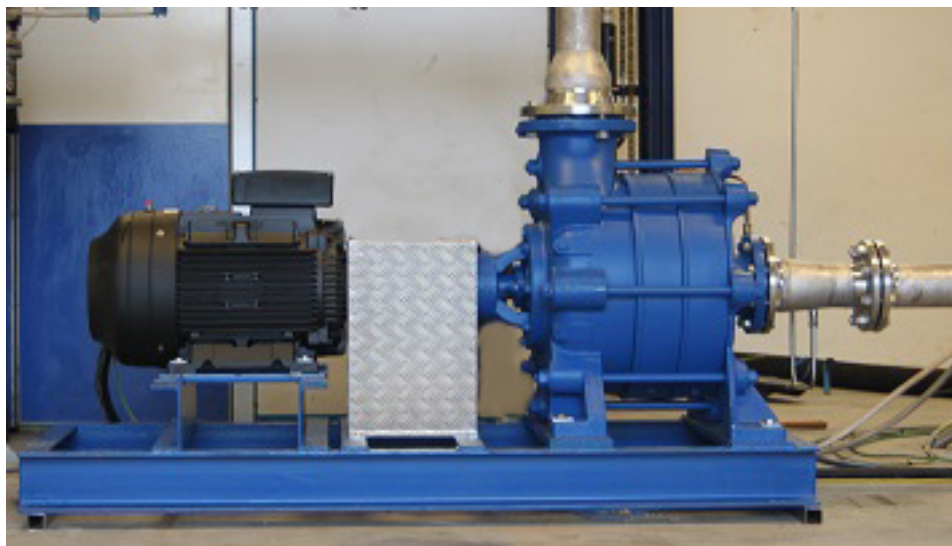
Figure 4.4: Pump setup at Varhaug

4.2.2   Measurement points

After discussing the placement of the measurements with the personnel at Ty-
phonix, some changes had to be made. This was due to size limitations regarding
the hull fittings which were to be placed on the outside of the pump, and after
discussions with Nocente and personnel at Typhonix, the new measurement points
can be seen in Figure 4.5. Measurement number 1 and 2 were to establish a velocity
distribution at the inlet of the diffuser, number 3 was to measure the velocity in
the diffuser throat and number 4 was established on request from Typhonix.
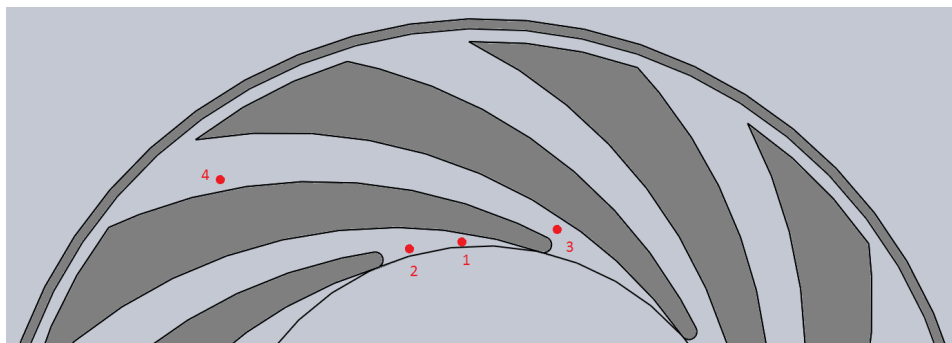
Figure 4.5: The new measurement points

Accurate positioning of the holes in the diffuser proved to be difficult. Fortunately,
a part of the diffuser was possible to dismount, revealing the internal channels,

see figures 4.6 and 4.7. The dismounted ring had clear prints from the diffuser channels, making it possible to position holes 1, 2 and 3 accurate.

Figure 4.6: Internal channels of the diffuser

Figure 4.7: Diffuser ring with holes 1, 2 and 3

Hole number 4 had to be positioned based on an estimate of where the diffuser channel would be in the outer region, as accurate measurements proved to be difficult. This resulted in a position close to the side wall of the channel, as shown in Figure 4.5.

It was also chosen to position hole 3 and 4 in another diffuser channel than hole 1 and 2. This was done to avoid any possible disturbances caused by hole 1 and 2 on measuring in hole number 3.

4.2.3   Measurement setup

The setup used in the pump measurements consisted of a flow meter upstream the pump, the knife pitot with two differential pressure transmitters, a DAQ-card for data acquisition and a computer for logging. The centrifugal pump was controlled from a computer close to the rig where it was possible to adjust the rotational speed of the pump. The back pressure valve was manually controlled, and was placed shortly downstream the centrifugal pump.

Data acquisition

For the data acquisition, the same setup as described in 4.1.2 was used. The only changes were to the LabView program, as several parameters had to be registered manually. The front panel of the LabView program can be seen in Appendix B.2.

Flow measurements

The volume flow was read from a magnetic flow meter of the type Rosemount 8705 Magnetic flow meter. This was manually read and registered in LabView for each operational point.

Rotational speed

The engine driving the centrifugal pump was of the type Busck IE2 and was frequency controlled. It was run from the computer, where the frequency could be set. The measurements were performed at different rotational speeds, and the frequency was manually registered in LabView for each measurement.

Pitot measurements

The pitot measurements were performed using the same pitot setup as described in 4.1.2. In addition, a disk showing the angle of the pitot was used. Lines were drawn on the pump radially outwards from the center and used as references when reading the angle. The angle was then registered in LabView.

The pitot penetrated the pump casing through a hull fitting, and entered the diffuser through a hole in the diffuser ring. The measured differential pressure was registered in LabView and recalculated to velocities using the calibration constants from the calibration in the swirl rig. The pitot measurement setup can be seen in Figure 4.8 where all the holes in pump casing are visible.
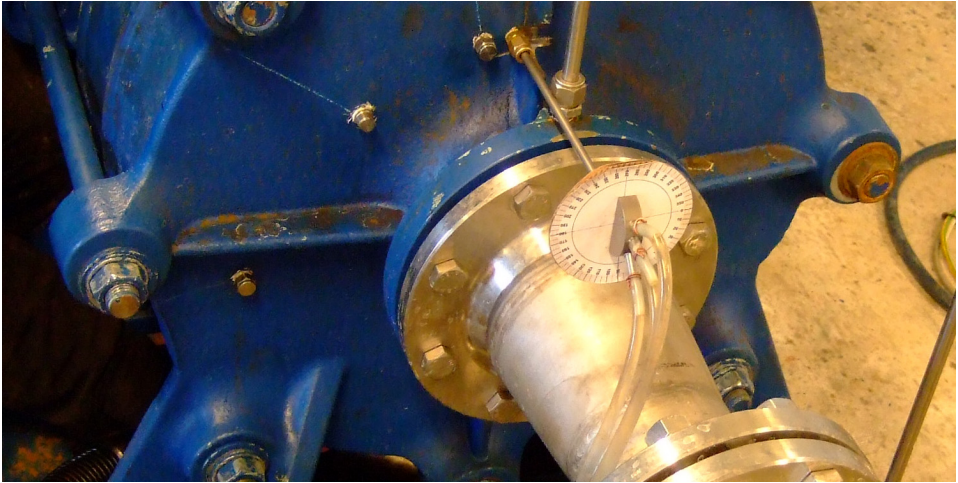
Figure 4.8: Pitot setup with angle measurement disk

4.2.4 Execution of measurements

The measurements were performed at motor supply frequencies 40, 50 and $60Hz$, and at volume flows $\frac{1}{2}Q_{design}$, $\frac{3}{4}Q_{design}$ and Q_{design}. The volume flow was controlled by manually adjusting the back pressure valve, while controlling the volume flow with the flow meter. When the correct operational point was achieved, the pitot was turned until the correct angle was found, and the angle was read from the disk. The measurement was then registered in LabView. All operational points were completed for a measurement position before the pitot was moved to the next position, as moving the pitot demanded the rig to be emptied from water.

Some difficulties were experienced adjusting the volume flow to the correct operational point, as the back pressure valve was difficult to move accurately enough.

At some of the measurements in position 1 and 2, it was difficult to find the correct angle of the flow. This was due to relatively high fluctuations in the differential pressures, probably caused by the blade passing of the impeller causing unstable flow conditions.

The set up of equipment and the measurements in total went very well, thanks to very good help from Olav Austbø, lab technician in Typhonix.

4.3 Pelton rigg calibration

As mentioned in section 4.1.3 the calibration done in the swirl rig experienced some difficulties, and it was decided to do a re-calibration in the pelton rig. In the pelton rig it is possible to do the calibration in a part of the pipe with a diameter

of 100mm, compared to the 150mm diameter on the swirl rig. This will give lesser vibrations, as well as the ability to reach higher velocities as the same centrifugal pump is used.

4.3.1   Rig description

The pelton rig is served by the same centrifugal pump as the swirl rigg, but the flow is redirected by adjusting some of the valves. The flow is then led through a flow meter before it is run through the turbine. Immediately upstream of the pelton nozzle, there are four pressure outlets, and one of these were used as entry point for the pitot. A schematic of the rig can be seen in Figure 4.9.
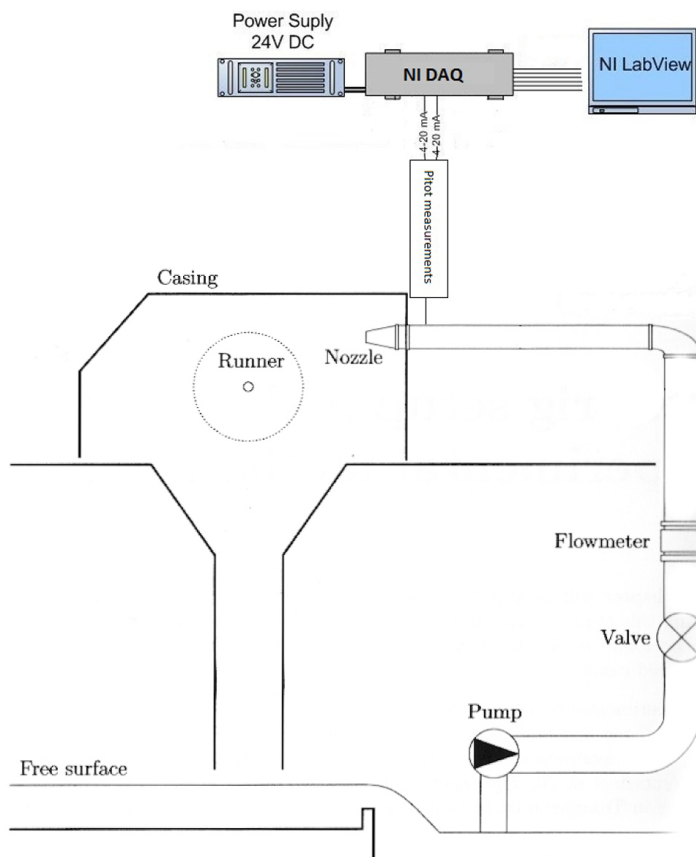
Figure 4.9: Schematic of pelton rig, modified from [3]

4.3.2 Measurement setup

The setup used in the pelton rig consisted of the flow meter, the pitot arrangement and the logging equipment. As the flow meter is connected directly to the control room, the volume flow and the pitot logging were performed independently.

Data acquisition

For data acquisition nearly the same setup was used as in 4.1.2. Some changes had to be made due to the different logging procedure of the volume flow. The front panel of LabView can be seen in Appendix B.3.

Flow measurements

The flow measurements were performed using the electromagnetic flow meter on the pelton rig of the type Optiflux F from Krohne. The calibration of the flow meter was performed by Stene and Wessel in their project work in October 2013, and the results can be seen in Table 4.3.

Name	Serial number	a	b	Max error %
Optiflux F	A03 36133	0.01240071	-0.024869287	0.84012

Table 4.3: Calibration results for flow meter on pelton rig

Pitot measurements

The pitot measurements were performed using the exact same setup as described in 4.1.2. The pitot was inserted through a hull fitting in one of the pressure outlets, where it was positioned at $\frac{3}{4}$radius out from the centre, according to the method described in 4.1. The pitot probe can be seen in Figure 4.10.

4.3.3 Execution of measurements

The re-calibration was performed by opening the pelton nozzle to full opening, and running the pump at different operational points. The desire was to achieve a flow velocity of up to 20 m/s, as the maximum measured velocity in the pump was in that region. Unfortunately, it was only possible to achieve 6.7 m/s due to high pressure in the rig. This is although a bit higher than what was achieved in the swirl rig, and no vibrations were experienced during the calibration.

16 measurements were performed in the pelton rig. First the velocity was raised from 0 to 6.7 m/s and then back to 0. At nearly maximum velocity, some leaks were discovered and tightened. These were later easily recognized in the results,
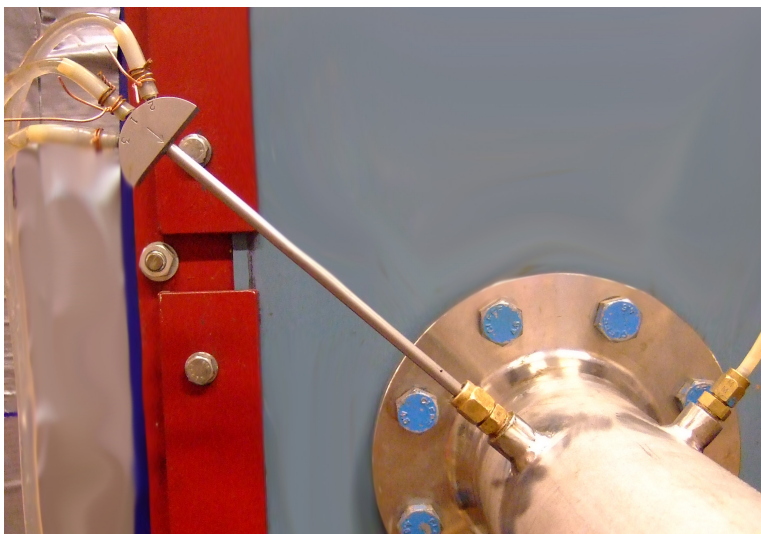
Figure 4.10: Introduction of pitot probe through hull fitting

making 7 of the measurements useless. As the rest of the measurements correlated with the swirl rig calibration, it was decided not to do the calibration again.

Controlling the volume flow of the pelton rig was significantly easier than using the swirl rig for the same purpose, and the measurements were a lot easier to carry out. This was mainly thanks to good help from PhD candidate Bjørn W. Solemslie who helped us with the pelton rig.

The results from the pitot calibration can be found in Appendix E.

Chapter 5

Results and discussion

In this chapter all results from the pump characteristics and velocity measurements are presented and compared to the theoretical solutions. A discussion of the results is carried out, and uncertainties or inaccuracies are considered.

5.1 Pump characteristics

Here the results from the testing of the characteristic curves of the pump will be presented, and they will be compared to the different approaches of estimation. The strengths and weaknesses of each method will be discussed, and in the end a comparison of them will be presented.

5.1.1 Test results

The pump characteristics were tested in the laboratory at the factory of Standart Pompa in Istanbul, and the full report can be seen in Appendix D. The head-capacity curve for the three-stage pump at 1480rpm can be seen in Figure 5.1.

As the pump design program in MATLAB is created for a one-stage pump, and the Standart pump is a three-stage pump, the head measured in the performance report was divided by three, assuming that each stage of the pump increases the head by the same amount. This assumption is based on the fact that all the stages are identical. The head-capacity curve of one of the three stages can be seen in Figure 5.2. Note that the units on the abscissa are different in figures 5.1 and 5.2.
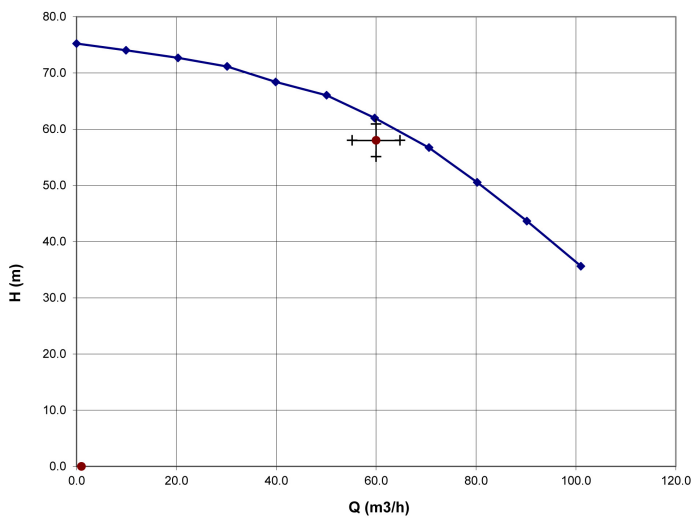
Figure 5.1: Measured head-capacity curve, three-stage
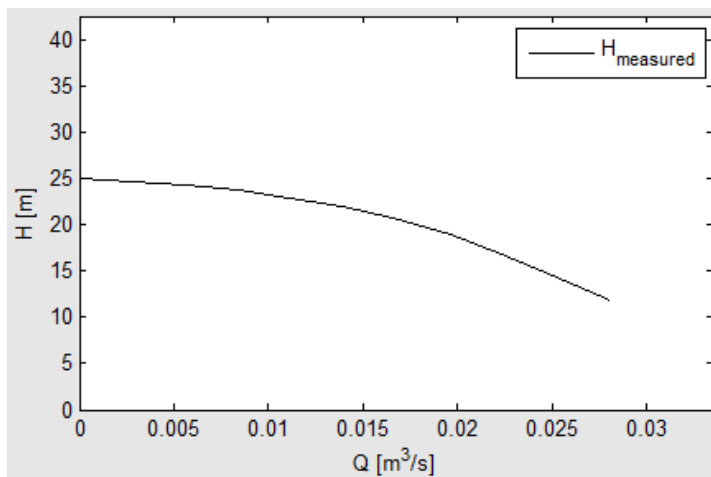
Figure 5.2: Measured head-capacity curve, one-stage

5.1.2 Numerical results

As a setup for the numerical approximations, four different calculation methods were used. These were implemented in MATLAB in a way where they could easily be compared, both to each other and to the reference values from Standart Pompa. The setup is described more thoroughly in chapter 3.

In this subsection each calculation method will be presented and compared to the reference values. The different input variables will be discussed, and strengths and weaknesses of the methods will be presented.

Traditional method with shock and friction factors

This method of calculation is the method described by, among others, Stepanoff [21], Brekke [5] and Łazarkiewicz and Troskolański [2]. It is a simple method of calculating an approximation of the characteristic curves of a pump based on the pump geometry and the volume flow.

One clear disadvantage with this method is the need for two constants which need to be found experimentally, as they are different from pump to pump [20, p. 176]. In this case, the head-capacity curve of the pump is known, making it possible to calculate reasonable constants in order to obtain the characteristic curves.

At $Q = 0$ the friction losses will theoretically be zero, so the only losses will be the shock losses. Knowing also that the shock losses are assumed to be zero at $Q = Q_{opt}$, it makes it possible to calculate the constants for a pump with known heads $H_{Q=0}$ and H_{opt}. This can be done using Equation (2.39), and the results are listed below.

Maximum head, $H_{Q=0}$	25.1 m
Head at BEP, H_{opt}	20.6 m
Friction constant, K_f	30640
Shock constant, K_s	30336

Table 5.1: Friction and shock loss constants

This will provide the head-capacity curve in Figure 5.3. There it is easily seen that the calculated head-capacity curve in red does not coincide very well with the measured curve in black. Apart from at $Q = 0$ and $Q = Q_{opt}$, where the calculated curve has been forced to match the measured curve through the constants, it deviates significantly. Especially the friction losses seem to be exaggerated at high flows, while the high shock losses at $Q = 0$ creates an unstable pump characteristics. Clearly this method is not reliable with these input.

In example 5.4 different friction and shock loss constants are used in order to obtain stable characteristics and lower losses in the upper flow regime. When using
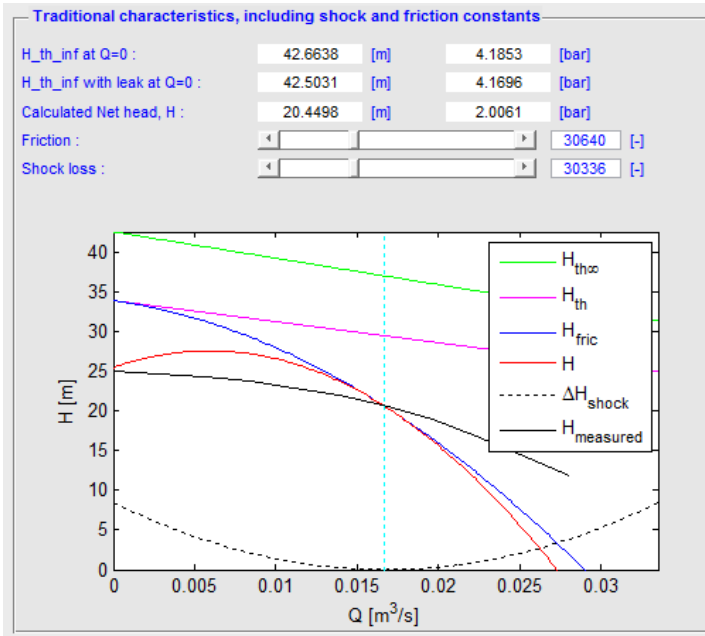
Figure 5.3: Head-capacity curve with calculated friction and shock loss constants

$K_f = K_s = 10000$, the calculated head-capacity curve seems to fit the measured curve quite well when it comes to shape, but it gives a head around 6 meters higher than the measured. This is an error of 29% at BEP, which clearly is not accurate enough.

It is difficult to assume what the reason for this mismatch may be, but by reducing the head all over it seems the curve could fit quite well. In Figure 5.5, the Pfleiderer correction factor C_p is increased to the double of the calculated, giving a curve which seems to fit well. This is although not a likely scenario, as the calculated slip is far larger than in any of the other calculation models.

In total, this method does not seem reliable for finding an approximation of the characteristic curves of a pump with known main dimensions. It may give an indication to what order of magnitude the head will be in, but as there are two unknown factors that need to be found experimentally, it will not be able to give a good prediction for a new pump design.
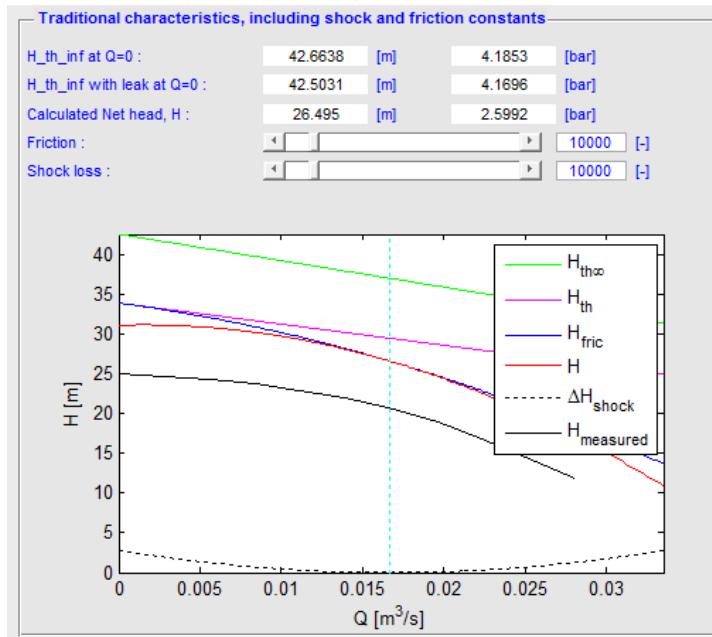
Figure 5.4: Head-capacity curve with approximated constants
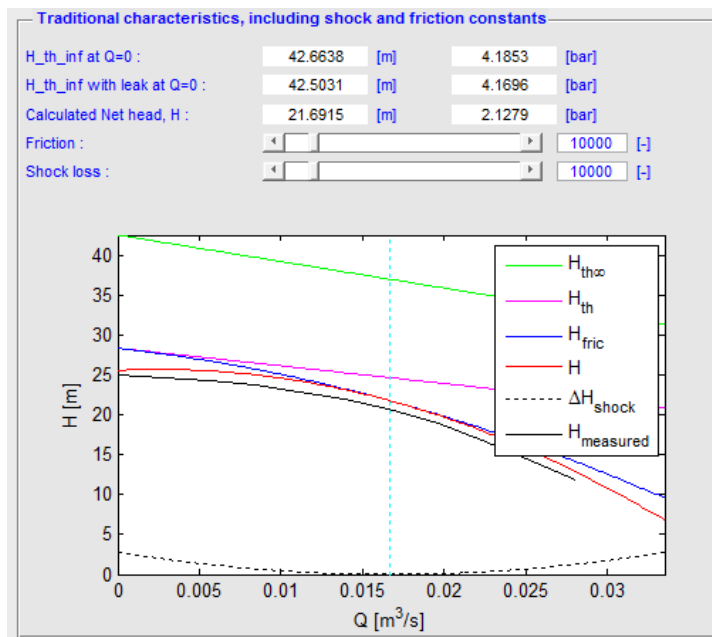
Figure 5.5: Head-capacity curve with increased slip

Traditional method with friction factor

This method is a simplification of the previous, giving the advantage of one less unknown. The simplification used assumes that all the shock losses can be approximated to equal the shock losses at the inlet, expressed by Equation (2.40). Using the same friction factor K_f as in the previous method, this gives a head-capacity curve as seen in Figure 5.6. This shows some of the same problems as in Figure 5.3, which was expected. Changing the friction factor to $K_f = 10000$ provides nearly the same solution as seen in Figure 5.4.
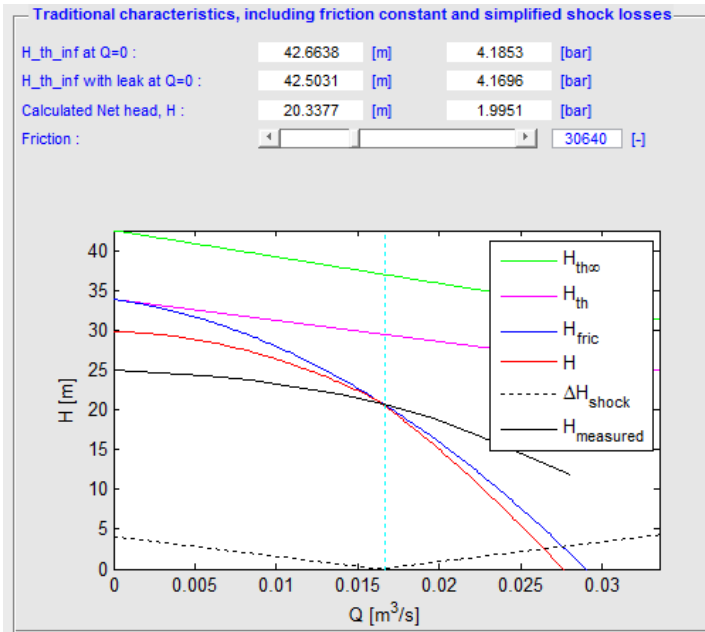
Figure 5.6: Head-capacity curve with simplified shock

This shows that the simplification made in this method may be useful, as the shapes of the curves are nearly similar. But these two methods still do not satisfy the user's need for an accurate head-capacity curve, as they both over-predict the head significantly at $Q < Q_{opt}$. Neither do they use any input regarding the diffuser or return channels, making obvious holes in the basis of the calculations.

Loss calculation method

This is by far the calculation method which requires the most input parameters. Compared with the two previous methods it requires 10-15 input parameters more, mostly regarding pump dimensions, but also other factors such as viscosity and roughness. For the pump used in this thesis, most of these parameters are known,

but a few have been necessary to estimate based on existing pictures or assumptions.

The main advantage of this approach is that there is only one factor that is not measurable. This is the coefficient ζ_{ov}, which is chosen between 0.2 and 1.5 depending on the design of the return channels where 0.2 is used for a good design, and 1.5 for a bad design. In this thesis a coefficient of $\zeta_{ov} = 1.5$ has been chosen, based on the fact that the return channels of the multistage pump have been extended significantly as a part of the testing procedures by Typhonix.

Using the input parameters as listed in Table 3.1, this provides the following head-capacity curve where the magnitude of the losses in the diffuser and the impeller can also be seen:
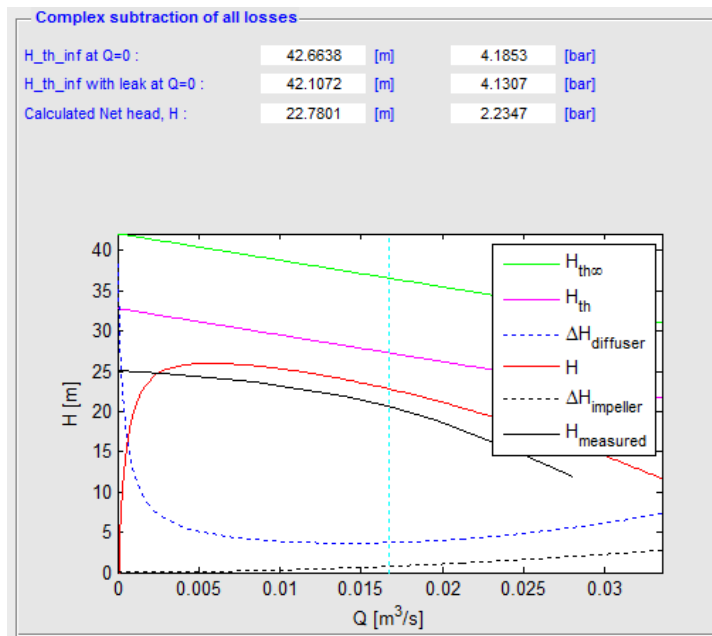
Figure 5.7: Head-capacity curve by calculating losses

Apart from the region at low volume flow, this model gave surprisingly good results. The calculated curve follows the shape of the tested, although it over-predicts the head by approximately 2 meters at BEP.

The very high diffuser losses at low flow rate comes from the calculation of the friction losses in the vaneless space between the impeller outlet and the diffuser throat. It is difficult to see that this behaviour is what will happen in a real case, as it would mean that all pressure is lost when a back pressure valve is closed.

As mentioned, the main disadvantage with this method is the need for detailed

input parameters, but if all parameters exist it seems likely that a good prediction of the head-capacity curve may be found, at least for most of the flow regime. It does over-predict the head to some extent, and this will be discussed further later.

Empirical method

Finally, the last method which has been looked into is an empirical approach to approximate the hydraulic efficiency and slip based on statistical data from other pumps. This requires approximately the same input parameters as the two traditional methods, but the losses are calculated using the statistical data presented in figures 2.7, 2.14 and 2.15. Calculating the head with Equation (2.44) then provides the following head-capacity curve:
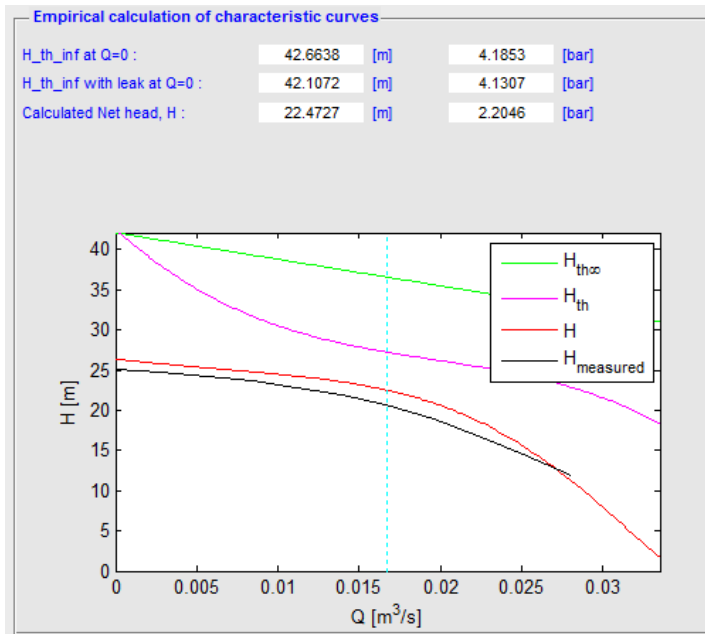
Figure 5.8: Head-capacity curve from empirical data

This method does not give any information about how the energy is lost, what kind of losses or where they may arise. Despite that, it does predict the head-capacity curve fairly well. Like the other methods it over-predicts the head a bit, and at BEP the error is close to 2 meters.

This seems to be a method which may give a good indication to how the characteristics of a pump with known main dimensions may look like, but it does not account for different diffuser or return channel design. This is a drawback, but in spite of that it predicts the curve impressively well.

It is important to note that the hydraulic efficiency estimation used here is based on multistage, single-entry impellers, and must be changed if the calculation method is to be used for another purpose.

5.1.3 Comparison

There are clearly significant differences between these four methods, both regarding input and output. Some of them need input regarding a few main dimensions, while others need twice the number of parameters or statistical approximations of the hydraulic efficiency. Clearly in the design process of a pump it is desirable to be able to predict the characteristics at an early point, and several of the details may not be known. Many of the parameters needed in the loss calculation model are still difficult to find when the complete pump design is known, making it difficult to create a reliable approximation at an early stage.

When it comes to the two traditional methods of calculating the head-capacity curves, widely used in the literature, the studies done here show that they can not be used to give a good prediction. They are unreliable without knowing the friction and shock loss factors, and even when these are calculated the results are not satisfying.

The empirical model does, however, seem to give a good approximation of the pump behaviour. This may not seem so strange, as it is based on existing pump designs, and should therefore give reasonable results for conventional pumps. It does however over-predict the head, but so does all the other methods.

The over-prediction of head which can be seen through all the different calculation models may arise from different factors. Throughout the calculations no-swirl conditions at the inlet have been assumed, something that in reality may be difficult to achieve for all stages in a multistage pump. If the return channels are not perfectly designed, a pre-swirl will ble present at the inlet of the following impeller causing a loss of head, according to Euler's equation (2.7). The multistage pump may also introduce losses which are not fully accounted for, such as leakages between the stages and higher disk friction losses.

The only model which to some extent accounts for the design of the diffuser is the loss calculation model. However, none of the models account for the design of the return channels, except a factor in the loss calculation model giving relatively insignificant effects. The multistage pump which has been used in these studies is a pump with modified diffuser and return channels, both being significantly longer than normal. This may also be the cause of the over-prediction of head, as these factors are not calculated.

5.2 Velocity triangles

In this section the results from the numerical calculations of the theoretical veloc-
ities will be compared to the results from the testing performed at Varhaug. Two
measurements were performed in the diffuser inlet (1 and 2), one in the diffuser
throat (3), and one in the diffuser outlet (4). The results will be presented in tables,
where the theoretical velocities and angles calculated in MATLAB are compared to
the measured, and all measurements will be discussed further regarding accuracy,
reliability and any other significant factors.

The rotational speed of the pump was calculated from the frequency of the engine,
and the relation was written on the data sheet on the engine. The frequencies
measured were 40, 50 and 60 Hz, which converted to rpm gives 1170, 1470 and
1770 rpm for this specific engine and operational conditions.

5.2.1 Diffuser inlet

Positions 1 and 2 were placed in the diffuser inlet, as close to the impeller as
practically possible. This was done to establish a velocity profile at the inlet of
the diffuser that could be used for further investigation. It was also an aim to find
the slip angle of the pump, as this is an angle which is defined different in the
literature, and apparently varies a lot.

The measured velocities and angles in the diffuser inlet, along with the theoretically
calculated values are presented in tables 5.2 and 5.3. Position 1 is placed quite close
to the pressure side of the diffuser, while position 2 is closer to the middle of the
diffuser inlet, see Figure 4.5.

Position 1								
		Velocity			Angle			
RPM	Flow	C_{th}	C_{meas}	Deviation	α_{th}	α_{meas}	Deviation	
	1/2	10.91	9.82	11.1%	13.5°	-4°	17.5°	
1170	3/4	10.66	9.17	16.2%	21.0°	-4°	25.0°	
	1/1	10.59	8.85	19.7%	28.7°	-7°	35.7°	
	1/2	13.90	14.30	2.8%	10.5°	-5°	15.5°	
1470	3/4	13.56	13.96	2.9%	16.3°	-5°	21.3°	
	1/1	13.36	13.16	1.5%	22.4°	-5°	27.4°	
	1/2	16.92	19.29	12.3%	8.6°	-4°	12.6°	
1770	3/4	16.51	19.88	17.0%	13.4°	-3°	16.4°	
	1/1	16.23	18.82	13.8%	18.3°	-3°	21.3°	

Table 5.2: Fluid properties in position 1

The first impression of the results is that they deviate significantly from the theoret-
ical values. It does not seem like the deviation is consistent, neither for the velocity

Position 2							
		Velocity			Angle		
RPM	Flow	C_{th}	C_{meas}	Deviation	α_{th}	α_{meas}	Deviation
	1/2	10.91	8.65	26.1%	13.5°	-1°	14.5°
1170	3/4	10.66	9.77	9.1%	21.0°	5°	16.0°
	1/1	10.59	9.22	14.9%	28.7°	8°	20.7°
	1/2	13.90	12.12	14.7%	10.5°	-7°	17.5°
1470	3/4	13.56	13.97	2.9%	16.3°	2°	14.3°
	1/1	13.36	14.37	7.0%	22.4°	5°	17.4°
	1/2	16.92	16.52	2.4%	8.6°	-10°	18.6°
1770	3/4	16.51	17.07	3.3%	13.4°	1°	12.4°
	1/1	16.23	19.26	15.7%	18.3°	4°	14.3°

Table 5.3: Fluid properties in position 2

nor the angle of the flow. A difference between the measured and theoretical velocity of up to 26.1% is registered, making it difficult to draw good conclusions from the measurements. If the difference between the measured and theoretical values was more consistent it could have been caused by the calibration, but it is not likely that a bad calibration could lead to these results.

Despite the fact that the flow velocities and angles deviate a lot from theory, it is interesting to investigate if the same trends and flow patterns can be found as in theory. A natural parameter to examine regarding the flow pattern is the angle of the flow. As the results show, these do also differ a lot from theory, and several of the measured angles are actually negative. This gives a negative meridional component of the absolute velocity, meaning that the flow is directed in towards the impeller, see Figure 5.9 where the effect of a positive and negative α is shown.
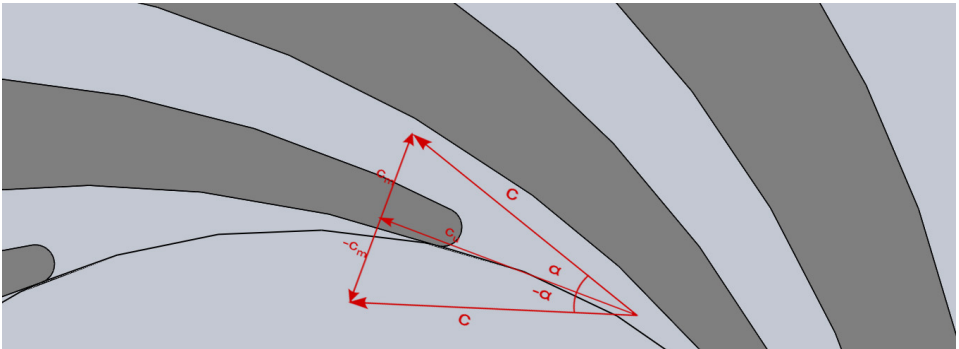
Figure 5.9: Negative flow angle α in diffuser inlet

The angles measured in position 1 do not seem to change consistent related to the flow or the rotational speed, but the angles measured in position 2 seem to become more positive as the flow increases, and also less positive as the rotational speed

increases. Both these trends are according to theory, as the theoretical angles show. They do, however, still deviate significantly from the theoretical flow angles, and a negative α is registered in both positions. In total, no good conclusions can be drawn from the measured flow angles in the experiment.

When it comes to the velocities, theoretically they should in these two positions should be equal for the same operational conditions, but the measurements show a different behaviour. In position 1 the velocities generally show the same trend as the theoretical velocities, as they decrease with increasing volume flow. The measurements at 1470 rpm are quite close to the theoretical velocity, but as the angle of the flow is negative for all measurements these results can not be trusted. In position 2 the velocities are actually increasing with increasing flow rates, the opposite of what the theory says.

The reason for the theoretical reduction of absolute velocity with increasing flow rates is the increase in the meridional component. This is easily seen in Figure 5.10 where the absolute velocity c to the left is larger than to the right, but the flow rate is larger to the right.
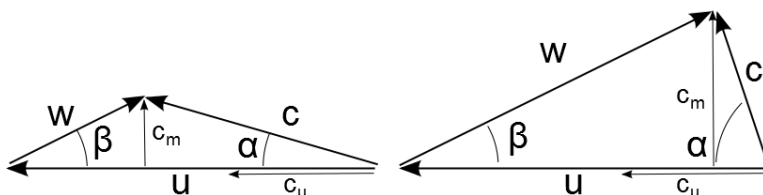
Figure 5.10: Effect of changing flow

5.2.2   Diffuser throat

Position 3 in the measurements was placed in the diffuser throat in the inlet of the diffuser, see Figure 4.5. This is an interesting value because the flow will here theoretically be aligned with the direction of the diffuser, and the flow velocity will only depend on the flow rate. The same velocities should therefore be measured for all rotational speeds. This is of course only in theory, and as Feng, Benra and Domen [8] discovered in their research the flow will in reality fluctuate well beyond the diffuser inlet throat.

The results from the measurements are presented in Table 5.4, along with the theoretical values. The theoretical angle has been measured from available drawings in SolidWorks, and is set equal to the angle of the centre in the diffusing channel in the throat.

The results from the diffuser throat show some of the same tendencies as the results from the diffuser inlet. The measurements generally deviate a lot from the theoretical values, both regarding velocities and angles.

Position 3								
		Velocity				Angle		
RPM	Flow	C_{th}	C_{meas}	Deviation	α_{th}	α_{meas}	Deviation	
	1/2	4.23	5.99	29.4%	16º	35º	-19º	
1170	3/4	6.35	6.69	5.1%	16º	37º	-21º	
	1/1	8.47	7.47	13.4%	16º	34º	-18º	
	1/2	4.23	7.99	47.1%	16º	27º	-11º	
1470	3/4	6.35	7.30	13.0%	16º	31º	-15º	
	1/1	8.47	8.85	4.3%	16º	30º	-14º	
	1/2	4.23	9.30	54.5%	16º	25º	-9º	
1770	3/4	6.35	10.60	40.1%	16º	23º	-7º	
	1/1	8.47	10.99	22.9%	16º	27º	-11º	

Table 5.4: Fluid properties in position 3

The flow angles are here positive meaning that the measured flow direction is outwards, which seems more correct than the measurements from the diffuser inlet. The angles measured here are more positive than the theoretical, giving a flow direction approximately as seen in Figure 5.11. This seems to be not so unlikely, but the highly irregular behaviour of the angle in the different measurements make it difficult to draw any good conclusions about the flow direction here as well.
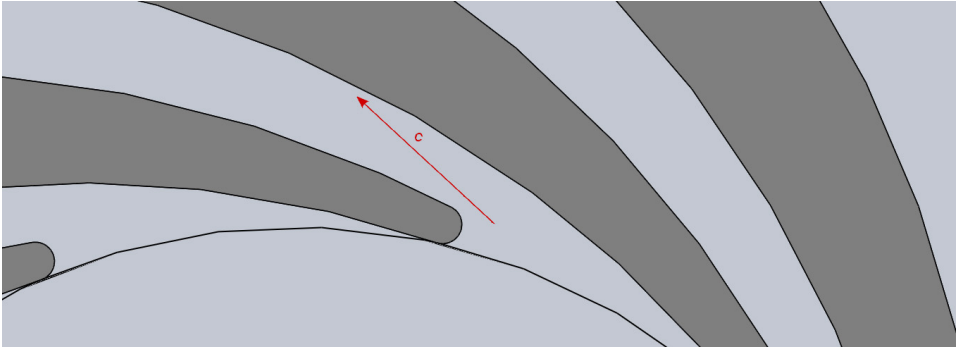
Figure 5.11: Flow direction in diffuser throat

The measured velocities are increasing at increasing volume flow for all rotational speed, as expected. As the total cross sectional area of the diffuser channels is constant and the volume flow is changed from half to full it was expected to find that the velocity was doubled, but only a increase of 10 to 25% is found. An explanation for this could be a large constant leakage between the stages of the pump, or the water extracted to cool the shaft bearing, but that would not explain why the measured velocity at full flow of 1170 rpm is below the theoretical value, nor why the measured velocity of 3/4 flow at 1470 rpm is below half and full flow at the same rotational speed.

In total the measurements in position 3 seem to show the same trends as the theory would imply for most of the measurements, but the fluctuating angles can not give any good conclusions. They do all increase with increasing rotational speed which is expected, as the velocity in front of the throat will then have a larger peripheral component c_u. They do not, however, change regularly related to the volume flow, which would be expected as the rotational speed clearly has an impact.

5.2.3 Diffuser outlet

Position 4 is measured just before the diffuser outlet, close to the inner wall of the diffusing channel, see Figure 4.5. This position was of special interest for Typhonix, as they wanted to investigate whether the rotational speed influences the flow in this position or not. The results are presented in Table 5.5.

Position 4								
		Velocity			Angle			
RPM	Flow	C_{th}	C_{meas}	Deviation %	α_{th}	α_{meas}	Deviation	
	1/2	1.40	1.88	25.5%	35°	-57°	92°	
1170	3/4	2.10	1.92	9.4%	35°	-57°	92°	
	1/1	2.80	2.17	29.0%	35°	-57°	92°	
	1/2	1.40	2.03	31.0%	35°	-57°	92°	
1470	3/4	2.10	2.11	0.5%	35°	-57°	92°	
	1/1	2.80	2.27	23.3%	35°	-57°	92°	
	1/2	1.40	2.15	34.9%	35°	-64°	99°	
1770	3/4	2.10	2.37	11.4%	35°	-60°	95°	
	1/1	2.80	2.55	9.8%	35°	-60°	95°	

Table 5.5: Fluid properties in position 4

The velocities measured here show the same trends as they theoretically should for increasing flow, but also here significant deviations are measured. As in position 3, the change in velocity when increasing from half to full flow is less than expected showing an increase from 12 to 19%. The results also show that the velocities do have a change related to the rotational speed of the impeller for the same volume flow, showing that the velocity profile created by the impeller still has an effect well beyond the diffuser throat. An increase of the rotational speed from 1170 to 1770 rpm, or 51%, gives an increase in the measured velocity for the same flow rate of 14 to 23%. This was not expected, but is an additional indication of the complex flow patterns within a pump, further investigated by Feng, Benra and Domen [8].

The flow angles measured show a nearly constant behaviour, but the actual direction is a very different than expected. An α of -57 to -64 means that the flow direction will be approximately as shown in Figure 5.12 where the red arrow indicates the measured flow angle and the black arrow indicates the expected.

The measurements from position 4 show that the velocities do change relative to
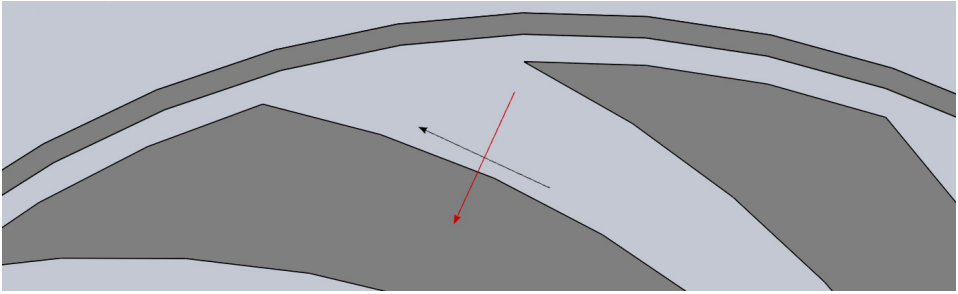
Figure 5.12: Flow direction in diffuser outlet

the rotational speed of the impeller, but the magnitude of the velocity and the measured angles can not be trusted. There is an increase in the velocity for higher volume flows, which is expected, but the relation between the rotational speed and the flow velocity was not expected.

5.3 Uncertainty

The results from the pump measurements show that the pitot-static probe did not give satisfying accuracy. Some of the measurement points seem to correlate with theory, at least when it comes to trends when changing rotational speed and volume flow. The angles measured are not at all in the expected range, and especially in the diffuser inlet the flow angles seem highly unlikely.

The reasons for the inaccurate measurement results could, as mentioned, be a bad calibration, but that would have given a more consistent behaviour, and probably also a better relation to the theory. In the project thesis of Finstad [9] problems with the pitot setup was also experienced, and the calibration is mentioned as one possible cause.

The introduction of a pitot probe into the relatively small dimensions of the diffuser was expected to disturb the flow to some degree, but these results show that the flow disturbance has probably been significant. Neither the angles, nor the flow velocities are according to theory, and for several of the measurements the flow behaviour seems both unlikely and shows irregular behaviour for different operational conditions. As seen in Figure 5.13 the pitot probe with a diameter of 6.4mm causes some of the diffuser area to be blocked, and this has probably resulted in a flow disturbance big enough to make the measurements unreliable. The measurements are also taken very close to the front and back walls of the diffuser, as they are taken in the center of the 15mm high diffuser, leaving only 7-8mm to each wall.
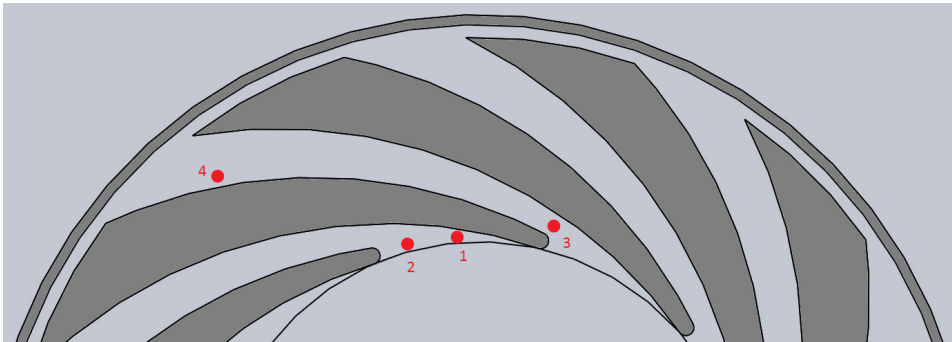
Figure 5.13: Size of the pitot probe

Chapter 6

Conclusion and Further Work

The aim of this thesis has been to find the velocity distribution at the outlet of the impeller of a centrifugal pump, both theoretically and by measurements. In addition it was an aim to verify the calculation of the characteristic curves done by a centrifugal pump design program in MATLAB.

The calculation and measurements of the outlet velocities from the pump impeller has proven to be more difficult than expected. According to theory an even velocity distribution was expected, thus making the velocity profile easy to find. The measurements done with a pitot probe unreliable results, both regarding the flow velocity and the flow direction. The expected trends for increased volume flow and rotational speed were found for most of the measurements, but the magnitude of the results are very different from theory.

The conclusion regarding the velocity profile at the outlet of a centrifugal pump impeller is that the flow in this narrow area is very complex and difficult to find analytically. Conducting CFD simulations is another approach which could give useful results.

The use of a pitot for these measurements has also proven to be difficult, as it is an intrusive method disturbing the flow significantly. LDV was considered as an alternative, but due to practical and time limitations it was not performed. LDV is a good method for fluctuating flows, and could have given better results if a good set up of equipment was achieved.

As a further investigation of the outlet velocities, a CFD simulation could be performed in combination with LDV measurements. Both these tasks are difficult and time consuming, and LDV measurements may be impossible to carry out on the industrial centrifugal pump used in this thesis. It would, however, be possible to bring the pump to the Waterpower Laboratory, as the research program of Ty-

phonix is finished. A set up at the Waterpower Laboratory could be interesting, and hopefully be used for several purposes.

According to available literature, there are many ways to calculate the characteristic curves of a centrifugal pump. The characteristics are clearly difficult to approximate, but four methods of approximation have been tested and compared to the measured characteristics of a multistage pump.

The methods have shown quite different results, but the traditional way of calculating the characteristic curves described by Stepanoff and Brekke has shown the least accurate results. This method is however the simplest, both with and without the shock loss simplification. It can be used to give an indication to what order of magnitude the head-capacity curves will be in, but it can not be trusted in a design process.

A better option is to use the empirical method where the slip and hydraulic efficiency is scaled based on empirical data. This gave good results, and may give a very good indication of the characteristics of a conventional pump. The method of loss calculation also proved to give good results, but many detailed input parameters are needed.

Investigating the losses in a centrifugal pump closer could give a better understanding of them, and provide a simple calculation model giving better results than the calculation in the traditional model. It would also be interesting to investigate other centrifugal pumps, both single- and multistage and compare them to the different calculation models. Time has unfortunately not been found to do that during this thesis.

Bibliography

[1] Harold H. Anderson. *Centrifugal Pumps and Allied Machinery*. Elsevier Advanced Technology, 4th edition, 1994.

[2] Stephen Łazarkiewicz and Adam T. Troskolański. *Impeller Pumps*. Pergamon Press, 1965.

[3] Lorentz Fjellanger Barstad. Cfd analysis of a pelton turbine. Master's thesis, NTNU, 2012.

[4] Hermod Brekke. Grunnkurs i hydrauliske strømningsmaskiner. Vannkraftlaboratoriet NTNU, 2000.

[5] Hermod Brekke. Pumper & Turbiner. Vannkraftlaboratoriet NTNU, 2003.

[6] Prof. Ole Gunnar Dahlhaug. Private communication, September 2013. NTNU.

[7] S. Larry Dixon and Cesare A. Hall. *Fluid Mechanics and Thermodynamics of Turbomachinery*. Elsevier, 6th edition, 2010.

[8] Jianjun Feng, Friedrich-Karl Benra, and Hans Josef Dohmen. Investigation of periodically unsteady flow in a radial pump by cfd simulations and ldv measurements. *Journal of Turbomachinery*, 133, 2011.

[9] Pål Henrik Enger Finstad. Vanninjeksjon i sugerør. Project thesis, NTNU, 2008.

[10] Sverre Stefanussen Foslie. Design of centrifugal pump for produced water. Project thesis, NTNU, 2013.

[11] Håkon Hjort Francke. *Increasing Hydro Turbine Operation Range and Efficiencies Using Water Injection in Draft Tubes*. PhD thesis, NTNU, 2010.

[12] Johann Friedrich Gülich. *Centrifugal Pumps*. Springer, 2nd edition, 2010.

[13] Jón Bergmann Heimisson. 3D geometry of runners for centrifugal pumps. Master's thesis, NTNU, 2007.

[14] Igor J. Karassik. *Engineers' Guide to Centrifugal Pumps*. McGraw-Hill, 1964.

[15] Arne Kjølle. Hydraulisk måleteknikk. Vannkraftlaboratoriet NTNU, 2003.

[16] Grigori I. Krivchenko. *Hydraulic Machines: Turbines and Pumps*. Lewis, 2nd edition, 1994.

[17] Neutrium. Absolute roughness of pipe material, Desember 2013. URL `http://neutrium.net/fluid_flow/absolute-roughness/`.

[18] Prof. Torbjørn Kristian Nielsen. Private communication, November 2013. NTNU.

[19] Sigrid Marie Skodje. Real time modelling of flow systems. Master's thesis, NTNU, 2013.

[20] Alexey J. Stepanoff. *Centrifugal and Axial Flow Pumps*. Wiley, 1948.

[21] Alexey J. Stepanoff. *Centrifugal and Axial Flow Pumps.* Wiley, 2nd edition, 1957.

[22] John Tuzson. *Centrifugal Pump Design.* Wiley, 2000.

[23] Anthony J. Wheeler and Ahmad R. Ganji. *Introduction to Engineering Experimentation.* Pearson Education, 2004.

[24] Frank M. White. *Fluid Mechanics.* McGraw-Hill, 6th edition, 2008.

Appendices

Appendix A

Loss calculations

These are the equations listed in *Centrifugal Pumps* by J.F. Gülich which can be used to estimate the hydraulic losses in the impeller and diffuser.

Impeller loss:	$h_{La} = h_{La,s} + h_{La,f}$	$(A.1)$
Shock loss at impeller inlet:	$h_{La,s} = \frac{0.3}{2g}(w_{m1} - w_{q1})^2$	$(A.2)$
Relative velocity vector:	$w_{m1} = \sqrt{c_{m1}^2 + (u_1 - c_{u1})^2}$	$(A.3)$
Velocity in impeller throat:	$w_{q1} = \frac{Q_{La}}{z_{La}A_{q1}} = \frac{Q_{La}}{z_{La}a_1 b_1}$	$(A.4)$
Friction and mixing losses:	$h_{La,f} = 2\frac{c_d}{g}\frac{L_{sch}}{D_h}w_{av}^2$	$(A.5)$
Dissipation coefficient:	$c_d = (c_f + 0.0015)(1.1 + 4\frac{b_2}{d_2})$	$(A.6)$
Friction coefficient:	$c_f = \frac{0.136}{\left\{-\log\left(0.2\frac{\varepsilon}{L_{sch}} + \frac{12.5}{\mathrm{Re}}\right)\right\}^{2.15}}$	$(A.7)$
Reynold's number:	$\mathrm{Re} = \frac{w_{av}L_{sch}}{\nu}$	$(A.8)$
Average relative velocity:	$w_{av} = \frac{2Q_{La}}{z_{La}(a_2 b_2 + a_1 b_1)}$	$(A.9)$
Hydraulic diameter:	$D_h = \frac{2(a_2 b_2 + a_1 b_1)}{a_1 + b_1 + a_2 + b_2}$	$(A.10)$

Table A.1: Calculation of impeller losses

Diffuser loss:	$h_{Le} = h_{2-3} + \frac{c_{q3}^2}{2g} \left\{ 0.3\left(\frac{c_2}{c_{q3}} - 1\right)^2 + 1 - c_p - \frac{1-\zeta_{ov}}{A_R^2} \right\}$	$(A.11)$
Friction losses in inlet region:	$h_{2-3} \qquad = \qquad \frac{u_2^2}{2g}(c_f \qquad +$ $0.0015) \left(\frac{a_3}{d_2} + \frac{b_3}{d_2}\right) \frac{\pi^3 \left(\frac{c_{m2}b_2}{u_2 d_2}\right)^2}{8\left(z_{Le}\frac{a_3 b_3}{d_2}\right)^3} \left(1 + \frac{c_2}{c_{q3}}\right)^3$	$(A.12)$
Flow velocity in throat:	$c_{q3} = \frac{Q_{Le}}{z_{Le}a_3 b_3}$	$(A.13)$
Area ratio:	$A_R = \frac{a_4 b_4}{a_3 b_3}$	$(A.14)$
Diffuser c_p from figure A.1:	$c_p = f\left(A_R, \frac{L_{3-4}}{R_1}\right)$	$(A.15)$
Diffuser c_p-coefficient:	$\frac{L_{3-4}}{R_1} = L_{3-4}\sqrt{\frac{\pi}{a_3 b_3}}$	$(A.16)$

Table A.2: Calculation of diffuser losses

The coefficient ζ_{ov} is chosen between 0.2 and 1.5 depending on the design of the return channels. With an optimal flow design, $\zeta_{ov} = 0.2$ could be attainable, while a bad design may give $\zeta_{ov} = 1$.
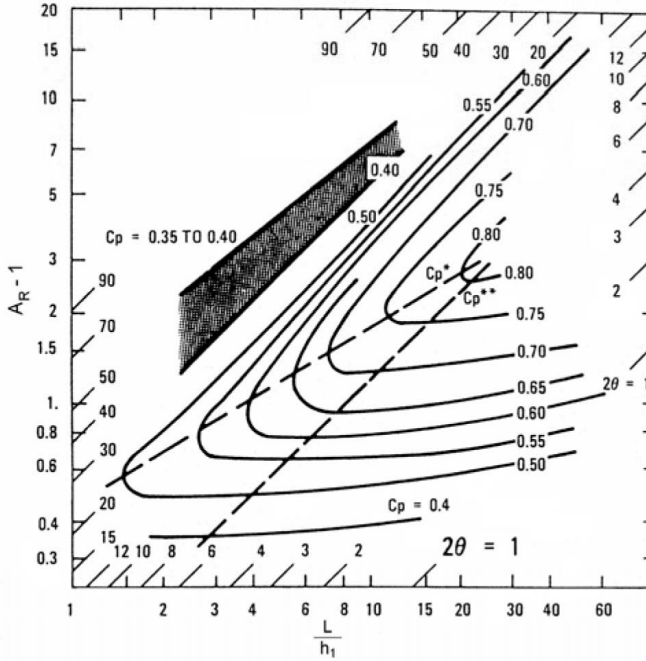
Figure A.1: Diffuser coefficient, c_p [12]

Appendix B

LabView programs

B.1 Swirl rig calibration
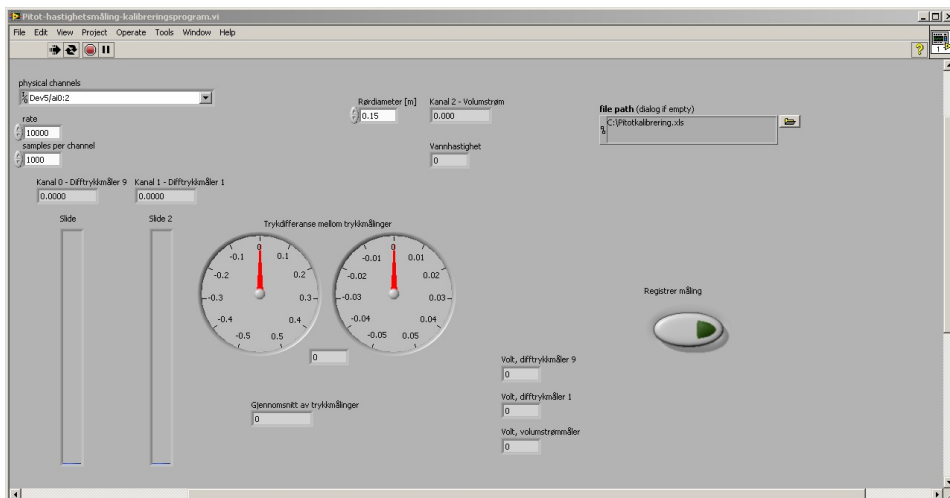
Figure B.1: Front panel of LabView program for calibration in swirl rig

B.2   Pump measurements
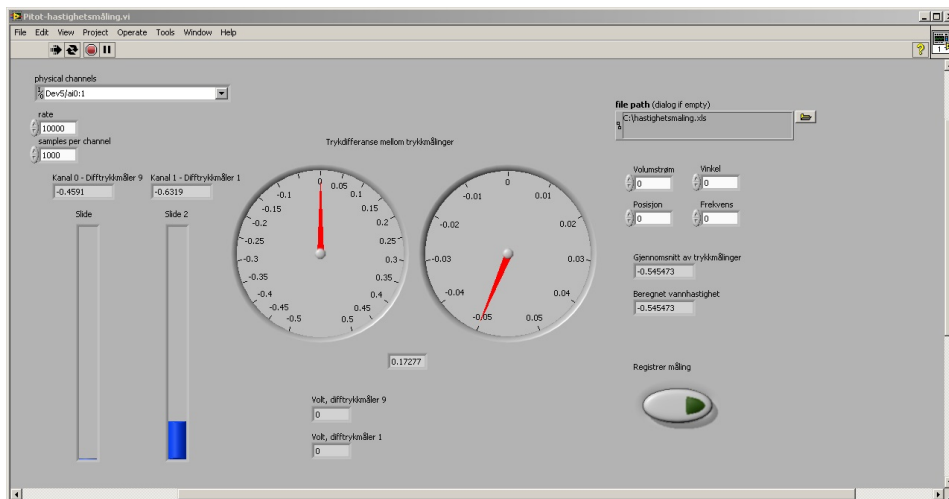
Figure B.2: Front panel of LabView program for pump measurements

B.3   Pelton rig calibration
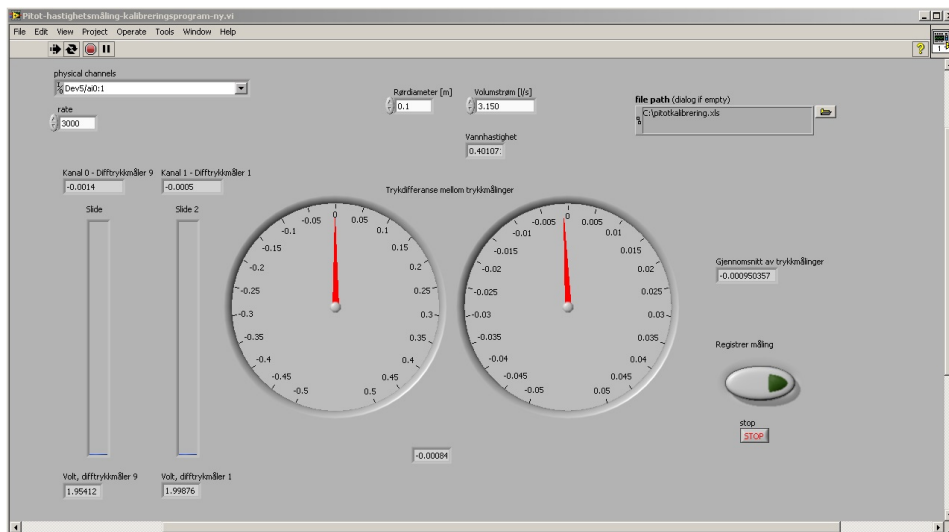
Figure B.3: Front panel of LabView program for calibration in swirl rig

Appendix C

Pitot tube

NOTES: 1. MAXIMUM TEMPERATURE 900°F
2. PRESSURE TIGHT (P)

YAW

PITCH

FLOW

PLUS
+

MINUS
−

MINUS
−

PLUS
+

SENSING HOLE SIZE
P_1 = .020 Ø HOLE
P_2 = .022 Ø HOLE
P_3 = .022 Ø HOLE

TYPE: WEDGE

P_1

P_2

P_3

.250 Ø

24.0

1 1/4

.156Ø SWAGED
TO .125Ø TYP.
(3) PLACES

(P) TYP.
(3) PLACES

(P)

1
2
3

DESIGN
CHECKED
DRAWN HJW
DATE 02/14/02

United Sensor Corp.

SIZE B   DWG NO. W-250-   -CD CUST.DWG
SCALE   SHEET   OF   REV

Appendix D

Pump performance report

Standart Pompa ve Makina San. Tic. A.Ş.
Dudullu Org. Sanayi Bolgesi 2. Cadde No:9
34775 Esenkent - Ümraniye - İstanbul - TR
t : +90 216 466 89 00   f : +90 216 415 88 60

Stand No: 2	1/2
T / D :	8/20/2013
Ref :	1
Test No :	per_710

Standart
POMPA ve MAKİNA SANAYİ TİC. AŞ.

Pompa Deney Raporu / Pump Test Report

Müşteri / Customer : TYPHONIX   **Proj. :**

Pompa Bilgileri / Pump Data

Tip / Type : SKM-E 150/3   **D$_{çark/Imp}$:** 264 mm   **DNe :** 125 mm
Seri / Serial : 1   **Tasarım / Design :**   **DNb :** 150 mm

Ölçme Sistemi / Measurement System

Man. (Emme/Suct.) : 0-3 bar(mutlak)   **Debi / Flow :** DN 300   **D$_1$:** 125 mm
Man. (Basma/Disch.) : 0-10 bar   **Δ z :** 0.85 m   **D$_2$:** 158 mm
T$_{ort/amb}$: 29.4 °C   **P$_{atm}$:** 996.8 mbar   **T$_{Su / Liq.}$:** 28.2 °C
Test Sıvısı / Liquid : Su   **ρ :** 1.00 kg/dm^3 **P$_{buh / vap}$:** 0.390 m

Motor Bilgileri / Motor Data

Üret./ Manuf. : WAT   **P :** 30 kW   **Volt. :** 380 V   **cos Φ :** 0.86
Tip / Type : QH 200L4C   **n :** 1465 rpm   **I :** 57.3 A
Seri / Serial : 30774   **Fre. :** 50 Hz   **η$_m$:** 92.3 %

Çalışma Noktası Bilgileri / Operating Conditions

Sıvı / Liquid : Su   **ρ :** 1.000 kg/dm^3 **Sıcaklık / Temp. :** 20.0 °C

	n rpm	Q m3/h	H m	η$_p$ %	η$_s$ %	n rpm	Q m3/h	H m	η$_p$ %	η$_s$ %
Anma / Rated	1480	60.0	58.0	-	-	-	-	-	-	-
Deney / Test		0.0	0.0	-	-	-	-	-	-	-

Ölçümler / Measurements

No	n rpm	Q m3/h	ρ$_{giriş/suct}$ barA	ρ$_{çıkış/disch}$ bar	v²/2g m	H m	P$_1$ kW	η$_m$ %	P$_2$ kW	η$_p$ %
1	1488.7	101.6	0.78	3.24	-0.16	36.04	19.55	91.4	17.88	55.6
2	1489.2	90.8	0.79	4.05	-0.13	44.19	19.23	91.4	17.57	62.0
3	1489.2	80.7	0.80	4.74	-0.10	51.17	18.61	91.2	16.97	66.1
4	1489.4	71.0	0.81	5.35	-0.08	57.43	17.78	91.1	16.19	68.4
5	1490.4	60.1	0.82	5.89	-0.06	62.86	16.67	90.9	15.15	67.7
6	1490.8	50.5	0.82	6.29	-0.04	66.99	15.50	90.7	14.05	65.3
7	1492.0	40.2	0.83	6.54	-0.03	69.51	14.07	90.4	12.72	59.7
8	1492.9	30.4	0.83	6.83	-0.02	72.40	12.56	90.1	11.32	52.9
9	1493.4	20.5	0.83	6.99	-0.01	74.00	10.95	89.8	9.83	41.9
10	1494.6	10.0	0.83	7.13	0.00	75.50	9.41	89.5	8.43	24.4
11	1495.6	0.0	0.84	7.26	0.00	76.82	8.18	89.3	7.30	0.0
12										
13										
14										
15										

Anma Şartlarında / Rated Conditions

No	n rpm	Q m3/h	H m	P$_2$ kW @ 1,00	P$_2$ kW @ 1	η$_p$ %
1	1480.0	101.0	35.62	17.56	17.56	55.8
2	1480.0	90.2	43.65	17.24	17.24	62.2
3	1480.0	80.2	50.54	16.66	16.66	66.3
4	1480.0	70.6	56.71	15.89	15.89	68.6
5	1480.0	59.7	61.99	14.84	14.84	68.0
6	1480.0	50.1	66.02	13.75	13.75	65.6
7	1480.0	39.9	68.40	12.42	12.42	59.9
8	1480.0	30.2	71.16	11.03	11.03	53.1
9	1480.0	20.3	72.67	9.57	9.57	42.1
10	1480.0	9.9	74.03	8.18	8.18	24.5
11	1480.0	0.0	75.22	7.08	7.08	0.0
12						
13						
14						
15						

Malzemeler / Materials

Gövde / Casing :
Difüzör / Diffuser :
Çark / Impeller :
Mil / Shaft :

Açıklamalar / Comments

Test Sınıfı / Class : ISO 9906 Class 2 Tol. : Q ±8%, H ±5%, η -5%

Tip / Type :	SKM-E 150/3	**Stand No:** 2 2/2
D$_{çark/Imp}$:	264 mm	**T / D :** 8/20/2013
Seri / Serial :	1	**Ref :** 1
n :	1480 rpm	**Test No :** per_710

Standart
POMPA ve MAKİNA SANAYİ TİC. AŞ.

Test Sınıfı / Class : ISO 9906 Class 2 Tol. : Q ±8%, H ±5%, η -5%
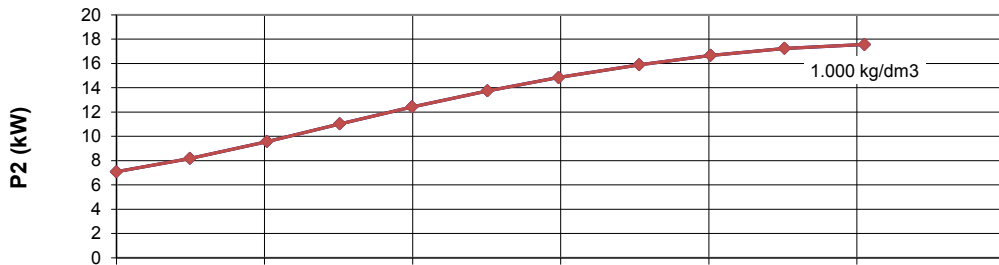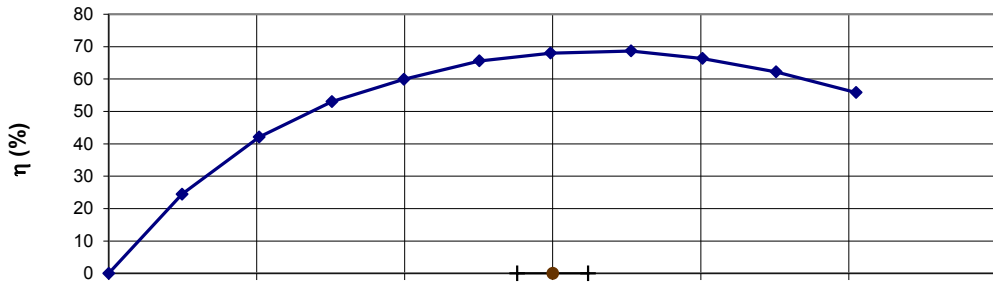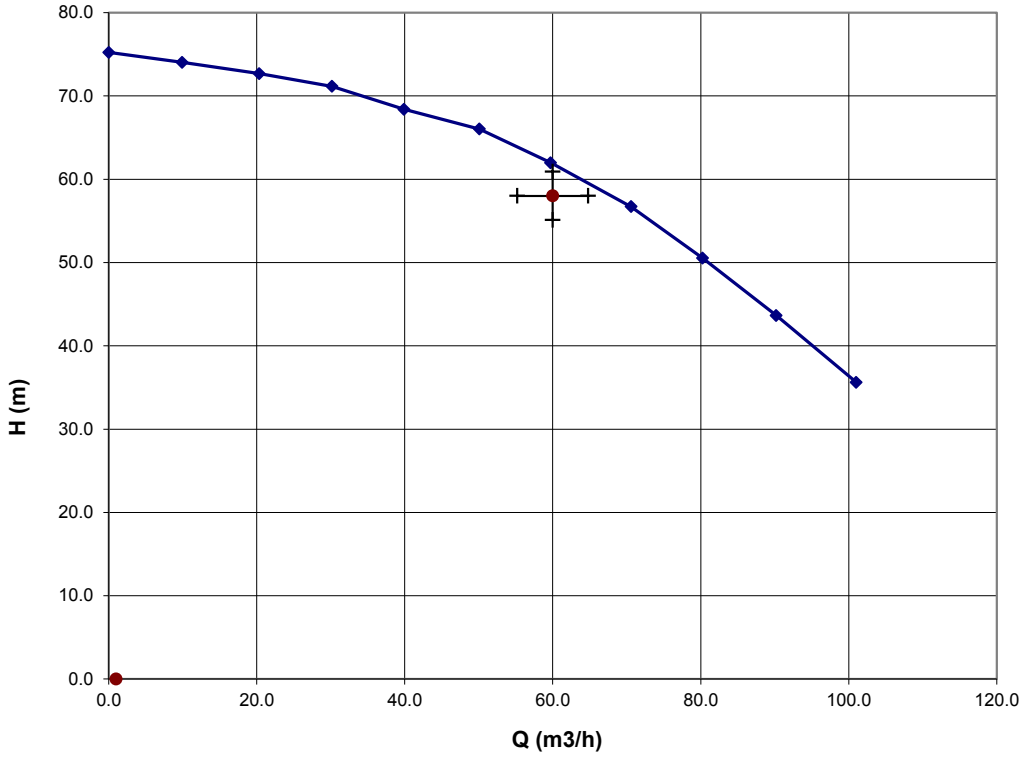
Appendix E

Pitot calibration

The results from the pitot calibrations are presented here, and a discussion regarding which is to be used for further calculations is carried out.

The calibration performed in the swirl rig gave linear results, but as the velocity was limited to approximately 5 m/s and some vibrations were observed, it was decided to do a re-calibration in the pelton rig.

The calibration results from the pelton rig proved to be less linear than the swirl results, and fewer measurements were carried out. It was, however, possible to increase the velocity to 6,7 m/s, a bit higher than in the swirl rig.

As the results from the swirl rig was both more linear, and closer in time to the experiments in Varhaug, it was decided to use the swirl calibration results for further calculations.

Name	a	b	R^2
Swirl calibration	25.898	1.4185	0.9878
Pelton calibration	25.767	0.5371	0.966

Table E.1: Calibration results for pitot-static probe

The calibration measurements and the calibration curves can be seen in the following figures and tables.
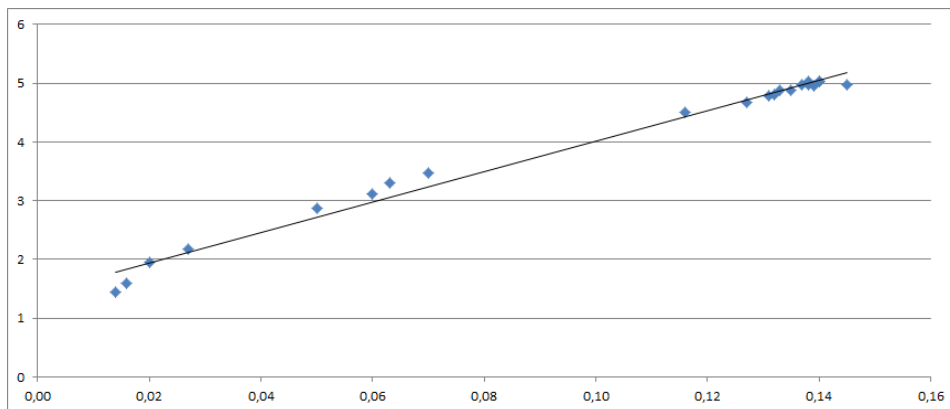
Figure E.1: Results from swirl calibration

Measured [m/s]	Pressure [bar]	Best linear fit [m/s]	Deviation
1.441	0.014	1.781	0.340
1.592	0.016	1.833	0.241
1.957	0.020	1.936	-0.021
2.174	0.027	2.118	-0.056
2.872	0.050	2.713	-0.159
3.113	0.060	2.972	-0.141
3.302	0.063	3.050	-0.252
3.471	0.070	3.231	-0.240
4.513	0.116	4.423	-0.090
4.678	0.127	4.708	0.030
4.790	0.131	4.811	0.021
4.796	0.132	4.837	0.041
4.882	0.133	4.863	-0.019
4.878	0.135	4.915	0.037
4.950	0.139	5.018	0.068
4.965	0.137	4.967	0.002
4.982	0.138	4.992	0.010
4.969	0.145	5.174	0.205
5.021	0.138	4.992	-0.029
5.039	0.140	5.044	0.005
5.038	0.140	5.044	0.006

Table E.2: Calibration data from swirl calibration
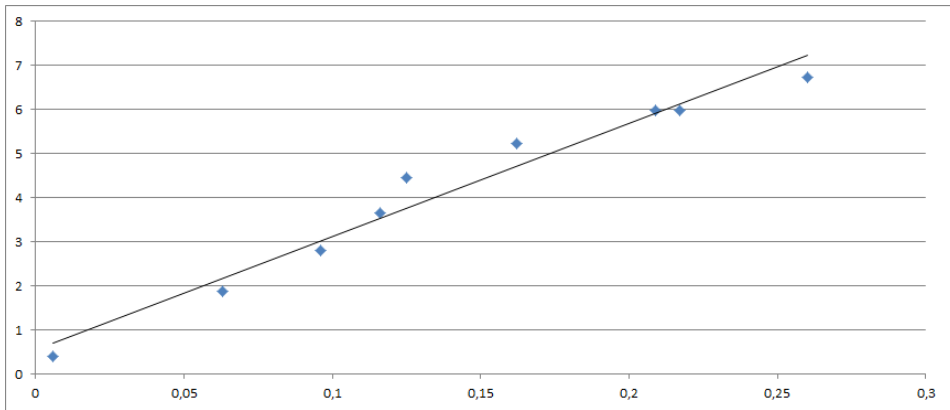
Figure E.2: Results from pelton calibration

Measured [m/s]	Pressure [bar]	Best linear fit [m/s]	Deviation
5.992	0.209	5.922	-0.070
6.743	0.260	7.237	0.494
5.981	0.217	6.129	0.147
5.222	0.162	4.711	-0.510
4.449	0.125	3.758	-0.691
3.653	0.116	3.526	-0.127
2.814	0.096	3.011	0.196
1.883	0.063	2.160	0.278
0.409	0.006	0.692	0.283

Table E.3: Calibration data from pelton calibration

Appendix F

Risk assessment

The risk assessment performed before the calibration in the swirl rig is presented on the following pages.

Risikovurderingsrapport

SWIRL-rigg

Prosjekttittel	SWIRL-rigg
Apparatur	SWIRL-rigg
Enhet	NTNU
Apparaturansvarlig	Bård Brandåstrø
Prosjektleder	Torbjørn Nielsen
HMS-koordinator	Morten Grønli
HMS-ansvarlig (linjeleder)	Olav Bolland
Plassering	Vannkraftlaboratoriet, 2.etasje
Romnummer	21
Risikovurdering utført av	Sverre Stefanussen Foslie i samarbeid med Bård Brandåstrø

Godkjenning:

	Navn	Dato	Signatur
Prosjektleder	Torbjørn Nielsen		
HMS koordinator	Morten Grønli		
HMS ansvarlig (linjeleder)	Olav Bolland		

INNHOLDSFORTEGNELSE

1   INNLEDNING

Eksisterende swirlrigg plassert i 2. etasje på Vannkraftlaboratoriet. Riggen skal kjøres med 1 volumstrømsmåler og det skal gjøres målinger med et pitotrør tilkoblet to differensialtrykkmålere. Målingene skal registreres av en NI DAQ. Formålet er å kalibrere en knivpitot for å bruke den i videre målinger.

2   KONKLUSJON

Riggen er bygget til god laboratorium praksis (GLP).

Apparaturkortet får en gyldighet på **12 måneder**
Forsøk pågår kort får en gyldighet på **12 måneder**

3   ORGANISERING

Rolle	NTNU
Prosjektleder	Torbjørn Nielsen
Apparaturansvarlig	Bård Brandåstrø
Romansvarlig	
HMS koordinator	Morten Grønli
HMS ansvarlig (linjeleder):	Olav Bolland

4   RISIKOSTYRING AV PROSJEKTET

Hovedaktiviteter risikostyring	Nødvendige tiltak, dokumentasjon	DTG
Prosjekt initiering	Prosjekt initiering mal	
Veiledningsmøte	Skjema for Veiledningsmøte med pre-risikovurdering	
Innledende risikovurdering	Fareidentifikasjon – HAZID Skjema grovanalyse	
Vurdering av teknisk sikkerhet	Prosess-HAZOP Tekniske dokumentasjoner	
Vurdering av operasjonell sikkerhet	Prosedyre-HAZOP Opplæringsplan for operatører	
Sluttvurdering, kvalitetssikring	Uavhengig kontroll Utstedelse av apparaturkort Utstedelse av forsøk pågår kort	

5   TEGNINGER, FOTO, BESKRIVELSER AV FORSØKSOPPSETT

Vedlegg:
Prosess og Instrumenterings Diagram, (PID) skal inneholde:
- *Alle komponenter i forsøksoppsetningen*
- *Komponentliste med spesifikasjoner*

- *Tegninger og bilder som beskriver forsøksoppsetningen.*

Hvor oppholder operatør seg, hvor er gassflasker, avstegningsventiler for vann/luft.
Annen dokumentasjon som beskriver oppsett og virkemåte.

6 EVAKUERING FRA FORSØKSOPPSETNINGEN

Evakuering skjer på signal fra alarmklokker eller lokale gassalarmstasjon med egen lokal varsling med lyd og lys utenfor aktuelle rom, se 6.2
Evakuering fra rigg området foregår igjennom merkede nødutganger til møteplass, (hjørnet gamle kjemi/kjelhuset eller parkeringsplass 1a-b.)
Aksjon på rigg ved evakuering: *Pumpen til riggen skal være avslått.*

7 VARSLING

7.1 Før forsøkskjøring

Varsling per e-post, til **Liste iept-experiments@ivt.ntnu.no**
I e-posten skal det stå::
- Navn på forsøksleder:
- Navn på forsøksrigg:
- Tid for start: (dato og klokkeslett)
- Tid for stop: (dato og klokkeslett)

All forsøkskjøringen skal planlegges og legges inn i aktivitetskalender for lab. Forsøksleder må få bekreftelse på at forsøkene er klarert med øvrig labdrift før forsøk kan iverksettes.

7.2 Ved uønskede hendelser

BRANN
Ved brann en ikke selv er i stand til å slukke med rimelige lokalt tilgjengelige slukkemidler, skal nærmeste brannalarm utløses og arealet evakueres raskest mulig. En skal så være tilgjengelig for brannvesen/bygningsvaktmester for å påvise brannsted.
Om mulig varsles så:

NTNU	SINTEF
Morten Grønli, Mob: 918 97 515	Harald Mæhlum, Mob: 930 14 986
Olav Bolland: Mob: 918 97 209	Anne Karin T. Hemmingsen Mob: 930 19 669
NTNU – SINTEF Beredskapstelefon	800 80 388

GASSALARM
Ved gassalarm skal gassflasker stenges umiddelbart og området ventileres. Klarer man ikke innen rimelig tid å få ned nivået på gasskonsentrasjonen så utløses brannalarm og laben evakueres. Dedikert personell og eller brannvesen sjekker så lekkasjested for å fastslå om det er mulig å tette lekkasje og lufte ut området på en forsvarlig måte.
Varslingsrekkefølge som i overstående punkt.

PERSONSKADE
- Førstehjelpsutstyr i Brann/førstehjelpsstasjoner,

- Rop på hjelp,
- Start livreddende førstehjelp
- **Ring 113** hvis det er eller det er tvil om det er alvorlig skade.

ANDRE UØNSKEDE HENDELSER (AVVIK)
NTNU:
Rapportering av uønskede hendelser, Innsida, avviksmeldinger
https://innsida.ntnu.no/wiki/-/wiki/Norsk/Melde+avvik

SINTEF:
Synergi

8   VURDERING AV TEKNISK SIKKERHET

8.1   Fareidentifikasjon, HAZOP

Se kapittel 13 "Veiledning til rapport mal.
Forsøksoppsetningen deles inn i følgende noder:

Node 1	Pumpe til rigg	
Node 2	Testrigg	
Node 3	Sump	

Vedlegg, skjema: Hazop_mal
Vurdering: (Sikkerhet ivaretatt)

8.2   Brannfarlig, reaksjonsfarlig og trykksatt stoff og gass

Se kapittel 13 "Veiledning til rapport mal.
Inneholder forsøkene brannfarlig, reaksjonsfarlig og trykksatt stoff

JA	Eksplosjonsverndokument utarbeides og eller dokumentert trykktest, (kap 7.3)

Vurdering: *Vann ved lavt trykk*

8.3   Trykkpåkjent utstyr

Inneholder forsøksoppsetningen trykkpåkjent utstyr:

JA	

Vurdering: Eksisterende rigg

8.4   Påvirkning av ytre miljø (utslipp til luft/vann, støy, temperatur, rystelser, lukt)

Se kapittel 13 "Veiledning til rapport mal..

NEI	

8.5   Stråling

Se kapittel 13 "Veiledning til rapport mal.

NEI	

8.6 Bruk og behandling av kjemikalier

NEI	

8.7 El sikkerhet (behov for å avvike fra gjeldende forskrifter og normer)

NEI	

9 VURDERING AV OPERASJONELL SIKKERHET

Sikrer at etablerte prosedyrer dekker alle identifiserte risikoforhold som må håndteres gjennom operasjonelle barrierer og at operatører og teknisk utførende har tilstrekkelig kompetanse.

9.1 Prosedyre HAZOP

Se kapittel 13 "Veiledning til rapport mal.
Metoden er en undersøkelse av operasjonsprosedyrer, og identifiserer årsaker og farekilder for operasjonelle problemer.
Vedlegg: HAZOP_MAL_Prosedyre
Vurdering:

9.2 Drifts og nødstopps prosedyre

Se kapittel 13 "Veiledning til rapport mal.
Driftsprosedyren er en sjekkliste som skal fylles ut for hvert forsøk.
Nødstopp prosedyren skal sette forsøksoppsetningen i en harmløs tilstand ved uforutsette hendelser.

Vedlegg Prosedyre for drift av swirlrigg
Nødstopp prosedyre: Pumpa til rigg stoppes ved å trykke på nødstoppsbryter enten på østveggen ved peltonturbin eller inne i kontrollbua.

9.3 Opplæring av operatører

Dokument som viser Opplæringsplan for operatører utarbeides for alle forøksoppsetninger*.*
- *Hvilke krav er det til opplæring av operatører.*
- *Hva skal til for å bli selvstendig operatør*
- *Arbeidsbeskrivelse for operatører*

Vedlegg*:* Opplæringsplan for operatører

9.4 Tekniske modifikasjoner

9.5 Personlig verneutstyr

- *Det er påbudt med vernebriller i sonen anlegget er plassert i.*
- *Det skal benyttes hørselsvern ved drift av rigg.*

9.6 Generelt

- ▪ *Vann og trykklufttilførsel i slanger skal stenges/kobles fra ved nærmeste fastpunkt når riggen ikke er i bruk.*

9.7 Sikkerhetsutrustning

9.8 Spesielle tiltak

10 TALLFESTING AV RESTRISIKO – RISIKOMATRISE

Se kapittel 13 "Veiledning til rapport mal.

Risikomatrisen vil gi en visualisering og en samlet oversikt over aktivitetens risikoforhold slik at ledelse og brukere får et mest mulig komplett bilde av risikoforhold.

IDnr	Aktivitet-hendelse	Frekv-Sans	Kons	RV
	Ledningsbrudd Vannsprut med lavt trykk *Vernebriller skal benyttes*	1	B	B1
	Støy ved drift *Hørselsvern skal benyttes*	4	B	B4
	Feil bruk av utstyr, skade på utstyr *Driftsprosedyre skal følges*	1	C	C1

Vurdering restrisiko: *Deltakerne foretar en helhetsvurdering for å avgjøre om gjenværende risiko ved aktiviteten/prosessen er akseptabel. Avsperring og kjøring utenom arbeidstid*

11 LOVER FORSKRIFTER OG PÅLEGG SOM GJELDER

Se http://www.arbeidstilsynet.no/regelverk/index.html
- Lov om tilsyn med elektriske anlegg og elektrisk utstyr (1929)
- Arbeidsmiljøloven
- Forskrift om systematisk helse-, miljø- og sikkerhetsarbeid (HMS Internkontrollforskrift)
- Forskrift om sikkerhet ved arbeid og drift av elektriske anlegg (FSE 2006)
- Forskrift om elektriske forsyningsanlegg (FEF 2006)
- Forskrift om utstyr og sikkerhetssystem til bruk i eksplosjonsfarlig område NEK 420
- Forskrift om håndtering av brannfarlig, reaksjonsfarlig og trykksatt stoff samt utstyr og anlegg som benyttes ved håndteringen
- Forskrift om Håndtering av eksplosjonsfarlig stoff
- Forskrift om bruk av arbeidsutstyr.
- Forskrift om Arbeidsplasser og arbeidslokaler
- Forskrift om Bruk av personlig verneutstyr på arbeidsplassen
- Forskrift om Helse og sikkerhet i eksplosjonsfarlige atmosfærer
- Forskrift om Høytrykksspyling
- Forskrift om Maskiner
- Forskrift om Sikkerhetsskilting og signalgivning på arbeidsplassen
- Forskrift om Stillaser, stiger og arbeid på tak m.m.
- Forskrift om Sveising, termisk skjæring, termisk sprøyting, kullbuemeisling, lodding og sliping (varmt arbeid)
- Forskrift om Tekniske innretninger
- Forskrift om Tungt og ensformig arbeid
- Forskrift om Vern mot eksponering for kjemikalier på arbeidsplassen (Kjemikalieforskriften)
- Forskrift om Vern mot kunstig optisk stråling på arbeidsplassen
- Forskrift om Vern mot mekaniske vibrasjoner
- Forskrift om Vern mot støy på arbeidsplassen

Veiledninger fra arbeidstilsynet
se: http://www.arbeidstilsynet.no/regelverk/veiledninger.html

12 DOKUMENTASJON

- Tegninger, foto, beskrivelser av forsøksoppsetningen
- Hazop_mal
- Sertifikat for trykkpåkjent utstyr
- Håndtering avfall i NTNU
- Sikker bruk av LASERE, retningslinje
- HAZOP_MAL_Prosedyre
- Forsøksprosedyre
- Opplæringsplan for operatører
- Skjema for sikker jobb analyse, (SJA)
- Apparaturkortet
- Forsøk pågår kort

13 VEILEDNING TIL RAPPORTMAL

Kapittel 7 Vurdering av teknisk sikkerhet

Sikre at design av apparatur er optimalisert i forhold til teknisk sikkerhet.
Identifisere risikoforhold knyttet til valgt design, og eventuelt å initiere re-design for å sikre at størst mulig andel av risiko elimineres gjennom teknisk sikkerhet.
Punktene skal beskrive hva forsøksoppsetningen faktisk er i stand til å tåle og aksept for utslipp.

7.1 Fareidentifikasjon, HAZOP

Forsøksoppsetningen deles inn i noder: (eks M*otorenhet, pumpeenhet, kjøleenhet.)*
Ved hjelp av ledeord identifiseres årsak, konsekvens og sikkerhetstiltak. Konkluderes det med at tiltak er nødvendig anbefales disse på bakgrunn av dette. Tiltakene lukkes når de er utført og Hazop sluttføres.
(eks "No flow", årsak: rør er deformert, konsekvens: pumpe går varm, sikkerhetsforanstaltning: måling av flow med kobling opp mot nødstopp eller hvis konsekvensen ikke er kritisk benyttes manuell overvåkning og punktet legges inn i den operasjonelle prosedyren.)

7.2 Brannfarlig, reaksjonsfarlig og trykksatt stoff.

I henhold til Forskrift om håndtering av brannfarlig, reaksjonsfarlig og trykksatt stoff samt utstyr og anlegg som benyttes ved håndteringen

Brannfarlig stoff: Fast, flytende eller gassformig stoff, stoffblanding, samt stoff som forekommer i kombinasjoner av slike tilstander, som i kraft av sitt flammepunkt, kontakt med andre stoffer, trykk, temperatur eller andre kjemiske egenskaper representerer en fare for brann.

Reaksjonsfarlig stoff: Fast, flytende, eller gassformig stoff, stoffblanding, samt stoff som forekommer i kombinasjoner av slike tilstander, som ved kontakt med vann, ved sitt trykk, temperatur eller andre kjemiske forhold, representerer en fare for farlig reaksjon, eksplosjon eller utslipp av farlig gass, damp, støv eller tåke.

Trykksatt stoff: Annet fast, flytende eller gassformig stoff eller stoffblanding enn brann- eller reaksjonsfarlig stoff, som er under trykk, og som derved kan representere en fare ved ukontrollert utslipp.

Nærmere kriterier for klassifisering av brannfarlig, reaksjonsfarlig og trykksatt stoff er fastsatt i vedlegg 1 i veiledningen til forskriften "Brannfarlig, reaksjonsfarlig og trykksatt stoff"
http://www.dsb.no/Global/Publikasjoner/2009/Veiledning/Generell%20veiledning.pdf
http://www.dsb.no/Global/Publikasjoner/2010/Tema/Temaveiledning_bruk_av_farlig_stoff_Del_1.pdf
Rigg og areal skal gjennomgås med hensyn på vurdering av Ex sone
- Sone 0: Alltid eksplosiv atmosfære, for eksempel inne i tanker med gass, brennbar væske.
- Sone 1: Primær sone, tidvis eksplosiv atmosfære for eksempel et fylle tappe punkt

- Sone 2: Sekundert utslippssted, kan få eksplosiv atmosfære ved uhell, for eksempel ved flenser, ventiler og koblingspunkt

7.4 Påvirkning av ytre miljø

Med forurensning forstås: tilførsel av fast stoff, væske eller gass til luft, vann eller i grunnen støy og rystelser påvirkning av temperaturen som er eller kan være til skade eller ulempe for miljøet.
Regelverk: http://www.lovdata.no/all/hl-19810313-006.html#6
NTNU retningslinjer for avfall se: http://www.ntnu.no/hms/retningslinjer/HMSR18B.pdf

7.5 Stråling

Stråling defineres som

Ioniserende stråling: Elektromagnetisk stråling (i strålevernsammenheng med bølgelengde <100 nm) eller hurtige atomære partikler (f.eks alfa- og beta-partikler) som har evne til å ionisere atomer eller molekyler
Ikke-ioniserende stråling: Elektromagnetisk stråling (bølgelengde >100 nm), og ultralyd[1], som har liten eller ingen evne til å ionisere.
Strålekilder: Alle ioniserende og sterke ikke-ioniserende strålekilder.
Ioniserende strålekilder: Kilder som avgir ioniserende stråling, f.eks alle typer radioaktive kilder, røntgenapparater, elektronmikroskop
Sterke ikke-ioniserende strålekilder: Kilder som avgir sterk ikke-ioniserende stråling som kan skade helse og/eller ytre miljø, f.eks laser klasse 3B og 4, MR[2]-systemer, UVC[3]-kilder, kraftige IR-kilder[4]
[1] Ultralyd er akustisk stråling ("lyd") over det hørbare frekvensområdet (>20 kHz). I strålevernforskriften er ultralyd omtalt sammen med elektromagnetisk ikke-ioniserende stråling.   [2] MR (eg. NMR) - kjernemagnetisk resonans, metode som nyttes til å «avbilde» indre strukturer i ulike materialer.   [3] UVC er elektromagnetisk stråling i bølgelengdeområdet 100-280 nm.   [4] IR er elektromagnetisk stråling i bølgelengdeområdet 700 nm – 1 mm.

For hver laser skal det finnes en informasjonsperm(HMSRV3404B) som skal inneholde:
- Generell informasjon
- Navn på instrumentansvarlig og stedfortreder, og lokal strålevernskoordinator
- Sentrale data om apparaturen
- Instrumentspesifikk dokumentasjon
- Referanser til (evt kopier av) datablader, strålevernbestemmelser, o.l.
- Vurderinger av risikomomenter
- Instruks for brukere
- Instruks for praktisk bruk; oppstart, drift, avstenging, sikkerhetsforholdsregler, loggføring, avlåsing, evt. bruk av strålingsmåler, osv.
- Nødprosedyrer

Se ellers retningslinjen til NTNU for laser: http://www.ntnu.no/hms/retningslinjer/HMSR34B.pdf

7.6 Bruk og behandling av kjemikalier.

Her forstås kjemikalier som grunnstoff som kan utgjøre en fare for arbeidstakers sikkerhet og helse.
Se ellers: http://www.lovdata.no/cgi-wift/ldles?doc=/sf/sf/sf-20010430-0443.html
Sikkerhetsdatablar skal være i forøkenes HMS perm og kjemikaliene registrert i Stoffkartoteket.

Kapittel 8 Vurdering av operasjonell sikkerhet

Sikrer at etablerte prosedyrer dekker alle identifiserte risikoforhold som må håndteres gjennom operasjonelle barrierer og at operatører og teknisk utførende har tilstrekkelig kompetanse.

8.1 Prosedyre Hazop

Prosedyre-HAZOP gjennomføres som en systematisk gjennomgang av den aktuelle prosedyren ved hjelp av fastlagt HAZOP-metodikk og definerte ledeord. Prosedyren brytes ned i enkeltstående arbeidsoperasjoner (noder) og analyseres ved hjelp av ledeordene for å avdekke mulige avvik, uklarheter eller kilder til mangelfull gjennomføring og feil.

8.2 Drifts og nødstopp prosedyrer

Utarbeides for alle forsøksoppsetninger.

Driftsprosedyren skal stegvis beskrive gjennomføringen av et forsøk, inndelt i oppstart, under drift og avslutning. Prosedyren skal beskrive forutsetninger og tilstand for start, driftsparametere med hvor store avvik som tillates før forsøket avbrytes og hvilken tilstand riggen skal forlates.

Nødstopp-prosedyre beskriver hvordan en nødstopp skal skje, (utført av uinnvidde),
hva som skjer, (strøm/gass tilførsel) og
hvilke hendelser som skal aktivere nødstopp, (brannalarm, lekkasje).

Kapittel 9 Risikomatrise Tallfesting av restrisiko

For å synliggjøre samlet risiko, jevnfør skjema for risikovurdering, plottes hver enkelt aktivitets verdi for sannsynlighet og konsekvens inn i risikomatrisen. Bruk aktivitetens IDnr. Eksempel: Hvis aktivitet med IDnr. 1 har fått en risikoverdi D3 (sannsynlighet 3 x konsekvens D) settes aktivitetens IDnr i risikomatrisens felt for 3D. Slik settes alle aktivitetenes risikoverdier (IDnr) inn i risikomatrisen.

I risikomatrisen er ulike grader av risiko merket med rød, gul eller grønn. Når en aktivitets risiko havner på rød (= uakseptabel risiko), skal risikoreduserende tiltak gjennomføres. Ny vurdering gjennomføres etter at tiltak er iverksatt for å se om risikoverdien er kommet ned på akseptabelt nivå.

KONSEKVENS	**Svært alvorlig**	E1	E2	E3	E4	E5
	Alvorlig	D1	D2	D3	D4	D5
	Moderat	C1	C2	C3	C4	C5
	Liten	B1	B2	B3	B4	B5
	Svært liten	A1	A2	A3	A4	A5
		Svært liten	Liten	Middels	Stor	Svært Stor
		SANSYNLIGHET				

Prinsipp over akseptkriterium. Forklaring av fargene som er brukt i risikomatrisen.

Farge		Beskrivelse
Rød		Uakseptabel risiko. Tiltak skal gjennomføres for å redusere risikoen.
Gul		Vurderingsområde. Tiltak skal vurderes.
Grønn		Akseptabel risiko. Tiltak kan vurderes ut fra andre hensyn.

Vedlegg til Risikovurderingsrapport

SWIRL-rigg

Prosjekttittel	SWIRL-rigg
Apparatur	SWIRL-rigg
Enhet	NTNU
Apparaturansvarlig	Bård Brandåstrø
Prosjektleder	Torbjørn Nielsen
HMS-koordinator	Morten Grønli
HMS-ansvarlig (linjeleder)	Olav Bolland
Plassering	Vannkraftlaboratoriet, 2.etasje
Romnummer	21
Risikovurdering utført av	Sverre Stefanussen Foslie i samarbeid med Bård Brandåstrø

INNHOLDSFORTEGNELSE

VEDLEGG A: PROSESS OG INSTRUMENTERINGSDIAGRAM

NTNU   ⊙ SINTEF

VEDLEGG B: PROSESS OGHAZOP MAL

Project: **Node: 1**						**Page**	
Ref#	**Guideword**	**Causes**	**Consequences**	**Safeguards**	**Recommendations**	**Action**	**Date/Sign**
	No flow						
	Reverse flow						
	More flow						
	Less flow						
	More level						
	Less level						
	More pressure						
	Less pressure						
	More temperature						
	Less temperature						
	More viscosity						
	Less viscosity						
	Composition Change						
	Contamination						
	Relief						
	Instrumentation						
	Sampling						
	Corrosion/erosion						
	Service failure						
	Abnormal operation						
	Maintenance						

NTNU   **SINTEF**

Project: Node: 1						Page	
Ref#	Guideword	Causes	Consequences	Safeguards	Recommendations	Action	Date/Sign
	Ignition						
	Spare equipment						
	Safety						

VEDLEGG C: PRØVESERTIFIKAT FOR LOKAL TRYKKTESTING

**Trykk testen skal utføres I følge NS-EN 13445 del 5 (Inspeksjon og prøving).
Se også prosedyre for trykktesting gjeldende for VATL lab**

Trykkpåkjent utstyr:	
Benyttes i rigg:	
Design trykk for utstyr (bara):	
Maksimum tillatt trykk (bara): (i.e. burst pressure om kjent)	
Maksimum driftstrykk i denne rigg:	

Prøvetrykket skal fastlegges i følge standarden og med hensyn til maksimum tillatt trykk.

Prøvetrykk (bara):			
X maksimum driftstrykk: I følge standard			
Test medium:			
Temperatur (°C)			
Start tid:		Trykk (bara):	
Slutt tid:		Trykk (bara):	
Maksimum driftstrykk i denne rigg:			

Eventuelle repetisjoner fra atm. trykk til maksimum prøvetrykk:…………….

Test trykket, dato for testing og maksimum tillatt driftstrykk skal markers på (skilt eller innslått)

_____   _____

Sted og dato   Signatur

NTNU   SINTEF
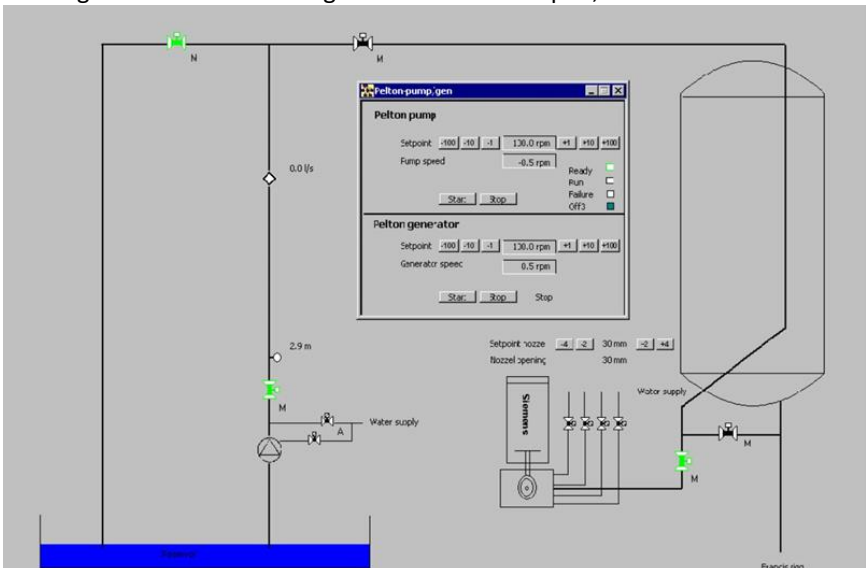
VEDLEGG D: HAZOP MAL PROSEDYRE

Project: Node: 1						Page	
Ref#	**Guideword**	**Causes**	**Consequences**	**Safeguards**	**Recommendations**	**Action**	**Date/Sign**
	Uklar	Prosedyre er laget for ambisiøs eller preget av forvirring					
	Trinn på feil plass	Prosedyren vil lede til at handlinger blir gjennomført i feil mønster/rekkefølge					
	Feil handling	Prosedyrens handling er feil spesifisert					
	Uriktig informasjon	Informasjon som er gitt i forkant av handling er feil spesifisert					
	Trinn utelatt	Manglende trinn, eller trinn krever for mye av operatør					
	Trinn mislykket	Trinn har stor sannsynlighet for å mislykkes					
	Påvirkning og effekter fra andre	Prosedyrens prestasjoner vil trolig bli påvirket av andre kilder					

VEDLEGG E: FORSØKSPROSEDYRE

Prosjekt	Dato	Signatur
Swirl Rigg		
Apparatur		
SWIRL Rigg		
Prosjektleder		
Torbjørn Nielsen		

	Conditions for the experiment:	Completed
	Experiments should be run in normal working hours, 08:00-16:00 during winter time and 08.00-15.00 during summer time. Experiments outside normal working hours shall be approved.	ok
	One person must always be present while running experiments, and should be approved as an experimental leader.	ok
	An early warning is given according to the lab rules, and accepted by authorized personnel.	ok
	Be sure that everyone taking part of the experiment is wearing the necessary protecting equipment and is aware of the shut down procedure and escape routes.	ok
	Preparations	**Carried out**
	Post the "Experiment in progress" sign.	
	Make sure all the valves are in correct position, so that the water goes to the swirl rig and not the Pelton-rig. Green valves are open, black are closed.	
	The pump is controlled from the small window "Pelton pump/gen". The pump set point should be at 100 rpm before start up. The pump is controlled by the buttons to the right and left for the set point window	
	Start-up	
	The pump must be at 500 rpm before the water is let into the rig	
	When starting, the rig must be emptied for air. Follow the procedure in the	

	next steps	
	Open valve V3 (this may be left open the entire start-up)	
	Open the vent valves L1 and L2, and close the backpressure valve VT completely	
	To fill the rig with water, drive the pump to 600rpm	
	When the water surface is above the Plexiglas section, control that V2 is open and close valve V1 and vent valve L1	
	When there is a continuously water stream through L2, close L2 and open L1. Then open V1 and closes V2. Hopefully all air is now above the pipe where V2 and L2 is mounted, and will be vented through L1. When there is a continuously water stream in L1 the system is emptied of air	
	Left over air can be vented by opening V1 and V2 so that the flow approaches maximum. Make sure that the venting valves are closed before opening the back pressure valve. If the static pressure drops below the atmospheric pressure, air will be sucked in, and the venting will have to be repeated	
	Open the back pressure valve VT in small steps while you increase the pump speed to 900rpm	
	If the nozzle is not in use, remember to close valve V3	
	During the experiment	**Ved kjøring**
	To adjust operating point, adjust the back pressure valve VT, V2 and V1 (and V3 if in use)	
	Remember that by adjusting one valve, this will affect the operation point of the rest of the rig. The loss coefficient can become large when dealing with low flow and when the valves are almost closed	
	End of experiment	
	The pump speed should be reduced to 100 rpm before shutdown	
	Remove all obstructions/barriers/signs around the experiment.	
	Tidy up and return all tools and equipment.	
	Tidy and cleanup work areas.	
	Return equipment and systems back to their normal operation settings (fire alarm)	
	To reflect on before the next experiment and experience useful for others	
	Was the experiment completed as planned and on scheduled in professional terms?	
	Was the competence which was needed for security and completion of the experiment available to you?	
	Do you have any information/ knowledge from the experiment that you should document and share with fellow colleagues?	

Operator(s):

Navn	Dato	Signatur
Sverre Stefanussen Foslie		

VEDLEGG F: OPPLÆRINGSPLAN FOR OPPERATØRER

Prosjekt	Dato	Signatur
Swirl Rigg		
Apparatur		
SWIRL Rigg		
Prosjektleder		
Torbjørn Nielsen		

	Gjennomført HMS kurs for EPT lab	
	Runde i lab	
	Rutiner/regler og Arbeidstid	
	Kjenner til evakueringsprosedyrer	
	Aktivitetskalender	
	Innmelding av forsøk til: iept-experiments@ivt.ntnu.no	
	Gjennomgang av Swirl-rigg	
	Gjennomgang av komponenter i rigg	
	Gjennomgang av kritiske komponenter	
	Driftsprosedyre	
	Nødstopprosedyre	
	Nærmeste brann/førstehjelpsstsajon	
	Kunne forklare og svare på spørsmål om oppsettet	

Jeg erklærer herved at jeg har gjennomgått og forstått HMS-regelverket, har fått hensiktsmessig opplæring for å kjøre dette eksperimentet og er klar over mitt personlige ansvar ved å arbeide i EPT laboratorier.

Operator(s):

Navn	Dato	Signatur
Sverre Stefanussen Foslie		

VEDLEGG G: SKJEMA FOR SIKKER JOBB ANALYSE

SJA tittel:		
Dato:	Sted:	
Kryss av for utfylt sjekkliste:		

Deltakere:		
SJA-ansvarlig:		

Arbeidsbeskrivelse: (Hva og hvordan?)

Risiko forbundet med arbeidet:

Beskyttelse/sikring: (tiltaksplan, se neste side)

Konklusjon/kommentar:

Anbefaling/godkjenning:	Dato/Signatur:	Anbefaling/godkjenning:	Dato/Signatur:
SJA-ansvarlig:		HMS koordinator	
Ansvarlig for utføring:		Annen (stilling):	

HMS aspekt	Ja	Nei	NA	Kommentar / tiltak	Ansv.
Dokumentasjon, erfaring, kompetanse					
Kjent arbeidsoperasjon?					
Kjennskap til erfaringer/uønskede hendelser fra tilsvarende operasjoner?					
Nødvendig personell?					
Kommunikasjon og koordinering					
Mulig konflikt med andre operasjoner?					
Håndtering av en evnt. hendelse (alarm, evakuering)?					
Behov for ekstra vakt?					
Arbeidsstedet					
Uvante arbeidsstillinger?					
Arbeid i tanker, kummer el.lignende?					
Arbeid i grøfter eller sjakter?					
Rent og ryddig?					
Verneutstyr ut over det personlige?					
Vær, vind, sikt, belysning, ventilasjon?					
Bruk av stillaser/lift/seler/stropper?					
Arbeid i høyden?					
Ioniserende stråling?					
Rømningsveier OK?					
Kjemiske farer					
Bruk av helseskadelige/giftige/etsende kjemikalier?					
Bruk av brannfarlige eller eksplosjonsfarlige kjemikalier?					
Er broken risikovurdert?					
Biologisk materiale?					
Støv/asbest/isolasjonsmateriale?					
Mekaniske farer					
Stabilitet/styrke/spenning?					
Klem/kutt/slag?					
Støy/trykk/temperatur?					
Behandling av avfall?					
Behov for spesialverktøy?					
Elektriske farer					
Strøm/spenning/over 1000V?					
Støt/krypstrøm?					
Tap av strømtilførsel?					
Området					
Behov for befaring?					
Merking/skilting/avsperring?					
Miljømessige konsekvenser?					
Sentrale fysiske sikkerhetssystemer					
Arbeid på sikkerhetssystemer?					
Frakobling av sikkerhetssystemer?					
Annet					

APPARATURKORT / UNITCARD

Dette kortet SKAL henges godt synlig på apparaturen!
This card MUST be posted on a visible place on the unit!

Apparatur (Unit)	**Dato Godkjent** (Date Approved)
Swirl-Rigg	
Faglig Ansvarlig (Scientific Responsible)	**Telefon mobil/privat** (Phone no. mobile/private)
Torbjørn Nielsen	+4791897572
Apparaturansvarlig (Unit Responsible) Sverre Stefanussen Foslie (student) Bård Brandåstrø (ansatt)	**Telefon mobil/privat** (Phone no. mobile/private) +4792842070 +4791897257
Sikkerhetsrisikoer (Safety hazards) Støy, sprut, rørbrudd.	
Sikkerhetsregler (Safety rules) 	
Nødstopp prosedyre (Emergency shutdown) Pumpa til rigg stoppes ved å trykke på nødstoppsbryter enten på østveggen ved peltonturbin eller inne i kontrollbua.	

Her finner du (Here you will find):

Prosedyrer (Procedures)	I perm ved rigg
Bruksanvisning (Users manual)	I perm ved rigg

Nærmeste (Nearest)

Brannslukningsapparat (fire extinguisher)	Ved inngangen til lunsjrommet
Førstehjelpsskap (first aid cabinet)	1.etasje ved utgang mot øst

NTNU
Institutt for energi og prosessteknikk

Dato

_____

Signert

_____

FORSØK PÅGÅR /EXPERIMENT IN PROGRESS

Dette kortet SKAL henges opp før forsøk kan starte!
This card MUST be posted on the unit before the experiment startup!

Apparatur (Unit)	**Dato Godkjent** (Date Approved)
Swirl-Rigg	
Faglig Ansvarlig (Scientific Responsible)	**Telefon mobil/privat** (Phone no. mobile/private)
Torbjørn Nielsen	+4791897572
Apparaturansvarlig (Unit Responsible) Sverre Stefanussen Foslie(student) Bård Brandåstrø (ansatt)	**Telefon mobil/privat** (Phone no. mobile/private) +4792842070 +4791897257
Godkjente operatører (Approved Operators)	
Sigrid Marie Skodje	
Prosjekt (Project)	**Prosjektleder (Project leader)**
Swirl-rigg	Torbjørn Nielsen
Forsøkstid / Experimental time (start - stop)	
November 2013	
Kort beskrivelse av forsøket og relaterte farer (Short description of the experiment and related hazards**)**	
Drift av swirlrigg med ulike volumstrømmer og måling med pitot Farer: støy, sprut, rørbrudd.	

NTNU
Institutt for energi og prosessteknikk

Dato

_____

Signert

_____

Appendix G

Matlab program code

Following is an extract of the program code used for the pump design program in Matlab. The full program code can be found in the digital appendices.

```matlab
declare_global_variables;

%ccccccccccccccccccccccccccccccccccccccccccccccccccccccccccccccccccccc
% Design parameter
%ccccccccccccccccccccccccccccccccccccccccccccccccccccccccccccccccccccc
n = valg_design_rotspeed;
param_omega = n*2*pi/60;
Q = valg_design_flow;
H = valg_design_nethead;
g = valg_design_gP;

%ccccccccccccccccccccccccccccccccccccccccccccccccccccccccccccccccccccc
% Calculate specific speeds
%ccccccccccccccccccccccccccccccccccccccccccccccccccccccccccccccccccccc
n_sQ = n*Q^0.5/H^0.75;
n_sstar = n_sQ/g^0.75;
n_sQstar = (1000/60)*n_sstar;

set(hand_calc_sp_speed, ...
    'String',num2str(0.1*round(10*n_sQ)), ...
    'Value',n_sQ);

set(hand_calc_sp_speed_dimless, ...
    'String',num2str(0.1*round(10*n_sstar)), ...
    'Value', n_sstar);

%ccccccccccccccccccccccccccccccccccccccccccccccccccccccccccccccccccccc
%
% Calculate outlet values
%
%ccccccccccccccccccccccccccccccccccccccccccccccccccccccccccccccccccccc

%ccccccccccccccccccccccccccccccccccccccccccccccccccccccccccccccccccccc
% Calculate outlet area
% A_2 not taking into account vane thickness
%ccccccccccccccccccccccccccccccccccccccccccccccccccccccccccccccccccccc
D_2     = valg_design_D2;
R_2     = 0.5*D_2;
D_2_red = D_2/R_2; % Should be 2
R_2_red = 0.5*D_2_red; % Defined as 11


b_2     = valg_design_b2;
b_2_red = b_2/R_2;
set(hand_value_b2, ...
    'String',num2str(b_2), ...
    'Value',b_2);

A_2     = R_2    *2*pi*b_2;
A_2_red = R_2_red*2*pi*b_2_red; % A_2/A_2; % Defined as 1
param_A2     = A_2;
param_A2_red = A_2_red;
set(hand_calc_A2, ...
    'String',num2str(A_2), ...
    'Value',A_2);




%ccccccccccccccccccccccccccccccccccccccccccccccccccccccccccccccccccccc
% Calculate Peripherial velocity, U_2
%ccccccccccccccccccccccccccccccccccccccccccccccccccccccccccccccccccccc
```

```matlab
U_2     = R_2*param_omega;
U_2_red = U_2/U_2; % Defined as 1;
set(hand_calc_U2, ...
    'String',num2str(U_2), ...
    'Value',U_2);
set(hand_calc_U2_red, ...
    'String',num2str(U_2_red), ...
    'Value',U_2_red);
set(hand_calc_U2slip, ...
    'String',num2str(U_2), ...
    'Value',U_2);
set(hand_calc_U2slip_red, ...
    'String',num2str(U_2_red), ...
    'Value',U_2_red);

%cccccccccccccccccccccccccccccccccccccccccccccccccccccccccccccccccccccccc
% Calculate outlet meridional component of absolute velocity, C_m2
%cccccccccccccccccccccccccccccccccccccccccccccccccccccccccccccccccccccccc
C_m2      = Q/A_2;
C_m2_red = C_m2/U_2;
set(hand_calc_Cm2, ...
    'String',num2str(C_m2), ...
    'Value',C_m2);
set(hand_calc_Cm2_red, ...
    'String',num2str(C_m2_red), ...
    'Value',C_m2_red);
set(hand_calc_Cm2slip, ...
    'String',num2str(C_m2), ...
    'Value',C_m2);
set(hand_calc_Cm2slip_red, ...
    'String',num2str(C_m2_red), ...
    'Value',C_m2_red);

%cccccccccccccccccccccccccccccccccccccccccccccccccccccccccccccccccccccccc
% Calculate relative outlet velocity, W_2
% also setting the W_2slip values
%cccccccccccccccccccccccccccccccccccccccccccccccccccccccccccccccccccccccc
beta_2  = valg_design_beta2;

W_2     = C_m2/sind(beta_2);
W_2_red = W_2/U_2;
set(hand_calc_W2, ...
    'String',num2str(W_2), ...
    'Value',W_2);
set(hand_calc_W2_red, ...
    'String',num2str(W_2_red), ...
    'Value',W_2_red);


%cccccccccccccccccccccccccccccccccccccccccccccccccccccccccccccccccccccccc
% Calculate outlet peripheral component of relative velocity, W_U2
% also setting the W_U2slip values
%cccccccccccccccccccccccccccccccccccccccccccccccccccccccccccccccccccccccc
W_U2     = C_m2/tand(beta_2);
W_U2_red = W_U2/U_2;
set(hand_calc_WU2, ...
    'String',num2str(W_U2), ...
    'Value',W_U2);
set(hand_calc_WU2_red, ...
    'String',num2str(W_U2_red), ...
    'Value',W_U2_red);
```

```matlab
%cccccccccccccccccccccccccccccccccccccccccccccccccccccccccccccccccccc
% Calculate C_U2
% also setting the W_U2slip values
%cccccccccccccccccccccccccccccccccccccccccccccccccccccccccccccccccccc
C_U2     = U_2-W_U2;
C_U2_red = C_U2/U_2;
set(hand_calc_CU2, ...
    'String',num2str(C_U2), ...
    'Value',C_U2);
set(hand_calc_CU2_red, ...
    'String',num2str(C_U2_red), ...
    'Value',C_U2_red);




%cccccccccccccccccccccccccccccccccccccccccccccccccccccccccccccccccccc
%
% Calculate inlet values
%
%cccccccccccccccccccccccccccccccccccccccccccccccccccccccccccccccccccc

%cccccccccccccccccccccccccccccccccccccccccccccccccccccccccccccccccccc
% Calculate impeller eye diameter, D_1
%cccccccccccccccccccccccccccccccccccccccccccccccccccccccccccccccccccc

D_1       = valg_design_D1;
D_1i      = valg_design_D1i;
D_n       = valg_design_Dn;
R_1i      = 0.5*D_1i;
D_1i_red  = D_1i/R_2;
D_n_red   = D_n/R_2;
R_1i_red  = 0.5*D_1i_red;
R_n_red   = 0.5*D_n_red;
R_1       = 0.5*D_1;
D_1_red   = D_1/R_2;
R_1_red   = 0.5*D_1_red;
set(hand_calc_D1, ...
    'String',num2str(D_1), ...
    'Value',D_1);




%cccccccccccccccccccccccccccccccccccccccccccccccccccccccccccccccccccc
% Calculate inlet area, A_1
%cccccccccccccccccccccccccccccccccccccccccccccccccccccccccccccccccccc
A_1     = (pi)/4*(D_1^2-D_n^2);
A2_A1   = A_2/A_1;
A_1_red = A_2_red/A2_A1;

set(hand_calc_A1, ...
    'String',num2str(A_1), ...
    'Value',A_1);

set(hand_calc_ratA, ...
    'String',num2str(A2_A1), ...
    'Value',A2_A1);

param_A1     = A_1;
param_A1_red = A_1_red;
```

```matlab
%cccccccccccccccccccccccccccccccccccccccccccccccccccccccccccccccccccccccc
% Calculate inlet mean streamline diamter, D_1m
%cccccccccccccccccccccccccccccccccccccccccccccccccccccccccccccccccccccccc
D_1m     = sqrt((D_1^2+D_1i^2)*0.5);
D_1m_red = D_1m/R_2;
set(hand_calc_D1m, ...
    'String',num2str(D_1m), ....
    'Value',D_1m);

%cccccccccccccccccccccccccccccccccccccccccccccccccccccccccccccccccccccccc
% Calculate inlet circumferential velocity, U_1
%cccccccccccccccccccccccccccccccccccccccccccccccccccccccccccccccccccccccc
U_1_ring     = param_omega*D_1*0.5;
U_1_ring_red = U_1_ring/U_1_ring; % Defined as 1
set(hand_calc_U1_ring, ...
    'String',num2str(U_1_ring), ...
    'Value',U_1_ring);
set(hand_calc_U1_ring_red, ...
    'String',num2str(U_1_ring_red), ...
    'Value',U_1_ring_red);

U_1_merid     = param_omega*D_1m*0.5;
U_1_merid_red = U_1_merid/U_1_ring;
set(hand_calc_U1_merid, ...
    'String',num2str(U_1_merid), ...
    'Value',U_1_merid);
set(hand_calc_U1_merid_red, ...
    'String',num2str(U_1_merid_red), ...
    'Value',U_1_merid_red);

U_1_boss     = param_omega*D_1i*0.5;
U_1_boss_red = U_1_boss/U_1_ring;
set(hand_calc_U1_boss, ...
    'String',num2str(U_1_boss), ...
    'Value',U_1_boss);
set(hand_calc_U1_boss_red, ...
    'String',num2str(U_1_boss_red), ...
    'Value',U_1_boss_red);

%cccccccccccccccccccccccccccccccccccccccccccccccccccccccccccccccccccccccc
% Calculate inlet meridional component of absolute velocity, C_m1
%cccccccccccccccccccccccccccccccccccccccccccccccccccccccccccccccccccccccc
C_m1_ring = Q/A_1;
C_m1_ring_red = C_m1_ring/U_1_ring;
set(hand_calc_Cm1_ring, ...
    'String',num2str(C_m1_ring), ...
    'Value',C_m1_ring);
set(hand_calc_Cm1_ring_red, ...
    'String',num2str(C_m1_ring_red), ...
    'Value',C_m1_ring_red);

C_m1_merid = Q/A_1;
C_m1_merid_red = C_m1_merid/U_1_ring;
set(hand_calc_Cm1_merid, ...
    'String',num2str(C_m1_merid), ...
    'Value',C_m1_merid);
set(hand_calc_Cm1_merid_red, ...
    'String',num2str(C_m1_merid_red), ...
    'Value',C_m1_merid_red);

C_m1_boss = Q/A_1;
C_m1_boss_red = C_m1_boss/U_1_ring;
```

```matlab
set(hand_calc_Cm1_boss, ...
    'String',num2str(C_m1_boss), ...
    'Value',C_m1_boss);
set(hand_calc_Cm1_boss_red, ...
    'String',num2str(C_m1_boss_red), ...
    'Value',C_m1_boss_red);

%ccccccccccccccccccccccccccccccccccccccccccccccccccccccccccccccccccccccc
% Calculate angle of inlet at boss, beta_1
%ccccccccccccccccccccccccccccccccccccccccccccccccccccccccccccccccccccccc
beta_1_ring = atand(C_m1_ring/U_1_ring);
set(hand_calc_beta1_ring, ...
    'String',num2str(beta_1_ring), ...
    'Value',beta_1_ring);

beta_1_merid = atand(C_m1_merid/U_1_merid);
set(hand_calc_beta1_merid, ...
    'String',num2str(beta_1_merid), ...
    'Value',beta_1_merid);

beta_1_boss = atand(C_m1_boss/U_1_boss);
set(hand_calc_beta1_boss, ...
    'String',num2str(beta_1_boss), ...
    'Value',beta_1_boss);

%ccccccccccccccccccccccccccccccccccccccccccccccccccccccccccccccccccccccc
% Calculate other usesful velocities
% C_U1 at ring, merid and boss
% W_1 at ring, merid and boss
%ccccccccccccccccccccccccccccccccccccccccccccccccccccccccccccccccccccccc
C_U1_ring  = U_1_ring - Q/(A_1*tand(beta_1_ring));
C_U1_merid = U_1_merid- Q/(A_1*tand(beta_1_merid));
C_U1_boss  = U_1_boss - Q/(A_1*tand(beta_1_boss));
W_1_ring   = C_U1_ring/ sind(beta_1_ring );
W_1_merid  = C_U1_merid/sind(beta_1_merid);
W_1_boss   = C_U1_boss/ sind(beta_1_boss );

C_U1_ring_red  = C_U1_ring /U_1_ring;
C_U1_merid_red = C_U1_merid/U_1_ring;
C_U1_boss_red  = C_U1_boss /U_1_ring;
W_1_ring_red   = W_1_ring  /U_1_ring;
W_1_merid_red  = W_1_merid /U_1_ring;
W_1_boss_red   = W_1_boss  /U_1_ring;


%ccccccccccccccccccccccccccccccccccccccccccccccccccccccccccccccccccccccc
%
% Calculate slip values
%
%ccccccccccccccccccccccccccccccccccccccccccccccccccccccccccccccccccccccc

Z       = valg_design_Z;
eps_lim = exp(-8.16*sin(beta_2)/Z);
D_2     = valg_design_D2;
kw      = 1;
f1      = 0.98;

if D_1m/D_2 > eps_lim
    kw = 1-((D_1m/D_2-eps_lim)/(1-eps_lim))^3;
end

slip_coeff = f1*(1-sqrt(sind(beta_2))/Z^0.70)*kw;
```

```matlab
set(hand_calc_slip_coeff, ...
    'String',num2str(slip_coeff), ...
    'Value',slip_coeff);

%Calculate blade blockage
e_2     = valg_design_tout;
block_2 = (1-e_2*Z/(pi*D_2*sind(beta_2)))^-1;

%Calculate CU2slip
%C_U2slip_old = C_U2-(1-slip_coeff)*U_2;
C_U2slip = U_2*(slip_coeff-C_m2*block_2/(U_2*tand(beta_2)));
C_U2slip_red = C_U2slip/U_2;
set(hand_calc_CU2slip, ...
    'String',num2str(C_U2slip), ...
    'Value',C_U2slip);
set(hand_calc_CU2slip_red, ...
    'String',num2str(C_U2slip_red), ...
    'Value',C_U2slip_red);

%Calculate beta_2slip and slip_angle
beta_2slip = atand(C_m2_red/(1-C_U2slip_red));
slip_angle = beta_2-beta_2slip;

%Calculate W_2slip
W_2slip = C_m2/sind(beta_2slip);
W_2slip_red = W_2slip/U_2;
set(hand_calc_W2slip, ...
    'String',num2str(W_2slip), ...
    'Value',W_2slip);
set(hand_calc_W2slip_red, ...
    'String',num2str(W_2slip_red), ...
    'Value',W_2slip_red);

%Calculate W_U2slip
W_U2slip = C_m2/tand(beta_2slip);
W_U2slip_red = W_U2slip/U_2;
set(hand_calc_WU2slip, ...
    'String',num2str(W_U2slip), ...
    'Value',W_U2slip);
set(hand_calc_WU2slip_red, ...
    'String',num2str(W_U2slip_red), ...
    'Value',W_U2slip_red);

%cccccccccccccccccccccccccccccccccccccccccccccccccccccccccccccccccccccccccc
% Calculate absolute angles at outlet, alpha_2 and alpha_2slip
%cccccccccccccccccccccccccccccccccccccccccccccccccccccccccccccccccccccccccc

alpha_2     = atand(C_m2/C_U2);
alpha_2slip = atand(C_m2/C_U2slip);


%cccccccccccccccccccccccccccccccccccccccccccccccccccccccccccccccccccccccccc
% Update outlet angles
% also setting the beta2slip values
%cccccccccccccccccccccccccccccccccccccccccccccccccccccccccccccccccccccccccc
set(hand_value_beta2, ...
    'String',num2str(beta_2), ...
    'Value',beta_2);
set(hand_calc_beta2, ...
    'String',num2str(valg_design_beta2))
```

```matlab
set(hand_calc_beta2slip, ...
    'String',num2str(beta_2slip))


% set(hand_value_slip, ...
%     'String',num2str(slip_angle), ...
%     'Value',slip_angle);
set(hand_calc_slip, ...
    'String',num2str(slip_angle), ...
    'Value',slip_angle);

set(hand_calc_alpha2, ...
    'String',num2str(alpha_2), ...
    'Value',alpha_2);

set(hand_calc_alpha2slip, ...
    'String',num2str(alpha_2slip), ...
    'Value',alpha_2slip);




%ccccccccccccccccccccccccccccccccccccccccccccccccccccccccccccccccccccccccc
%
% Calculate the optimal hydraulic efficiency
%
%ccccccccccccccccccccccccccccccccccccccccccccccccccccccccccccccccccccccccc
if Q>1
    a=0.5;
else
    a=1;
end

m=0.08*a*(1/Q)^0.15*(45/n_sQ)^0.06;

eta_opt=1-0.065*(1/Q)^m-0.23*(0.3-log10(n_sQ/23))^2*(1/Q)^0.05;

%ccccccccccccccccccccccccccccccccccccccccccccccccccccccccccccccccccccccccc
%
% UPDATE the pump characteristics
%
%ccccccccccccccccccccccccccccccccccccccccccccccccccccccccccccccccccccccccc
set(hand_calc_eta_opt, ...
    'String',num2str(eta_opt));

% Set the calculated theoretical head
set(hand_calc_theoretical_head, ...
    'String',num2str(get(hand_calc_U2,'Value')^2/valg_design_gP));

% Set the calculated theoretical head in bar
set(hand_calc_theoretical_head_bar, ...
    'String',num2str(get(hand_calc_U2,'Value')^2*valg_design_rhoP*10^-5));

[hand_axes_charac,calc_net_head,x_max,y_max,calc_pfleiderer_slip] ...
    = draw_charac_curves( ...
        hand_axes_charac, ...
        valg_design_flow, ...
        get(hand_calc_U2,'Value'), ...
        get(hand_calc_U1_merid,'Value'), ...
        get(hand_calc_CU2,'Value'), ...
        valg_design_D2, ...
        D_1, ...
        get(hand_value_b2,'Value'), ...
        valg_design_beta2, ...
```

```matlab
        beta_1_merid, ...
        A_1, ...
        get(hand_calc_slip,'Value'), ...
        param_omega, ...
        valg_charac_friction, ...
        valg_charac_shockloss, ...
        valg_design_gP, ...
        valg_design_Z, ...
        valg_design_nethead ...
    );

% Set the calculated theoretical head with volume loss
set(hand_calc_theoretical_head_leakage,'String',num2str(y_max));

% Set the calculated theoretical head in bar with volume loss
set(hand_calc_theoretical_head_leakage_bar,'String',num2str(y_max*valg_design_rhoP*valg
_design_gP*10^-5));

% Set the calculated slip factor based on design_flow as Pfleiderer slip
set(hand_calc_pfleiderer,'String',num2str(calc_pfleiderer_slip));

% Set the calculated net head
set(hand_calc_net_head,'String',num2str(calc_net_head));

% Set the calculated net head in bar
set(hand_calc_net_head_bar,'String',num2str(calc_net_head*valg_design_rhoP*valg_design_
gP*10^-5));




% % set(hand_calc_pfleiderer,'String',num2str(pfleiderer));

% set(hand_axes_charac, ...
%     'XLim',[0 x_max], ...
%     'YLim',[0 y_max]);


%cccccccccccccccccccccccccccccccccccccccccccccccccccccccccccccccccccccccccc
%
% UPDATE the inlet velocity plot
%
%cccccccccccccccccccccccccccccccccccccccccccccccccccccccccccccccccccccccccc
[hand_plot_U1_ring,  hand_text_U1_ring, ...
 hand_plot_C1_ring,  hand_text_C1_ring, ...
 hand_plot_W1_ring,  hand_text_W1_ring, ...
 hand_plot_U1_merid,  ...
 hand_plot_W1_merid, hand_text_W1_merid, ...
 hand_plot_U1_boss,   ...
 hand_plot_W1_boss,  hand_text_W1_boss] = ...
    inlet_velocity_plot_update( ...
    hand_plot_U1_ring,  hand_text_U1_ring, ...
    hand_plot_C1_ring,  hand_text_C1_ring, ...
    hand_plot_W1_ring,  hand_text_W1_ring, ...
    hand_plot_U1_merid,  ...
    hand_plot_W1_merid, hand_text_W1_merid, ...
    hand_plot_U1_boss,   ...
    hand_plot_W1_boss,  hand_text_W1_boss, ...
    U_1_ring_red,       C_m1_ring_red, ...
    U_1_merid_red,      C_m1_merid_red, ...
    U_1_boss_red,       C_m1_boss_red);


%cccccccccccccccccccccccccccccccccccccccccccccccccccccccccccccccccccccccccc
```

```matlab
%
% UPDATE the outlet velocity plot
%
%ccccccccccccccccccccccccccccccccccccccccccccccccccccccccccccccccccccc
[hand_plot_U2,hand_text_U2, ...
 hand_plot_C2,hand_text_C2, ...
 hand_plot_W2,hand_text_W2, ...
 hand_plot_CU2,hand_text_CU2, ...
 hand_plot_Cm2,hand_text_Cm2, ...
 hand_plot_C2slip,hand_text_C2slip, ...
 hand_plot_W2slip,hand_text_W2slip, ...
 hand_plot_CU2slip,hand_text_CU2slip, ...
 hand_plot_Cm2slip] = ...
    outlet_velocity_plot_update( ...
    hand_plot_U2,   hand_text_U2, ...
    hand_plot_C2,   hand_text_C2, ...
    hand_plot_W2,   hand_text_W2, ...
    hand_plot_CU2, hand_text_CU2, ...
    hand_plot_Cm2, hand_text_Cm2, ...
    hand_plot_C2slip,  hand_text_C2slip, ...
    hand_plot_W2slip,  hand_text_W2slip, ...
    hand_plot_CU2slip, hand_text_CU2slip, ...
    hand_plot_Cm2slip, ...
    U_2_red,C_m2_red,C_U2_red,C_U2slip_red);
```

```matlab
%cccccccccccccccccccccccccccccccccccccccccccccccccccccccccccccccccccccccc
% Design parameters
%cccccccccccccccccccccccccccccccccccccccccccccccccccccccccccccccccccccccc
D_2 = valg_design_D2;
D_3 = valg_design_D3;
D_4 = valg_design_D4;
b_3 = valg_design_b3;
b_4 = valg_design_b4;
a_3 = valg_design_a3;
n   = valg_npoints_cross_diffuser;
m   = valg_npoints_stream_diffuser;
%cccccccccccccccccccccccccccccccccccccccccccccccccccccccccccccccccccccccc
%
% Calculate inlet values
%
%cccccccccccccccccccccccccccccccccccccccccccccccccccccccccccccccccccccccc

%cccccccccccccccccccccccccccccccccccccccccccccccccccccccccccccccccccccccc
% Calculate inlet peripheral velocity component of absolute velocity, C_u3
%cccccccccccccccccccccccccccccccccccccccccccccccccccccccccccccccccccccccc

C_U2slip    = get(hand_calc_CU2slip,'Value');

C_U3        = D_2*C_U2slip/D_3;
C_U3block   = C_U3;

set(hand_calc_CU3, ...
    'String',num2str(C_U3), ...
    'Value',C_U3);

set(hand_calc_CU3block, ...
    'String',num2str(C_U3block), ...
    'Value',C_U3block);

%cccccccccccccccccccccccccccccccccccccccccccccccccccccccccccccccccccccccc
% Calculate inlet peripheral velocity component of absolute velocity, C_u3,
% without slip
%cccccccccccccccccccccccccccccccccccccccccccccccccccccccccccccccccccccccc

C_U2    = get(hand_calc_CU2,'Value');

C_U3noslip       = D_2*C_U2/D_3;
C_U3noslipblock  = C_U3noslip;

set(hand_calc_CU3noslip, ...
    'String',num2str(C_U3noslip), ...
    'Value',C_U3noslip);

set(hand_calc_CU3noslipblock, ...
    'String',num2str(C_U3noslipblock), ...
    'Value',C_U3noslipblock);


%cccccccccccccccccccccccccccccccccccccccccccccccccccccccccccccccccccccccc
% Calculate meridional component of absolute velocity before diffuser inlet
%cccccccccccccccccccccccccccccccccccccccccccccccccccccccccccccccccccccccc
Q       = valg_design_flow;

C_m3    = Q/(pi*D_3*b_3);

set(hand_calc_Cm3, ...
    'String',num2str(C_m3), ...
    'Value',C_m3);
```

```matlab
C3      = sqrt(C_m3^2+C_U3^2);

set(hand_calc_C3, ...
    'String',num2str(C3), ...
    'Value',C3);

%cccccccccccccccccccccccccccccccccccccccccccccccccccccccccccccccccccccccc
% Calculate diffuser throat velocity
%cccccccccccccccccccccccccccccccccccccccccccccccccccccccccccccccccccccccc
Q       = valg_design_flow;
Z_Le    = valg_design_ZLe;    %Number of diffuser vanes


C_q3    = Q/(Z_Le*a_3*b_3);

set(hand_calc_CQ3, ...
    'String',num2str(C_q3), ...
    'Value',C_q3);

%cccccccccccccccccccccccccccccccccccccccccccccccccccccccccccccccccccccccc
% Calculate absolute flow angle before diffuser inlet
%cccccccccccccccccccccccccccccccccccccccccccccccccccccccccccccccccccccccc
alpha_3 = atand(C_m3/C_U3);

set(hand_calc_alpha3, ...
    'String',num2str(alpha_3), ...
    'Value',alpha_3);

%cccccccccccccccccccccccccccccccccccccccccccccccccccccccccccccccccccccccc
% Calculate flow conditions after diffuser inlet (with blade blockage)
%cccccccccccccccccccccccccccccccccccccccccccccccccccccccccccccccccccccccc

e_3     = valg_design_e3;       %Blade thickness at diffuser inlet

alpha_3B = valg_design_alpha3B; %Blade angle at diffuser inlet

block_3 = (1-Z_Le*e_3/(pi*D_3*sind(alpha_3B)))^-1; %Blade blockage at diffuser inlet

C_m3block = Q*block_3/(pi*D_3*b_3);    %Meridional component of flow after diffuser
inlet
alpha_3block = atand(C_m3block/C_U3);   %Flow angle after diffuser inlet
C3block = sqrt(C_m3block^2+C_U3^2);

set(hand_calc_Cm3block, ...
    'String',num2str(C_m3block), ...
    'Value',C_m3block);
set(hand_calc_alpha3block, ...
    'String',num2str(alpha_3block), ...
    'Value',alpha_3block);
set(hand_calc_C3block, ...
    'String',num2str(C3block), ...
    'Value',C3block);
%cccccccccccccccccccccccccccccccccccccccccccccccccccccccccccccccccccccccc
%
% UPDATE the inlet velocity plot
%
%cccccccccccccccccccccccccccccccccccccccccccccccccccccccccccccccccccccccc
[hand_plot_C3,hand_text_C3, ...
 hand_plot_CU3,hand_text_CU3, ...
 hand_plot_Cm3,hand_text_Cm3, ...
 hand_plot_C3block,hand_text_C3block, ...
 hand_plot_CU3block,hand_text_CU3block, ...
```

```
hand_plot_Cm3block,hand_text_Cm3block] = ...
    inlet_velocity_plot_diffuser_update( ...
    hand_plot_C3,hand_text_C3, ...
    hand_plot_CU3,hand_text_CU3, ...
    hand_plot_Cm3,hand_text_Cm3, ...
    hand_plot_C3block,hand_text_C3block, ...
    hand_plot_CU3block,hand_text_CU3block, ...
    hand_plot_Cm3block,hand_text_Cm3block, ...
    C_U3, C_U3block, ...
    C_m3, C_m3block);
```

```matlab
%cccccccccccccccccccccccccccccccccccccccccccccccccccccccccccccccccccc
%
% Pump characteristics, traditional 1
% H = (1/(1+Cp))(Hthinfty)-KfQ^2-Ks(Q-Qopt)^2
%
%cccccccccccccccccccccccccccccccccccccccccccccccccccccccccccccccccccc


% Set the calculated theoretical head
set(hand_calc_theoretical_head_trad_1, ...
    'String',num2str(get(hand_calc_U2,'Value')^2/valg_design_gP));

% Set the calculated theoretical head in bar
set(hand_calc_theoretical_head_bar_trad_1, ...
    'String',num2str(get(hand_calc_U2,'Value')^2*valg_design_rhoP*10^-5));


[hand_axes_charac_trad_1,calc_net_head_trad_1,x_max_trad_1,y_max_trad_1,calc_pfleiderer
_slip_trad_1] ...
    = draw_charac_curves_trad_1( ...
        hand_axes_charac_trad_1, ...
        valg_design_flow, ...
        get(hand_calc_U2,'Value'), ...
        get(hand_calc_U1_merid,'Value'), ...
        get(hand_calc_CU2,'Value'), ...
        valg_design_D2, ...
        D_1, ...
        get(hand_value_b2,'Value'), ...
        valg_design_beta2, ...
        beta_1_merid, ...
        A_1, ...
        get(hand_calc_slip,'Value'), ...
        param_omega, ...
        valg_charac_friction_trad_1, ...
        valg_charac_shockloss_trad_1, ...
        valg_design_gP, ...
        valg_design_Z, ...
        valg_design_nethead ...
    );

% Set the calculated theoretical head with volume loss
set(hand_calc_theoretical_head_leakage_trad_1,'String',num2str(y_max_trad_1));

% Set the calculated theoretical head in bar with volume loss
set(hand_calc_theoretical_head_leakage_bar_trad_1,'String',num2str(y_max_trad_1*valg_de
sign_rhoP*valg_design_gP*10^-5));

% Set the calculated slip factor based on design_flow as Pfleiderer slip
set(hand_calc_pfleiderer_trad_1,'String',num2str(calc_pfleiderer_slip_trad_1));

% Set the calculated net head
set(hand_calc_net_head_trad_1,'String',num2str(calc_net_head_trad_1));

% Set the calculated net head in bar
set(hand_calc_net_head_bar_trad_1,'String',num2str(calc_net_head_trad_1*valg_design_rho
P*valg_design_gP*10^-5));


%cccccccccccccccccccccccccccccccccccccccccccccccccccccccccccccccccccc
%
% Pump characteristics, traditional 2
% H = (1/(1+Cp))(Hthinfty)-KfQ^2-(u1cu1/g)
```

```matlab
%
%ccccccccccccccccccccccccccccccccccccccccccccccccccccccccccccccccccccccccc


% Set the calculated theoretical head
set(hand_calc_theoretical_head_trad_2, ...
    'String',num2str(get(hand_calc_U2,'Value')^2/valg_design_gP));

% Set the calculated theoretical head in bar
set(hand_calc_theoretical_head_bar_trad_2, ...
    'String',num2str(get(hand_calc_U2,'Value')^2*valg_design_rhoP*10^-5));


[hand_axes_charac_trad_2,calc_net_head_trad_2,x_max_trad_2,y_max_trad_2,calc_pfleiderer
_slip_trad_2] ...
    = draw_charac_curves_trad_2( ...
        hand_axes_charac_trad_2, ...
        valg_design_flow, ...
        get(hand_calc_U2,'Value'), ...
        get(hand_calc_U1_merid,'Value'), ...
        get(hand_calc_CU2,'Value'), ...
        valg_design_D2, ...
        D_1, ...
        get(hand_value_b2,'Value'), ...
        valg_design_beta2, ...
        beta_1_merid, ...
        A_1, ...
        get(hand_calc_slip,'Value'), ...
        param_omega, ...
        valg_charac_friction_trad_2, ...
        valg_charac_shockloss_trad_2, ...
        valg_design_gP, ...
        valg_design_Z, ...
        valg_design_nethead ...
    );

% Set the calculated theoretical head with volume loss
set(hand_calc_theoretical_head_leakage_trad_2,'String',num2str(y_max_trad_2));

% Set the calculated theoretical head in bar with volume loss
set(hand_calc_theoretical_head_leakage_bar_trad_2,'String',num2str(y_max_trad_2*valg_de
sign_rhoP*valg_design_gP*10^-5));

% Set the calculated slip factor based on design_flow as Pfleiderer slip
set(hand_calc_pfleiderer_trad_2,'String',num2str(calc_pfleiderer_slip_trad_2));

% Set the calculated net head
set(hand_calc_net_head_trad_2,'String',num2str(calc_net_head_trad_2));

% Set the calculated net head in bar
set(hand_calc_net_head_bar_trad_2,'String',num2str(calc_net_head_trad_2*valg_design_rho
P*valg_design_gP*10^-5));


%ccccccccccccccccccccccccccccccccccccccccccccccccccccccccccccccccccccccccc
%
% Pump characteristics, loss calculation
% H = Gulich, including all losses
%
%ccccccccccccccccccccccccccccccccccccccccccccccccccccccccccccccccccccccccc


% Set the calculated theoretical head
```

```matlab
set(hand_calc_theoretical_head_trad_3, ...
    'String',num2str(get(hand_calc_U2,'Value')^2/valg_design_gP));

% Set the calculated theoretical head in bar
set(hand_calc_theoretical_head_bar_trad_3, ...
    'String',num2str(get(hand_calc_U2,'Value')^2*valg_design_rhoP*10^-5));


[hand_axes_charac_trad_3,calc_net_head_trad_3,x_max_trad_3,y_max_trad_3] ...
    = draw_charac_curves_trad_3( ...
        hand_axes_charac_trad_3, ...
        valg_design_flow, ...
        get(hand_calc_U2,'Value'), ...
        get(hand_calc_U1_merid,'Value'), ...
        get(hand_calc_CU2,'Value'), ...
        valg_design_D2, ...
        D_1, ...
        get(hand_value_b2,'Value'), ...
        valg_design_beta2, ...
        beta_1_merid, ...
        A_1, ...
        slip_coeff, ...
        eta_opt, ...
        block_2, ...
        valg_charac_shockloss_trad_3, ...
        valg_design_gP, ...
        valg_design_Z, ...
        valg_design_nethead, ...
        get(hand_calc_sp_speed,'Value') ...
    );

% Set the calculated theoretical head with volume loss
set(hand_calc_theoretical_head_leakage_trad_3,'String',num2str(y_max_trad_3));

% Set the calculated theoretical head in bar with volume loss
set(hand_calc_theoretical_head_leakage_bar_trad_3,'String',num2str(y_max_trad_3*valg_de
sign_rhoP*valg_design_gP*10^-5));

% Set the calculated net head
set(hand_calc_net_head_trad_3,'String',num2str(calc_net_head_trad_3));

% Set the calculated net head in bar
set(hand_calc_net_head_bar_trad_3,'String',num2str(calc_net_head_trad_3*valg_design_rho
P*valg_design_gP*10^-5));

%cccccccccccccccccccccccccccccccccccccccccccccccccccccccccccccccccccccccc
%
% Pump characteristics, empirical
% H = ...
%
%cccccccccccccccccccccccccccccccccccccccccccccccccccccccccccccccccccccccc


% Set the calculated theoretical head
set(hand_calc_theoretical_head_trad_4, ...
    'String',num2str(get(hand_calc_U2,'Value')^2/valg_design_gP));

% Set the calculated theoretical head in bar
set(hand_calc_theoretical_head_bar_trad_4, ...
    'String',num2str(get(hand_calc_U2,'Value')^2*valg_design_rhoP*10^-5));


[hand_axes_charac_trad_4,calc_net_head_trad_4,x_max_trad_4,y_max_trad_4] ...
```

```matlab
    = draw_charac_curves_trad_4( ...
        hand_axes_charac_trad_4, ...
        valg_design_flow, ...
        get(hand_calc_U2,'Value'), ...
        get(hand_calc_U1_merid,'Value'), ...
        get(hand_calc_CU2,'Value'), ...
        valg_design_D2, ...
        D_1, ...
        get(hand_value_b2,'Value'), ...
        valg_design_beta2, ...
        beta_1_merid, ...
        A_1, ...
        slip_coeff, ...
        eta_opt, ...
        block_2, ...
        valg_charac_shockloss_trad_4, ...
        valg_design_gP, ...
        valg_design_Z, ...
        valg_design_nethead, ...
        get(hand_calc_sp_speed,'Value') ...
    );

% Set the calculated theoretical head with volume loss
set(hand_calc_theoretical_head_leakage_trad_4,'String',num2str(y_max_trad_4));

% Set the calculated theoretical head in bar with volume loss
set(hand_calc_theoretical_head_leakage_bar_trad_4,'String',num2str(y_max_trad_4*valg_de
sign_rhoP*valg_design_gP*10^-5));

% Set the calculated net head
set(hand_calc_net_head_trad_4,'String',num2str(calc_net_head_trad_4));

% Set the calculated net head in bar
set(hand_calc_net_head_bar_trad_4,'String',num2str(calc_net_head_trad_4*valg_design_rho
P*valg_design_gP*10^-5));
```

```matlab
function [h_axes,h_design_calc,x_limit,y_limit,pfleiderer_slip] =  ...

draw_charac_curves_trad_1(h_axes,Q_design,U_2,U_1,C_U2,D_2,D_1,b_2,beta_2,beta_1,A_1,sl
ip,omega,fric,shock,g,Z,H)

set(gcf,'CurrentAxes',h_axes)

% Parameters used in the calculations
R_2 = 0.5*D_2;
A_2 = R_2*2*pi*b_2;

Q = 0;
step_size = Q_design/100;
i = 1;
eta_v_opt=0.02;
Q_Lopt=Q_design*eta_v_opt;
Ku=Q_Lopt/sqrt(H);

psi             = 1.1*(1+sind(beta_2))*(D_1/D_2);
pfleiderer_slip = 2*(psi/Z)*(1/(1-(D_1/D_2)^2));


W_U2temptemp       = (Q/A_2) / tand(beta_2); % should be 0 (zero)
C_U2temptemp       = U_2-W_U2temptemp;
Htemptemp  = (U_2/g)*C_U2temptemp;
Q_L        = Ku*sqrt(Htemptemp);
W_U2       = ((Q+Q_L)/A_2) / tand(beta_2);
C_U2       = U_2-W_U2;
h_th_inf   = (U_2/g)*C_U2; % U_2^2/g
h_th       = h_th_inf / (1+pfleiderer_slip);
h_fric     = h_th - fric*(Q+Q_L)^2;
dh_shock   = shock*((Q+Q_L)-(Q_design+Q_L))^2;
h          = h_fric - dh_shock;

Q = Q+step_size;

while (Q<(2*Q_design))
    W_U2temptemp    = (Q/A_2) / tand(beta_2); % should be 0 (zero)
    C_U2temptemp    = U_2-W_U2temptemp;
    Htemptemp       = (U_2/g)*C_U2temptemp;
    Q_L             = Ku*sqrt(Htemptemp);
    W_U2_temp       = ((Q+Q_L)/A_2)/tand(beta_2);
    C_U2_temp       = U_2-W_U2_temp;
    h_th_inf_temp   = (U_2/g)*(C_U2_temp);
    h_th_temp       = h_th_inf_temp/(1+pfleiderer_slip);
    h_fric_temp     = h_th_temp-fric*(Q+Q_L)^2;
    dh_shock_temp   = shock*((Q+Q_L)-(Q_design+Q_L))^2;
    h_temp          = h_fric_temp - dh_shock_temp;

    [W_U2]          = [W_U2       W_U2_temp];
    [h_th_inf]      = [h_th_inf   h_th_inf_temp];
    [h_th]          = [h_th       h_th_temp];
    [h_fric]        = [h_fric     h_fric_temp];
    [h]             = [h          h_temp];
    [dh_shock]      = [dh_shock   dh_shock_temp];

    Q = Q+step_size;
    i = i+1;
end

Q = linspace(0,Q,length(h_th_inf));

% [min_dh_shock,min_index] = min(dh_shock);
```

```
h_design_calc = h(101);

x_limit = Q(end);
y_limit = h_th_inf(1);

plot(h_axes,Q,h_th_inf,'g', ...
    Q,h_th,'m', ...
    Q,h_fric,'b', ...
    Q,h,'r', ...
    Q,dh_shock,':k', ...
    [0 9.9 20.3 30.2 39.9 50.1 59.7 70.6 80.2 90.2 101]/3600,[75.22 74.03 72.67 71.16
68.40 66.02 61.99 56.71 50.54 43.65 35.62]/3,'k', ...
    [Q_design Q_design],[0 max(h_th_inf)],'c:')


legend('H_{th\infty}','H_{th}','H_{fric}','H','\DeltaH_{shock}','H_{measured}')
set(h_axes,'XLim',[0 x_limit],'YLim',[0 y_limit]);

xlabel('Q [m^3/s]');
ylabel('H [m]');
```

```matlab
function [h_axes,h_design_calc,x_limit,y_limit,pfleiderer_slip] =  ...

draw_charac_curves_trad_2(h_axes,Q_design,U_2,U_1,C_U2,D_2,D_1,b_2,beta_2,beta_1,A_1,sl
ip,omega,fric,shock,g,Z,H)

set(gcf,'CurrentAxes',h_axes)

% Parameters used in the calculations
R_2 = 0.5*D_2;
A_2 = R_2*2*pi*b_2;

Q = 0;
step_size = Q_design/100;
i = 1;
eta_v_opt=0.02;
Q_Lopt=Q_design*eta_v_opt;
Ku=Q_Lopt/sqrt(H);

psi             = 1.1*(1+sind(beta_2))*(D_1/D_2);
pfleiderer_slip = 2*(psi/Z)*(1/(1-(D_1/D_2)^2));


W_U2temptemp      = (Q/A_2) / tand(beta_2); % should be 0 (zero)
C_U2temptemp      = U_2-W_U2temptemp;
Htemptemp   = (U_2/g)*C_U2temptemp;
Q_L         = Ku*sqrt(Htemptemp);
W_U2        = ((Q+Q_L)/A_2) / tand(beta_2);
W_U1        = ((Q+Q_L)/A_1) / tand(beta_1);
C_U2        = U_2-W_U2;
C_U1        = U_1-W_U1;
h_th_inf    = (U_2/g)*C_U2; % U_2^2/g
h_th        = h_th_inf / (1+pfleiderer_slip);
h_fric      = h_th - fric*(Q+Q_L)^2;

dh_shock    = abs((U_1*C_U1)/g);
h           = h_fric - dh_shock;

Q = Q+step_size;

while (Q<(2*Q_design))
    W_U2temptemp      = (Q/A_2) / tand(beta_2); % should be 0 (zero)
    C_U2temptemp      = U_2-W_U2temptemp;
    Htemptemp         = (U_2/g)*C_U2temptemp;
    Q_L               = Ku*sqrt(Htemptemp);
    W_U2_temp         = ((Q+Q_L)/A_2)/tand(beta_2);
    W_U1_temp         = ((Q+Q_L)/A_1)/tand(beta_1);
    C_U2_temp         = U_2-W_U2_temp;
    C_U1_temp         = U_1-W_U1_temp;
    h_th_inf_temp     = (U_2/g)*(C_U2_temp);
    h_th_temp         = h_th_inf_temp/(1+pfleiderer_slip);
    h_fric_temp       = h_th_temp-fric*(Q+Q_L)^2;
    dh_shock_temp     = abs((U_1*C_U1_temp)/g);
    h_temp            = h_fric_temp - dh_shock_temp;

    [W_U2]            = [W_U2       W_U2_temp];
    [h_th_inf]        = [h_th_inf   h_th_inf_temp];
    [h_th]            = [h_th       h_th_temp];
    [h_fric]          = [h_fric     h_fric_temp];
    [h]               = [h          h_temp];
    [dh_shock]        = [dh_shock   dh_shock_temp];

    Q = Q+step_size;
    i = i+1;
```

```matlab
end

Q = linspace(0,Q,length(h_th_inf));

% [min_dh_shock,min_index] = min(dh_shock);
h_design_calc = h(101);

x_limit = Q(end);
y_limit = h_th_inf(1);

plot(h_axes,Q,h_th_inf,'g', ...
    Q,h_th,'m', ...
    Q,h_fric,'b', ...
    Q,h,'r', ...
    Q,dh_shock,':k', ...
    [0 9.9 20.3 30.2 39.9 50.1 59.7 70.6 80.2 90.2 101]/3600,[75.22 74.03 72.67 71.16
68.40 66.02 61.99 56.71 50.54 43.65 35.62]/3,'k', ...
    [Q_design Q_design],[0 max(h_th_inf)],'c:')


legend('H_{th\infty}','H_{th}','H_{fric}','H','\DeltaH_{shock}','H_{measured}')
set(h_axes,'XLim',[0 x_limit],'YLim',[0 y_limit]);

xlabel('Q [m^3/s]');
ylabel('H [m]');
```

```matlab
function [h_axes,h_design_calc,x_limit,y_limit] =  ...

draw_charac_curves_trad_3(h_axes,Q_design,U_2,U_1,C_U2,D_2,D_1,b_2,beta_2,beta_1,A_1,sl
ipcoeff,omega,fric,shock,g,Z,H,nq)

set(gcf,'CurrentAxes',h_axes)

% Parameters used in the calculations
R_2 = 0.5*D_2;
A_2 = R_2*2*pi*b_2;

% Some dimensions
a1       = 0.018;        % Inlet throat dimension (estimated)
b1       = 0.0324;       % Inlet throat dimension
a2       = 0.04;         % Outlet throat dimension (estimated)
b2       = 0.013;        % Outlet height
Lsch     = 0.14;         % Impeller blade length (estimated)
visc     = 0.553*10^-6;  % Kinematic viscosity water 50C
eps      = 0.5*10^-3;    % Absolute roughness of moderately corroded carbon steel
(http://neutrium.net/fluid_flow/absolute-roughness/)
a3       = 0.0127;       % Diffuser inlet throat width
b3       = 0.0155;       % Diffuser inlet throat height
a4       = 0.0276;       % Diffuser outlet throat width
b4       = 0.0184;       % Diffuser outlet throat height
cp       = 0.72;         % Diffuser cp from figure
Z_Le     = 10;           % Diffuser vanes
zetaov   = 1.5;          % Return channel design coefficient, between 0.2 and 1.5. 0.2
is good design, 1.0 is bad design

Q = 0;
step_size = Q_design/100;
i = 1;
Q_Lopt=2*4.1/(nq^1.6)*Q_design;
Ku=Q_Lopt/sqrt(H);

A_R        = (a4*b4)/(a3*b3);
Dh         = (2*(a2*b2+a1*b1))/(a1+b1+a2+b2);


W_U2temptemp      = (Q/A_2) / tand(beta_2); % should be 0 (zero)
C_U2temptemp      = U_2-W_U2temptemp;
Htemptemp  = (U_2/g)*C_U2temptemp;
Q_L        = Ku*sqrt(Htemptemp);
W_Q1       = (Q+Q_L)/(Z*a1*b1);
W_U1       = ((Q+Q_L)/A_1) / tand(beta_1);
C_U1       = U_1-W_U1;
C_M1       = (Q+Q_L)/A_1;
W_M1       = sqrt(C_M1^2+(U_1-C_U1)^2);
h_Las      = 0.3/(2*g)*(W_M1-W_Q1)^2;
W_av       = 2*(Q+Q_L)/(Z*(a2*b2+a1*b1));
Re         = W_av*Lsch/visc;
cf         = 0.136/((-log10(0.2*eps/Lsch+12.5/Re))^2.15);
cd         = (cf+0.0015)*(1.1+4*b2/D_2);
h_Laf      = 2*cd/g*Lsch/Dh*W_av^2;
h_La       = h_Las+h_Laf; % Total impeller loss
W_U2       = ((Q+Q_L)/A_2) / tand(beta_2);
C_U2       = U_2-W_U2;
C_U2slip   = slipcoeff*U_2-W_U2;
C_M2       = (Q+Q_L)/A_2;
C_2slip    = sqrt(C_M2^2+C_U2slip^2);
C_Q3       = (Q+0.5*Q_L)/(Z_Le*a3*b3);
```

```matlab
h_23          =
U_2^2/(2*g)*(cf+0.0015)*(a3/D_2+b3/D_2)*pi^3*((C_M2*b2)/(U_2*D_2))^2/(8*(Z_Le*(a3*b3)/(
D_2)))^3*(1+C_2slip/C_Q3)^3;
h_Le          = h_23+C_Q3^2/(2*g)*(0.3*(C_2slip/C_Q3-1)^2+1-cp-(1-zetaov)/A_R^2); % Total
diffuser loss
h_th_inf      = (U_2/g)*C_U2; % U_2^2/g
h_th          = (U_2/g)*C_U2slip;
h             = h_th - h_La-h_Le;


Q = Q+step_size;

while (Q<(2*Q_design))
    W_U2temptemp     = (Q/A_2) / tand(beta_2); % should be 0 (zero)
    C_U2temptemp     = U_2-W_U2temptemp;
    Htemptemp        = (U_2/g)*C_U2temptemp;
    Q_L_temp         = Ku*sqrt(Htemptemp);
    W_U2_temp        = ((Q+Q_L_temp)/A_2)/tand(beta_2);
    W_Q1_temp        = (Q+Q_L_temp)/(Z*a1*b1);
    W_U1_temp        = ((Q+Q_L_temp)/A_1)/tand(beta_1);
    C_U2_temp        = U_2-W_U2_temp;
    C_U2slip_temp    = slipcoeff*U_2-W_U2_temp;
    C_U1_temp        = U_1-W_U1_temp;
    C_M1_temp        = (Q+Q_L_temp)/A_1;
    W_M1_temp        = sqrt(C_M1_temp^2+(U_1-C_U1_temp)^2);
    h_Las_temp       = 0.3/(2*g)*(W_M1_temp-W_Q1_temp)^2;
    W_av_temp        = 2*(Q+Q_L_temp)/(Z*(a2*b2+a1*b1));
    Re_temp          = W_av_temp*Lsch/visc;
    cf_temp          = 0.136/((-log10(0.2*eps/Lsch+12.5/Re_temp))^2.15);
    cd_temp          = (cf_temp+0.0015)*(1.1+4*b2/D_2);
    h_Laf_temp       = 2*cd_temp/g*Lsch/Dh*W_av_temp^2;
    h_La_temp        = h_Las_temp+h_Laf_temp; % Total impeller loss
    C_M2_temp        = (Q+Q_L_temp)/A_2;
    C_2slip_temp     = sqrt(C_M2_temp^2+C_U2slip^2);
    C_Q3_temp        = (Q+0.5*Q_L_temp)/(Z_Le*a3*b3);
    h_23_temp        =
U_2^2/(2*g)*(cf_temp+0.0015)*(a3/D_2+b3/D_2)*pi^3*((C_M2_temp*b2)/(U_2*D_2))^2/(8*(Z_Le
*(a3*b3)/(D_2)))^3*(1+C_2slip_temp/C_Q3_temp)^3;
    h_Le_temp        = h_23_temp+C_Q3_temp^2/(2*g)*(0.3*(C_2slip_temp/C_Q3_temp-1)^2+1-
cp-(1-zetaov)/A_R^2); % Total diffuser loss
    h_th_inf_temp    = (U_2/g)*(C_U2_temp);
    h_th_temp        = (U_2/g)*(C_U2slip_temp);
    h_temp           = h_th_temp - h_La_temp-h_Le_temp;

    [W_U2]           = [W_U2        W_U2_temp];
    [h_th_inf]       = [h_th_inf    h_th_inf_temp];
    [h_th]           = [h_th        h_th_temp];
    [h_Le]           = [h_Le        h_Le_temp];
    [h_La]           = [h_La        h_La_temp];
    [h]              = [h           h_temp];

    Q = Q+step_size;
    i = i+1;
end

Q = linspace(0,Q,length(h_th_inf));

% [min_dh_shock,min_index] = min(h_Le);
h_design_calc = h(101);



x_limit = Q(end);
```

```matlab
y_limit = h_th_inf(1);

plot(h_axes,Q,h_th_inf,'g', ...
     Q,h_th,'m', ...
     Q,h_Le,':b', ...
     Q,h,'r', ...
     Q,h_La,':k', ...
     [0 9.9 20.3 30.2 39.9 50.1 59.7 70.6 80.2 90.2 101]/3600,[75.22 74.03 72.67 71.16
68.40 66.02 61.99 56.71 50.54 43.65 35.62]/3,'k', ...
     [Q_design Q_design],[0 max(h_th_inf)],'c:')

legend('H_{th\infty}','H_{th}','\DeltaH_{diffuser}','H','\DeltaH_{impeller}','H_{measur
ed}')
set(h_axes,'XLim',[0 x_limit],'YLim',[0 y_limit]);

xlabel('Q [m^3/s]');
ylabel('H [m]');
```

```matlab
function [h_axes,h_design_calc,x_limit,y_limit] =  ...

draw_charac_curves_trad_4(h_axes,Q_design,U_2,U_1,C_U2,D_2,D_1,b_2,beta_2,beta_1,A_1,sl
ipcoeff_opt,eta_opt,block_2,shock,g,Z,H,nq)

set(gcf,'CurrentAxes',h_axes)

% Parameters used in the calculations
R_2 = 0.5*D_2;
A_2 = R_2*2*pi*b_2;

Q = 0; %
step_size = (Q_design-Q)/100;
i = 1;
Q_Lopt=2*4.1/(nq^1.6)*Q_design;
Ku=Q_Lopt/sqrt(H);


W_U2temptemp        = (Q/A_2) / tand(beta_2); % should be 0 (zero)
C_U2temptemp        = U_2-W_U2temptemp;
Htemptemp           = (U_2/g)*C_U2temptemp;
Q_L                 = Ku*sqrt(Htemptemp);
slipcoeff           = slipcoeff_opt*(1.3746-
0.2483*((Q+Q_L)/(Q_design+Q_L))^3+0.8639*((Q+Q_L)/(Q_design+Q_L))^2-
0.9919*((Q+Q_L)/(Q_design+Q_L)));
W_U2                = ((Q+Q_L)/A_2) / tand(beta_2);
C_U2                = U_2-W_U2;
C_U2slip            = slipcoeff*U_2-W_U2;
h_th_inf            = (U_2/g)*C_U2; % U_2^2/g
h_th                = (U_2/g)*C_U2slip;
eta                 = eta_opt*(1-0.6*((Q+Q_L)/(Q_design+Q_L)-0.9)^2-
0.25*((Q+Q_L)/(Q_design+Q_L)-0.9)^3);
h                   = eta*U_2/g*(slipcoeff*U_2-W_U2*block_2); % Assuming non-rotational
inlet

Q = Q+step_size;

while (Q<(2*Q_design))
    W_U2temptemp    = (Q/A_2) / tand(beta_2); % should be 0 (zero)
    C_U2temptemp    = U_2-W_U2temptemp;
    Htemptemp       = (U_2/g)*C_U2temptemp;
    Q_L_temp        = Ku*sqrt(Htemptemp);
    slipcoeff_temp  = slipcoeff_opt*(1.3746-
0.2483*((Q+Q_L_temp)/(Q_design+Q_L_temp))^3+0.8639*((Q+Q_L_temp)/(Q_design+Q_L_temp))^2
-0.9919*((Q+Q_L_temp)/(Q_design+Q_L_temp)));
    W_U2_temp       = ((Q+Q_L_temp)/A_2)/tand(beta_2);
    C_U2_temp       = U_2-W_U2_temp;
    C_U2slip_temp   = slipcoeff_temp*U_2-W_U2_temp;
    h_th_inf_temp   = (U_2/g)*(C_U2_temp);
    h_th_temp       = (U_2/g)*(C_U2slip_temp);
    eta_temp        = eta_opt*(1-0.6*((Q+Q_L_temp)/(Q_design+Q_L_temp)-0.9)^2-
0.25*((Q+Q_L_temp)/(Q_design+Q_L_temp)-0.9)^3);
    h_temp          = eta_temp*U_2/g*(slipcoeff_temp*U_2-W_U2_temp*block_2);


    [W_U2]          = [W_U2        W_U2_temp];
    [h_th_inf]      = [h_th_inf    h_th_inf_temp];
    [h_th]          = [h_th        h_th_temp];
    [h]             = [h           h_temp];

    Q = Q+step_size;
    i = i+1;
end
```

```matlab
Q = linspace(0,Q,length(h_th_inf));

% [min_dh_shock,min_index] = min(h);
h_design_calc = h(101);

x_limit = Q(end);
y_limit = h_th_inf(1);



plot(h_axes,Q,h_th_inf,'g', ...
    Q,h_th,'m', ...
    Q,h,'r', ...
    [0 9.9 20.3 30.2 39.9 50.1 59.7 70.6 80.2 90.2 101]/3600,[75.22 74.03 72.67 71.16
68.40 66.02 61.99 56.71 50.54 43.65 35.62]/3,'k', ...
    [Q_design Q_design],[0 max(h_th_inf)],'c:')


legend('H_{th\infty}','H_{th}','H','H_{measured}')
set(h_axes,'XLim',[0 x_limit],'YLim',[0 y_limit]);

xlabel('Q [m^3/s]');
ylabel('H [m]');
```